INVESTIGATION OF THE STRUCTURED PACKING SURFACE TEXTURES INFLUENCE ON CO_2 ABSORPTION USING OPENFOAM

Phanindra PRASAD THUMMALA

PhD Thesis

Department of Environmental Engineering

Supervisor: Prof.Dr. Ümran TEZCAN ÜN

(Co-supervisor: Asst.Prof.Dr. Ahmet Ozan ÇELİK)

Eskişehir,

Anadolu University

Graduate School of Sciences

June, 2018

This thesis study was supported and funded by the board of the Scientific Research Projects Commission of Anadolu University under project Number BAP-1603F123

ABSTRACT

INVESTIGATION OF THE STRUCTURED PACKING SURFACE TEXTURES INFLUENCE ON CO_2 ABSORPTION USING OPENFOAM

Phanindra PRASAD THUMMALA

Department of Environmental Engineering,

Anadolu University, Graduate School of Sciences, June, 2018

Supervisor: Prof.Dr. Ümran TEZCAN ÜN

(Co-supervisor: Asst.Prof.Dr. Ahmet Ozan ÇELİK)

The scope of the present thesis is to effectively utilize the OpenFOAM (open source CFD software) to study influence of structured packing surface textures on absorption of CO_2 and find possibility of developing improved surface texture(s). The work mainly focuses on the three aspects: implementing an effective approach in OpenFOAM for modeling reactive mass transfer of CO_2, deriving the surface texture design parameters that can influence the overall mass transfer and suggest a possible new surface texture design.

CFD modeling of structured packing is carried in three scales: small-, meso- and large scales. Small scale analysis is carried to study the influence of micro scale phenomenon on the performance of the packing. Meso-scale analysis is usually carried to study the dry and wet pressure drop using representative elementary units (REU). Large scale analysis is carried to study the liquid distribution over a full scale column by modeling the column as porous medium.

This thesis focuses on small and meso scale. The novelty of the present thesis is in implementing the one fluid formulation for modeling the mass transfer across gas liquid interface along with developing user code required for effective post-processing. This thesis proposes a best practice of keeping “amplitude to base ratio of a texture <0.2” for designing the surface textures. A new texture was proposed and verified experimentally for its effectiveness in producing higher interfacial area. Also this thesis presents results of pressure drop analysis by considering detailed surface texture geometry at meso-scale for the first time.

Keywords: OpenFOAM, Surface texture, Amplitude to base ratio, Pressure drop, Structured packing column.

Özet

OPENFOAM KULLANARAK YAPILANDIRILMIŞ DOLGU YÜZEYİNİN CO_2 ABSORBSİYONU ÜZERİNDEKİ ETKİSİNİN İNCELENMESİ

Phanindra PRASAD THUMMALA

Çevre Mühendisliği Bölümü,

Anadolu Üniversitesi, Fen Bilimleri Enstitüsü, Haziran, 2018

Danışman: Prof.Dr. Ümran TEZCAN ÜN

(İkinci Danışman: Doç.Dr. Ahmet Ozan ÇELİK)

Bu tezin amacı, OpenFOAM'ı (açık kaynaklı Hesaplamalı Akışkanlar dinamiği (HAD) yazılımı) etkin bir şekilde kullanarak, yapılandırılmış dolgu yüzeyinin CO_2 absorbsiyonu üzerindeki etkisini incelemek ve yeni yüzey dokusu geliştirilme imkanı bulmaktır. Çalışma başlıca üç alana odaklanmıştır: CO_2'in reaktif kütle transferini modellemek için OpenFOAM'da etkili bir yaklaşımın uygulanması, tüm kütle transferini etkileyebilecek yüzey dokusu tasarım parametrelerinin türetilmesi ve olası yeni bir yüzey tasarımının önerilmesidir.

Yapılandırılmış dolgulunun HAD modellemesi üç ölçekte yürütülmektedir: küçük, orta ve büyük ölçekler.Küçük ölçekli analiz dolgunun performansında mikro ölçekli fenomenlerin etkisini belirlemek için yürütülmektedir. Mezo-ölçekli analiz genellikle Temsilci Temel Birimler (TTB) kullanarak kuru ve ıslak basınç düşüşünü inceleyerek yürütülür. Büyük ölçekli analiz tam ölçekli kolon üzerinde sıvının dağılımını kolonu gözenekli ortam olarak modelleyerek yapılır.

Bu tez küçük ve mezo ölçeğe odaklanmıştır. Bu tezin özgünlüğü, etkili bir işlem sonrası işlemler için gerekli olan kullanıcı kodu geliştirerek gaz sıvı ara yüzünde kütle transferinin modellenmesi için bir akışkan formülasyonunun uygulanmasındadır. Bu tez, yapılandırılmış dolgulu kolonunun yüzey dokusunu modellemede "genlik/taban oranını <0.2" tutulmasını önermektedir. HAD kullanılarak yeni bir doku geliştirilmiş ve daha yüksek ara yüzey alanı oluşturmadaki etkinliği için deneysel olarak doğrulanmıştır. Ayrıca bu tez, ilk kez mezo-ölçekte detaylı yüzey doku geometrisi göz önüne alınarak yapılandırılmış dolgulu kolonunun basınç düşüşü analiz sonuçlarını sunmaktadır.

Anahtar Kelimeler: OpenFOAM; Yüzey dokusu; genlik/taban oranı; basınç düşüşü; yapılandırılmış dolgulu kolon.

ACKNOWLEDGEMENT

I would like to express my sincere thanks to my supervisors Prof.Dr. Ümran Tezcan Ün and Asst.Prof.Dr. Ahmet Ozan Çelik for their continuous support and guidance during my PhD studies at Anadolu University, Turkey. I also would like to thank my jury members Prof.Hikmet Karakoç and Prof.Aysegül Aşkin for their constructive suggestions during the progress meetings of my PhD.

I'm also grateful for the financial support I received from Anadolu Univerity and Turkiye scholarships (YTB) for completely funding my studies.

I also would like to thank my parents Mr.Nagendra Prasad Thummala and Mrs.Hemalatha Prasad Thummala; family members Ravindra, Krishnaveni and Mrunalini; friends Masood, Abdullah, Fatima, Ayşe and others in my University; all the citizens of Turkey for everything.

Finally, I thank fellow *foamers* and CFD engineers across globe who shared their valuable inputs for implementing the OpenFOAM code.

Phanindra Prasad Thummala

07/06/2018

STATEMENT OF COMPLIANCE WITH ETHICAL PRINCIPLES AND RULES

I hereby truthfully declare that this thesis is an original work prepared by me; that I have behaved in accordance with the scientific ethical principles and rules throughout the stages of preparation, data collection, analysis and presentation of my work; that I have cited the sources of all the data and information that could be obtained within the scope of this study, and included these sources in the references section; and that this study has been scanned for plagiarism with "scientific plagiarism detection program" used by Anadolu University, and that "it does not have any plagiarism" whatsoever. I also declare that, if a case contrary to my declaration is detected in my work at any time, I hereby express my consent to all the ethical and legal consequences that are involved.

Phanindra Prasad Thummala

CONTENTS

Page

Page

Page

LIST OF TABLES

Page

LIST OF FIGURES

Page

Page

Page

NOMENCLATURE

C	:	molar concentration [mol/m^3]
D	:	mass diffusivity [m^2/s]
d	:	hydraulic diameter [m]
F	:	mass flux [mol/m^2-s]
g	:	acceleration of gravity [m/s^2]
H	:	Henry constant [-]
k	:	liquid side mass transfer coefficient [mol/Pa.s.m^2]
L	:	length of the flat plate [m]
R	:	universal gas constant [Pa.m^3.mol^{-1}.K^{-1}]
T	:	temperature [K]
v	:	velocity [m/s]
x	:	mole fraction in solvent
z	:	distance of grid cell from wall [m]
λ	:	base width[m]
A	:	half of the Amplitude of the texture height[m]
α	:	volume fraction[-]
ρ	:	density [kg/m^3]
μ	:	viscosity [Pa s]
β	:	plate inclination angle [degree]

θ	:	contact angle between liquid and solid wall [degree]
τ	:	time of exposure [s]
$\boldsymbol{k}$	:	surface curvature [m^{-1}]
σ	:	surface tension coefficient [Nm^{-1}]
δ	:	liquid film thickness[m]
G	:	gas phase
L	:	liquid phase
st	:	surface tension
w	:	wall
i	:	interface
Re	:	Reynolds number

1. INTRODUCTION

Carbon dioxide (CO_2) is one of the major greenhouse gases which are released to earth's atmosphere by human activity. Out of them majority of the CO_2 emission is from power plants consuming fossil fuels (IPCC 2005). Generally these kinds of emissions are referred as post combustion emissions. Using renewable energy sources will be the best way to reduce these emissions to zero, but the cost of energy produced by these technologies is expensive when compared to energy produced by consuming fossil fuels (Viebahn et al. 2012). Hence keeping the reduction of renewable energy cost as long term goal there is an urgent need to develop technologies which can capture the CO_2 at the source, before being released to atmosphere.

Reactive absorption is the absorption process enhanced due to the presence of chemical reactions in the liquid solvent (Yildirim et al. 2012). Reactive absorption of CO_2 using amine solvents like monoethanolamine (MEA, C_2H_7NO) is one of the best economically feasible method for capturing the CO_2 (Aaron & Tsouris 2005). This kind of technology can be readily integrated into existing power plants and is going to be the most preferable method for post combustion CO_2 mitigation by 2030 (Rochelle 2009). Typical post combustion amine scrubbing process or post combustion carbon capture (PCC) process integrated into natural gas combined cycle (NGCC) power plant looks like Figure 1.1 (Biliyok & Yeung 2013).

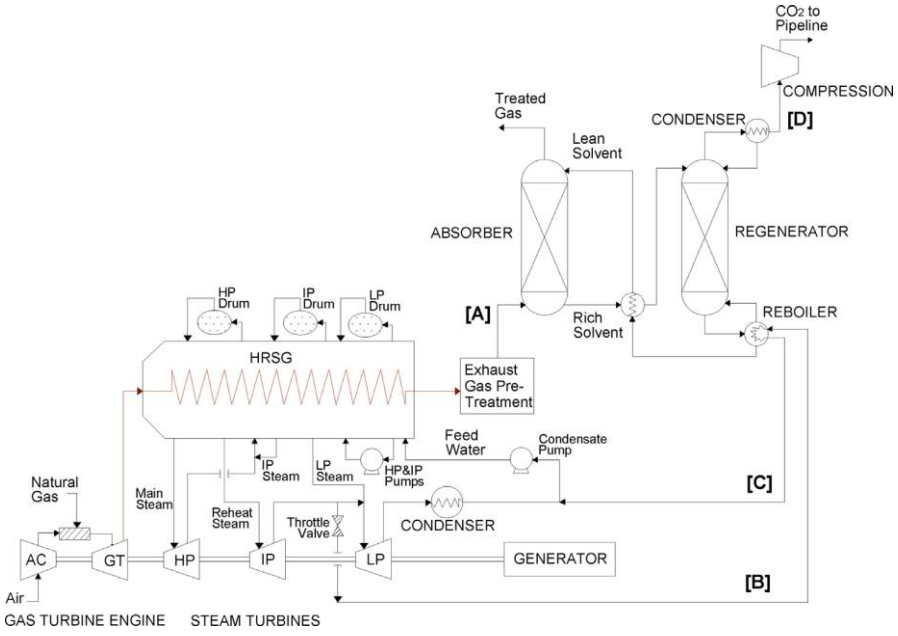

Figure 1.1 *Process flow diagram of integrated NGCC, PCC and compression plant*

The PCC process consists of two columns: absorber and regenerator. The absorber is a packed column filled with random or structured packing. The flue gas with CO_2 is injected in to the absorber from the bottom and the amine solvents are poured into the column from the top in a counter current fashion. The solvent will come into contact of the flue gas and reactive absorption of CO_2 takes place at the interface of the two fluids under flow. The CO_2 rich solvent leaving the absorber is then poured into regeneration column where in which the solvent is regenerated. The regeneration process cost nearly 60% of the total cost of PCC (Mores et al. 2012). Despite of the chemical penalty involved, the reactive absorption is found to be the most promising approach especially after the successful operation of Boundary dam project in Canada (Stéphenne 2014). This project began operating in the fall of 2014 and is the world's first commercial coal fired post combustion carbon capture project.

In general the structured packing columns are preferred over random packing due to small pressure losses and better efficiency (Yang et al. 2015). The structured packing columns are made of corrugated sheets that may have been chemically treated or mechanically roughened in order to improve wetting or promote wetting stability(Henry Z. Kister 1992; Zhao & Cerro 1992) . Hence in a structured column two kinds of structures can be identified: first, there is a macro-structure generated by corrugation (Figure 1.2 (a) & Figure 1.2 (b)(Nawrocki et al. 1991); The size of the base (2B) of these macro structures is generally in the order of 0.01 to 0.03m); and the second kind of structure is micro-structure which is associated with the surface treatment (Figure 1.3; the size of these micro structures is in the order of 0.001m). These micro structures are generally referred as "surface textures" due to their association with the surface of the sheets. The micro structures are found to enhance mass transfer by 20-100% (Kohrt et al. 2011).

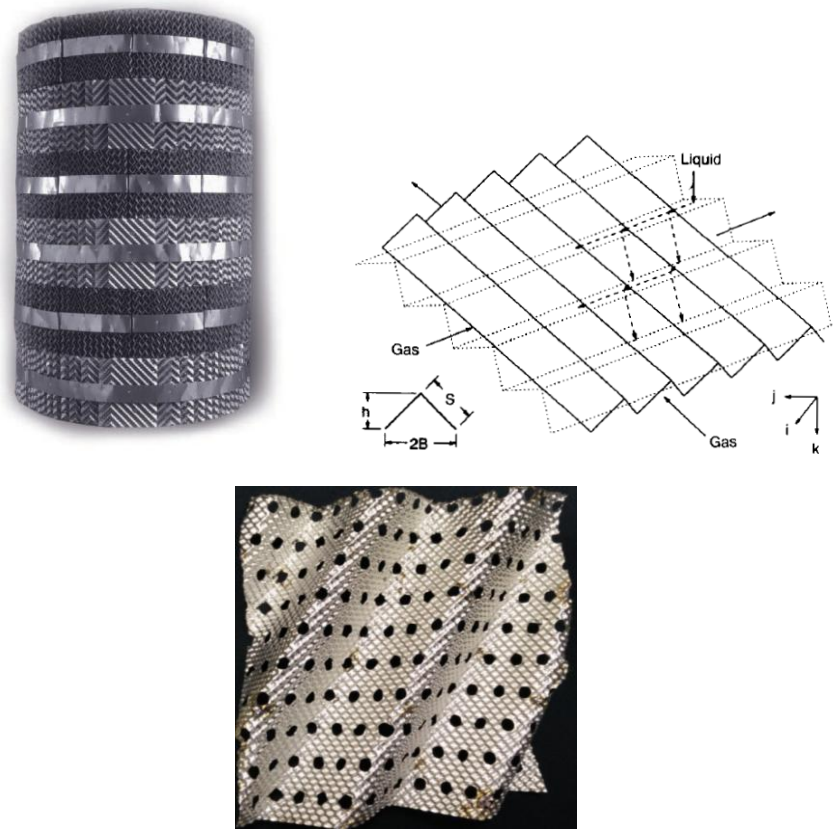

Figure.1.2 (a): *Six layers of commercial FLEXIPAC structured packing* **(b)** *Flow channel arrangement of structured packing* **(c)** *Structured packing sheets with micro-structure*

1.1 Thesis Subject and Objectives

The scope of the present thesis is to effectively utilize the OpenFOAM (Open source Field Operation and Manipulation) (Jasak & Weller 1995; Rusche 2002), an open source CFD (Computational Fluid Dynamics) software, to study influence of structured packing surface textures on absorption of CO_2 by reactive mass transfer into MEA solvent. Also find out possibility of developing improved surface texture(s). Overall the end results will be effectively useful for any future investigations related to designing of surface textures of structure packing columns for absorption.

Multiphase flow occurs in a wide spectrum of industrial reactor applications ranging from bubble columns, packed bed/trickle bed reactors and fluidized bed reactors. These reactors generally involve complex flow of two or more immiscible fluids across which the mass transfer takes place. Also the mass transfer in some cases is accompanied by chemical reactions, sometimes in the presence of solid catalysts, to enhance the rate of mass transfer. The analysis of these multiphase flows can be tackled

in three ways: by means of experimental work, with theoretical equations or using numerical models. Numerical methods are preferred over the experimental works for reducing the design phase expenses at small size lab scale investigations. They are preferred because of their ability to assess flow characteristics that cannot be accessed using experimental techniques. In the case of chemical absorption in structured packing columns, numerical models can be used to quantify aspects such as liquid film thickness and velocities, concentration profiles of chemical species within the liquid film, dry and wet pressure drop of the packing, liquid holdup, liquid spreading and interfacial area per unit volume of packing. All these features would be practically impossible to analyze inserting probes into the experimental devices without interfering with the flow. Experimental pilot setups are then developed on the basis of designs optimized by numerical methods and tests will be carried to find the suitability of developed designs for industrial applications.

In general numerical studies are carried at three different scales: small scale, meso-scale and large scale. The results of one scale can be used as a feed to another scale. The influence of surface texture that is of interest to the present thesis involves analysis at small and meso-scale due to its size. Hence a detailed overview of various approaches along with their capabilities used in the hydrodynamic analysis at these small and meso scales will be presented in Chapter 2. Also in the last decades many approaches were developed for modeling the mass transfer accompanied with and without reactions and a detailed discussion will be presented about these approaches in Chapter 2. This discussion helps in choosing the most appropriate approach for modeling the mass transfer in the present thesis.

In this thesis, OpenFOAM open source CFD software written basically in C++ is used to run simulations. Many features required for hydrodynamic and thermal analysis are available by default in this software. But a limited number of features are available for CFD analysis of mass transfer across immiscible phases. Hence the mass transfer model chosen from literature is implemented as an additional equation into the existing library. Also additional functions were developed to derive the most important aspects like film height, interfacial area and liquid hold up from the simulation results. Along with the development of these features a methodology was developed to reduce the overall computational resource time which is very important for analysis involving multiphase flow simulation.

The present thesis is thus dedicated to develop and implement additional functions required to model the mass transfer across immiscible phases, effectively use the resulting equations in analyzing the influence of surface textures on CO_2 absorption in structured packing columns, use the model equations to develop improved surface textures and propose limitations (if any) in this regard. The analyses of results specifically focus on the:

- Correct derivation of liquid hold up, film height distribution and interfacial area through developed additional functions
- The influence of surface texture's amplitude to base ratio on the film growth and mass transfer
- The influence of surface texture on the interfacial area under rivulet flow conditions to find the amount of actual solid area covered by liquid phase

1.2 Elements of Novelty:

The present thesis aims in introducing following new results regarding the development of surface texture by effectively utilizing CFD modeling:

1. This thesis discuss the most reliable approach called *one fluid formulation* for modeling the mass transfer across immiscible phases and suggests methods to overcome limitations found during its implementation in OpenFOAM. Also a procedure is suggested to reduce the overall computational resource required for simulating the system of equations
2. This thesis proposes a best practice of keeping "amplitude to base ratio of a texture <0.2". A new texture was developed and verified by CFD for its effectiveness of producing higher interfacial area at low liquid hold up when compared with existing commercial packing textures.
3. This thesis provides additional code that can be coupled to OpenFOAM library to visualize film height, liquid hold up and interfacial area.
4. This thesis derives the pressure drop by considering detailed surface texture geometry at meso-scale for the first time.

In short this thesis aims at presenting an integrated CFD approach using which new surface textures can be developed for structured packing columns used in post combustion CO_2 absorption units.

1.3 Progress of Research

This research begins with literature survey of technologies available for CCS by absorption and kinetics of reaction between CO_2 and amine solvents. Also the literature survey was focused on familiarization with the current modeling strategies along with their advantages and limitations.

A most reliable approach "*one fluid formulation*" for modeling mass transfer was chosen from open literature and was implemented in OpenFOAM. The chosen approach was based on "geometric reconstruction method" of representing the interface whereas the OpenFOAM is based on "algebraic method" of interface representation (details in Chapter3). Hence there were challenges in its implementation and deriving effective results. These limitations and a methodology to overcome some of them were investigated in the initial period of research. The analysis was carried initially on the simple geometries and validation was carried against the available results from the literature. The systems of equations were then applied for a flow over flat plate domain where gas liquid flow in counter current direction. This is a prerequisite step to find out the advantages and limitations of the current approach to model mass transfer over a structured plate. During this a procedure to overcome the difficulties like reducing computational resource was developed. Thereupon the system of equations were utilized effectively in order to find the effect of various design operating parameters of a surface texture on the mass transfer between gas liquid phase. The analysis was carried on triangular texture patterns of commercially available structured packing columns like Mellapak 250 and wave pattern developed and published in open literature. The analysis had resulted in the formulation of a best practice of "amplitude to base ratio <0.2" for designing a new texture. This was first of its kind of study carried using CFD. A new texture was developed using this best practice and was the verified by CFD for producing higher interfacial area at low liquid hold up when compared with existing commercial packing textures. Finally pressure drop analysis was carried at meso-scale by considering detailed geometry and detail analysis of the results were presented. Also, an experimental investigation using PIV (Particle Image Velocimetry) technique was carried for various solvents of interest to CO_2 absorption and bench mark results were produced for validating existing and future investigations.

1.4 Structure of Thesis

The work carried till date is organized into eight chapters and an appendix chapter. The appendix chapter show the code for implementation of "*one fluid formulation*" and code for deriving the results like film height, interfacial area and liquid holdup. The first four chapters form the foundation of the thesis and results are presented in the later chapters.

Overall the current report is organized as follows:

- Chapter1 introduces the context of the PhD and describes the importance of surface textures influence on the overall performance of the structured packing column. Also the chapter introduces the objectives of the thesis, the elements of novelty and the progress of research till date
- Chapter 2 constitutes the literature survey. The chapter gives a brief review of various works carried and published in open literature from the perspective of structured packing surface textures influence on CO_2 absorption. Also, various approaches used in CFD modeling of hydrodynamics and reactive mass transfer on structured columns with surface textures are discussed in detail.
- Chapter 3 gives an overview of mathematical theory of multiphase flows and the modeling of reactive mass transfer by 'one fluid formulation' in detail. Also the chapter discuss the fundamental difference between the "geometric reconstruct algorithm" used in commercial and "algebraic algorithm" used in OpenFOAM for constructing the gas-liquid interface surface. Since the original "*one fluid formulation*" was developed by "geometric reconstruct algorithm", an understanding of the mathematical difference is required to effectively utilize this approach. Also this chapter includes the details of validation of the implemented model with the results available in the open literature.
- Chapter 4 presents the results of physical mass transfer on flat plate by the system of equations and discuss the advantages and limitations in detail. Also procedure to overcome these limitations is suggested.
- Chapter 5 presents results of the applied model on commercial surface textures and deriving a best practice for designing a new texture surface
- Chapter 6 presents the results of the MEA solvent distribution on the flat, plate with commercial texture pattern and a developed new and improved texture

pattern. It also clearly shows how the new texture pattern is a significant improvement in terms of producing high interfacial area at low liquid hold up.

- Chapter 7 presents pressure drop analysis at meso-scale considering the detailed geometry of surface textures
- Chapter 8 presents final remarks along with outlining of the future research work which is of scientific significance that can be carried as an extension of this thesis.
- Appendix
    - OpenFOAM code for "one fluid formulation"
    - Post processing code for deriving the film height, interfacial area and liquid hold up.

2. LITERATURE REVIEW

This chapter presents a critical discussion of previous literature about the modeling of structured packing columns using three scale approaches, highlighting their advantages and limitations. Also the influence of the surface textures on reactive mass transfer in structured packing columns is discussed in detail. The aim of the review is to find the potential gaps in research. Since the novelty of the thesis lies in developing a possible new surface textures by using CFD modeling of physical and reactive mass transfer, a detail discussion of the available literature in regard to CFD modeling of physical and reactive mass transfer is also presented. Discussion of available approaches for modeling of reactive mass transfer is emphasized along with their advantages and disadvantages.

2.1 CFD Modeling of Hydrodynamics of Structured Packing with Surface Textures

Two approaches exist to tackle multiphase modeling: the Euler-Euler and the Euler- Lagrange approach. In the Euler-Lagrange approach the Navier-Stokes equations are solved for the continuous phase whereas a number of particles of the dispersed phase are tracked, exchanging mass, momentum and energy with the continuous phase. This approach is not appropriate in general for any application in which the volume fraction of the secondary phase cannot be omitted, i.e. such is the case of free-surface flows. On the other hand, in the Euler-Euler approach the concept of volume fraction of the different phases is introduced, which makes this approach suitable to track the interface between the fluids involved. The volume fraction constitutes a field of scalar values in space and time. The sum of the volume fraction of all the phases cannot be over one. Three different Euler-Euler models can be used in CFD:

- The VOF model (Hirt & Nichols 1981; Fluent Inc. 2011) solves a single set of momentum and mass conservation equations which is shared by the fluids. The interface is tracked using an additional transport equation for the volume fraction. This method is used when the tracking of the interface is interesting as it is the case in the present thesis.
- The mixture model also treats the phases as interpenetrating continua and prescribes relative velocities between the dispersed and the primary phase. This model is used for particle-laden and bubbly flows with low loading.

- The Eulerian model solves a set of momentum and mass conservation equations for each phase, coupling them with the interface exchange coefficients. The application range of this model is similar to that of the mixture model, including also fluidized beds and sedimentation.

The simulations performed in this thesis utilize the VOF method for the interface tracking of the free-surface flow within amine scrubbers.

2.2 Multi-scale Modeling of Structured Packing Columns

Even though the calculation power of modern computers has increased in multi fold in the last decades simulating the structured packing column with all the geometry details stands expensive. Multi-scale strategy is adopted and proven to be the best approach for simulating the structured packing columns by CFD (Sun et al. 2013; Raynal & Royon-Lebeaud 2007; Li et al. 2016).

The three scale strategy applied for CFD simulation of structured packing bed is shown in Figure 2.1 and is summarized below:

- Small-scale, consists of small 2D or 3D computational domains, often in the range of millimeters and up to about 10 centimeters. At this scale it is possible to implement an interface tracking method without an excessive computational cost due to the small size of the domain. Therefore, it is possible to describe the interaction between phases, solving aspects such as liquid spreading and reactive mass transfer. Also the simplicity of the geometry allows the user to implement a structured mesh, which considerably reduces the required computational time.
- Meso-scale models consist of a limited set of representative elementary units (REUs), normally used to analyze dry pressure drop by means of single-phase simulations, i.e. including only the gas phase. A small set of REUs presents the same dry pressure drop per unit length as the entire column. This is used to assess the performance of the structured packing in this regard. After the dry pressure drop is obtained, the wet pressure drop can be calculated using correction factors that take into account the effect of the presence of the liquid phase.
- Large-scale models simulate the entire reactor assuming that the structured packing behaves as a porous medium with a high void fraction, i.e. with the porosity in the range of 0.95–0.98, in terms of liquid spreading. Large-scale

simulations can also be used to study the influence of the different geometrical features such as liquid distributors, walls, etc. on the gas flow patterns.

A description of the CFD work done so far at the aforementioned different scales is included in the subsequent sections.

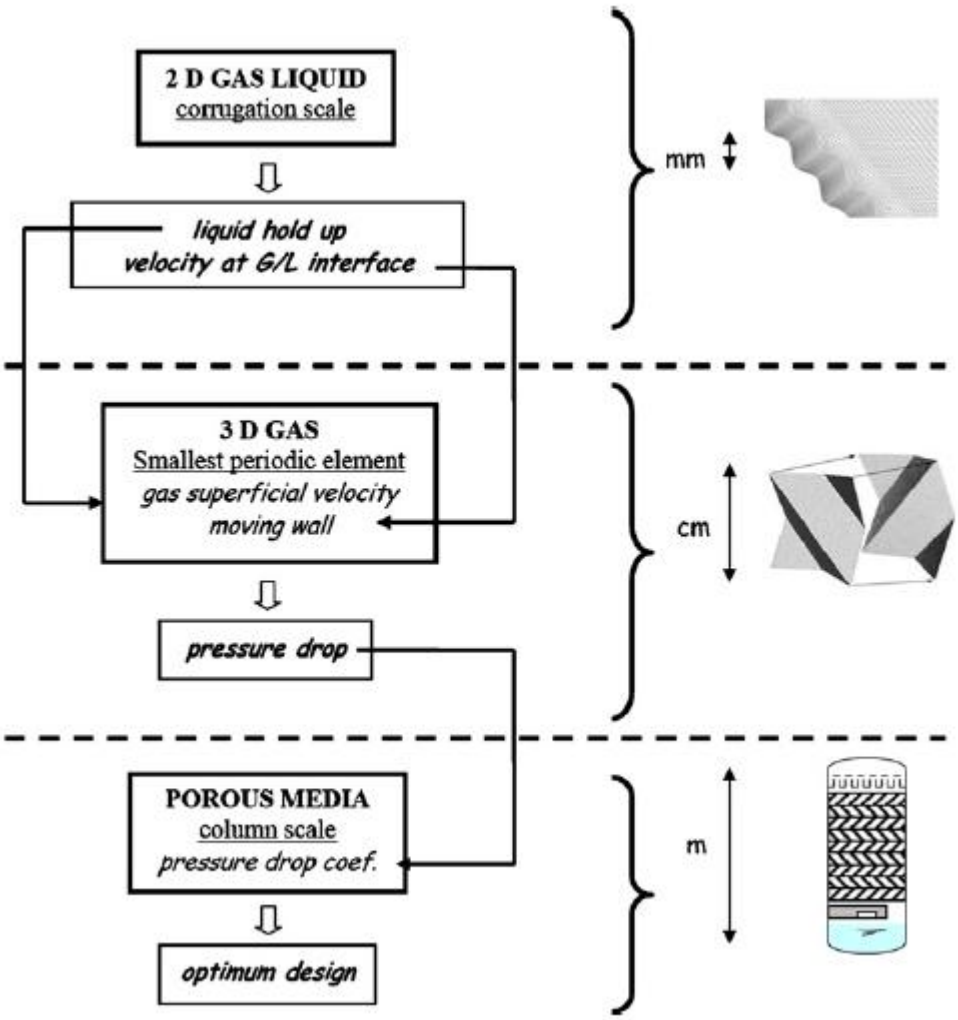

Figure 2.1: *The three scale strategy successfully applied for CFD simulation of structured packing beds(Raynal & Royon-Lebeaud 2007)*

2.2.1 Small-scale modeling

Small-scale modeling focuses mainly on tracking the interface between the fluids using small computational domains. By doing so, important flow features like liquid hold-up, interfacial area and the interaction between phases can be described in

great detail, e.g. influence of geometric surface texture, diffusion of species into the liquid film, formation of droplets, waves and other liquid structures, etc (Min & Park 2011; Valluri et al. 2005; Wehinger et al. 2013; Luo et al. 2014). Following discussion of the literature on small-scale modeling that follows focuses first on the hydrodynamics and continues with the reactive mass transfer.

The analysis of the hydrodynamics can be carried out with 2D or 3D simulations. 2D simulations offer the possibility of studying texture patterns on the solid surface and the development of the falling liquid film, i.e. velocity profiles , liquid film thickness and reactive mass transfer can be assessed (Valluri et al. 2005; Haroun & Raynal 2016). The liquid hold-up is thereafter calculated assuming that a perfectly developed liquid film covers the entire surface of the packing. The liquid hold-up is thus obtained multiplying the liquid film thickness from the simulations by the specific area of the packing. 3D simulations extend the capabilities of 2D, allowing assessing the formation of liquid irregularities (i.e. rivulets and droplets) that strongly influence the amount of interfacial area and the absorption rate (Li et al. 2016). The formation of liquid irregularities within the liquid phase is known as liquid maldistribution and involves the calculation of the gas liquid interface.

An attempt to use small-scale VOF simulations to determine the liquid hold-up on structured packing was carried out by Raynal and Royon-Lebeaud (Raynal & Royon-Lebeaud 2007). The authors consider a 2D computational domain with both a smooth wall and a wavy corrugation pattern simulating the texture of the wall along which the falling liquid film is developed. The two surface texture patterns used by the authors can be observed in Figure 2.2. The fact that the liquid film thickness has the same order of magnitude as the amplitude of the texture in the walls, i.e. approximately 0.3 mm, brings the hypothesis that the texture itself can heavily influence the development of the liquid film and the mass transfer (Kohrt et al. 2011). Apart from the substantial increase in the computational resources that the VOF model requires, the fact that a sufficiently fine mesh has to be applied in those areas of the domain where important gradients are to be found, constitutes a justification of the three-scales strategy. As a matter of fact, such degree of detail provided by a very refined mesh at the vicinity of the wall could not be attained in meso- or large-scale domains.

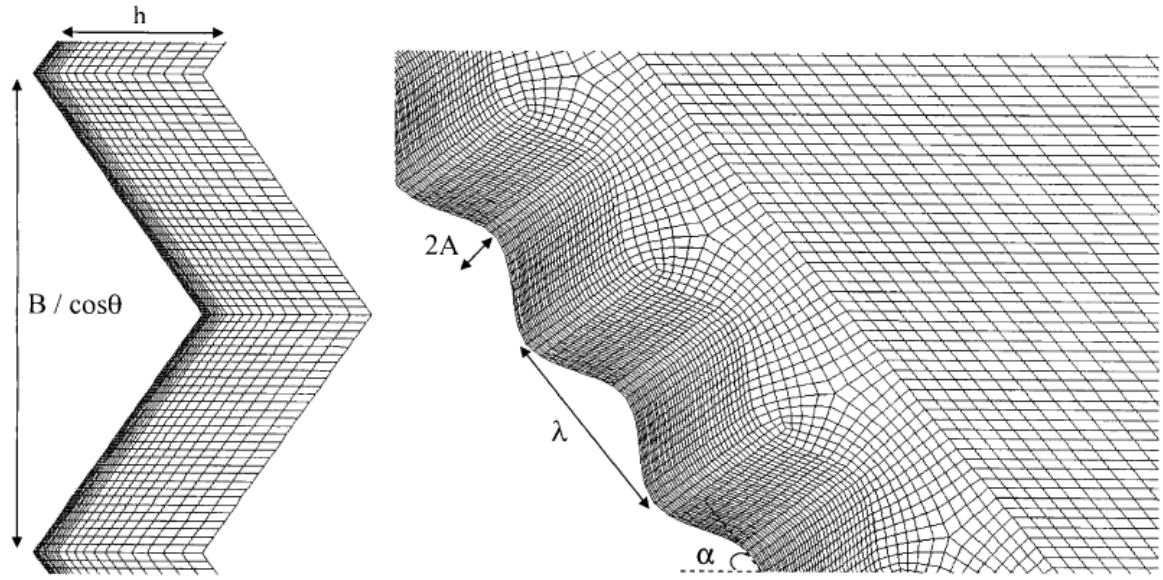

Figure 2.2: *Triangular and wavy surface texture patterns simulated by CFD in two dimensions (Raynal & Royon-Lebeaud 2007)*

The results obtained with the wall texture are in closer agreement with the experimental values than the results for the smooth wall. Discrepancy between experiments and between the film thicknesses obtained by both surface textures was found inevitable. Also, an analysis of the velocity field inside the liquid film had shown recirculation zones at the valleys of the corrugation. All these results had shown the authors that the higher liquid hold-up obtained in the simulations with rough walls compared to smooth walls is due to the presence of liquid in the valley regions and was useful in understanding the difference in the liquid holdup of smooth versus textured structured columns. The appearance of those recirculation zones suggests the occurrence of two different components that added to one another result in the total liquid hold-up: the static and the dynamic liquid hold-up. Later, Zakeri et al (Zakeri et al. 2012a) also suggested the appearance of the static and dynamic components. They defined the static liquid hold-up as the amount of liquid phase that cannot be renewed with the flow since it remains stuck at corners and dead spots.

The 2D approximation used presents a clear disadvantage of underestimating the liquid maldistribution that can occur in 3D simulations. This is so because the geometry of the domain itself can vary depending on the cross-section considered on the packing. Also, 2D simulations use strict counter-current flow inside the domain whereas a complicated combination of co- and counter-current flow regimes actually takes place

in a complex geometry such as a structured packing, with channels forming a particular angle with the vertical and between confronted channels belonging to different metallic sheets. To overcome the drawbacks presented by 2D simulations, Zheng et al (Zheng et al. 2013) studied the flow in an entire channel. The study is a first approximation to the development of an interface tracking model at meso-scale, but with a focus on hydrodynamics, analyzing liquid film thickness and pressure drop by not considering the actual repeating pattern in the packing.

Other works at small-scale includes CFD simulations of the liquid film formation over an inclined metallic plate. For instance, Iso et al (Iso et al. 2013) analyzed the wetting regimes achieved in the experiments as a function of the liquid load and concluded that the amount of area of the plate covered by the liquid depends on Weber number which is a function between gravity and the surface tension. According to the authors, large values of the Weber number result in a better liquid spreading whereas the interfacial area tends to the minimum energy state when surface tension prevails over gravity, resulting in the formation of round structures such as rivulets. Surface textures were found to help in avoiding the fluid channeling and increasing the amount of area available to produce mass transfer. The authors, in this work, also conducted an experiment analysis at pilot scale to check whether or not the assumption of including a particular texture on the surface of the packing could improve the CO_2 separation performance. The experiments confirmed the hypothesis of a better absorption rate for the textured pattern.

The liquid maldistribution phenomenon due to the prevalence of adhesive forces over cohesive forces is therefore found to be the most important flow characteristics that can be clearly observed at 3D small-scale CFD simulations. A significant amount of work has been found in the literature (Fourati et al. 2012; Aferka et al. 2011; Janzen et al. 2013) dealing with the visualization of the irregular distribution of liquid within the plate by measuring the liquid hold-up and the liquid spreading with gamma-ray, neutron radiography and X-ray tomography. The occurrence of liquid maldistribution was also tested by Oluji´c and Jansen (Olujić & Jansen 2015) , who support the fact that surface tension is a key factor in the distribution of liquid over a packing material.

The small-scale numerical studies described above had been focused mainly on the hydrodynamics and the tracking of the gas-liquid interface. It can be clearly observed that the small-scale analysis itself is adequate to implement reactive

absorption and to test its effects inside the liquid film by contrast with the implementation of chemical reactions that has been already observed at large-scale .However the number of works in relation to the reactive mass transfer at small or meso scale area few. It can be due the difficulty in the localized measurement of concentration distribution and film thickness at micro scales where as at large scales it is easier to measure the gas liquid concentrations at inlet and outlet of the reactors.

One of the preliminary works regarding the micro-scale reactive mass transfer was carried by Hu et al., (Hu et al. 2014) . They found that the interfacial mass transfer is a dependent of the vorticity in the vicinity of the interface. They also found that there exist two types of vortices, wall bounded vortices and interfacial vortices which can highly influence the reactive mass transfer of CO_2. Others attempts include the modeling of reactive mass transfer in a vertically falling film by Haroun et al (Haroun et al. 2010), direct numerical simulation of inter phase heat and mass transfer in evaporating flows by Haelssig et al (Haelssig et al. 2010) and Micro scale CFD modeling of reactive mass transfer in falling films by Sebastia-Saez et al. (Sebastia-Saez et al. 2014) and experimental and CFD studies on the effects of surface texture on liquid thickness, wetted area and mass transfer in wave-like structured packing by Yu et al., (Yu et al. 2018) . The first two are limited to two dimensional analyses and thus doesn't include the effect of liquid maldistribution on mass transfer. In their work, the authors present an analysis of the concentration profiles within the liquid film for a generic second order chemical reaction. The influence of the Hatta number and the contact time between the phases is observed in the results obtained. The concentration profiles obtained were classified into three regimes: one with an enhancement factor approximately equal to one, where the occurrence of the chemical reaction has no effect on the absorption rate; a second regime with a behavior comparable to a first order reaction, hence the name pseudo-first order regime; and a third regime in which the enhancement factor is higher than one but does not vary with the Hatta number anymore.

The later studies were on the 3D surface with and without surface textures on the mass transfer of O_2, but with the size of the surface texture fixed. In their studies, the mass transfer modeled as a source term which is a product of the mass transfer coefficient, derived from two film theory (Higbie 1935a), and the concentration gradient, where in which the concentration at the gas-liquid interface was calculated as a

fixed constant from the Henry's solubility law . The later studies clearly emphasized a need of detailed analysis to study the influence of geometric parameters of surface textures on liquid maldistribution and CO_2 mass transfer.

2.2.2 Meso-scale modeling

Modeling and analysis of dry and wet pressure drop has been the main aim of meso-scale studies. The use of representative elementary units (REU) results in the same pressure drop per unit length which is obtained by using full length column (Said et al. 2011; Petre et al. 2003; Hosseini et al. 2012; Li et al. 2016; Fernandes et al. 2009; Armstrong et al. 2013; Owens et al. 2013; Ding et al. 2015; Sebastia-Saez et al. 2014; Lautenschleger et al. 2015). The pressure drop in general is calculated in analogy with Darcy-Weisbach equation (Brown 2002) which predicts the pressure drop as a function of friction factor. The friction factor coefficient is obtained by curve fitting the experimental data and is many times unique to the geometry under evaluation.

Petre et al (Petre et al. 2003) presented the different types or REUs that can be observed in Figure 2.3. The most used REU is the one shown in Figure 2.3a, which corresponds to the bulk of the packing, being the others a representation of the geometries found near the column walls, below the liquid distributor at the top part of the column, etc.

Li et al (Li et al. 2016) has proposed a simple REU of the Figure 2.3(a), which is similar to the REU model proposed by Hosseini et al (Hosseini et al. 2012) , as shown in the Figure 2.4. In the current thesis, this model of REU was used for meso-scale analysis.

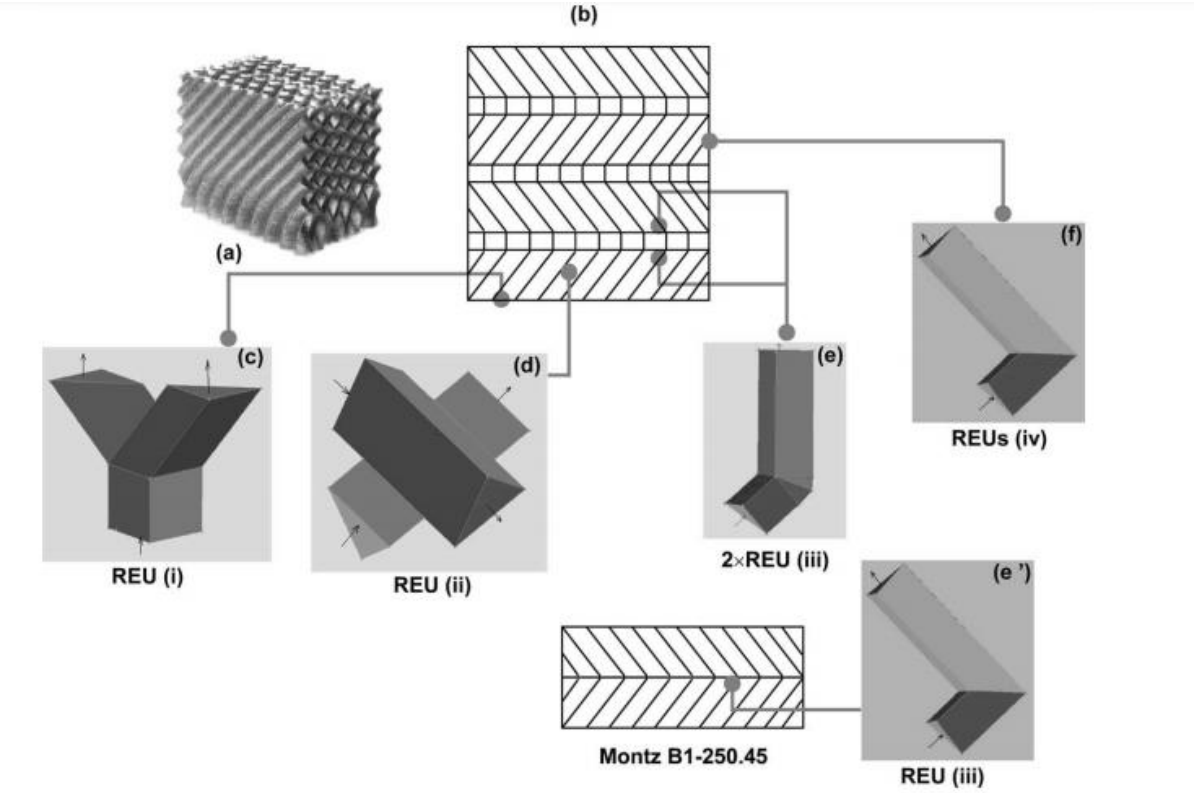

Figure 2.3: *Typical REUs approximating corrugated-sheet structured packings.* **(a)** *Montz B1-250 M;* **(b)** *Montz B1-250.45/B1V;* **(c)** *entrance region REU (mechanism i);* **(d)** *criss-crossing junction REU (mechanism ii);* **(e and e')** *interlayer transition REU (mechanism iii);* **(f)** *channel-wall transition REU (mechanism iv).*

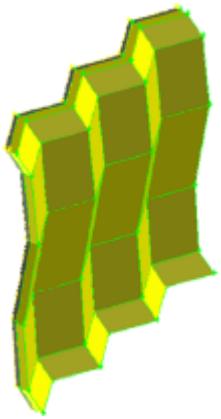

Figure 2.4: *Meso-scale 3D computational model (Li et al. 2016)*

Majority of the work reported in the open literature in regard of pressure drop has been experimental. Correlations were derived which are case specific and are available in abundant (Zivdar et al. 2006; Zakeri et al. 2012b; Rix & Olujic 2008; Li et al. 2016). The dry pressure drop can be derived as a sum of two components: the drag component and friction component. The drag component is due to the resistance offered by column walls and the transition regions between the packing sheets whereas the friction component is due the resistance offered by porous metallic packing sheets. It is observed that in the structured packing beds the frictional resistance is dominant when compared with the drag component of the pressure drop.

Said et al (Said et al. 2011) studied the pressure drop due to the friction term in a reduced number of REU and established a correlation for the pressure drop as a function of the dimensions of the packing itself. The influence of several turbulence models was also assessed. Boccardo et al (Boccardo et al. 2015) presented a new methodology, which according to authors, that is effective in terms of time and computational resource. The geometry is reproduced with the open source computer graphics code BlenderTM allowing users to build more complex geometries. The methodology is applied to the prediction of the void fraction inside the bed and the dry pressure drop. Recently Li et al (Li et al. 2016) studied dry and wet pressure drop for the effect of angle of inclination of corrugations of the structured packing and obtained the pressure drop as a function of kinetic energy of the gas. The authors have compared their results with commercial Mellapak 125X packing series. The authors have also studied the effect of pressure drop for wave type surface texture that was built by their own research group. Figure 2.5 depicts a typical pressure drop as a function of square root term of kinetic energy of gas. Since a square root term of gas is involved non linear behavior can be seen. This term is usually referred as F-factor in literature.

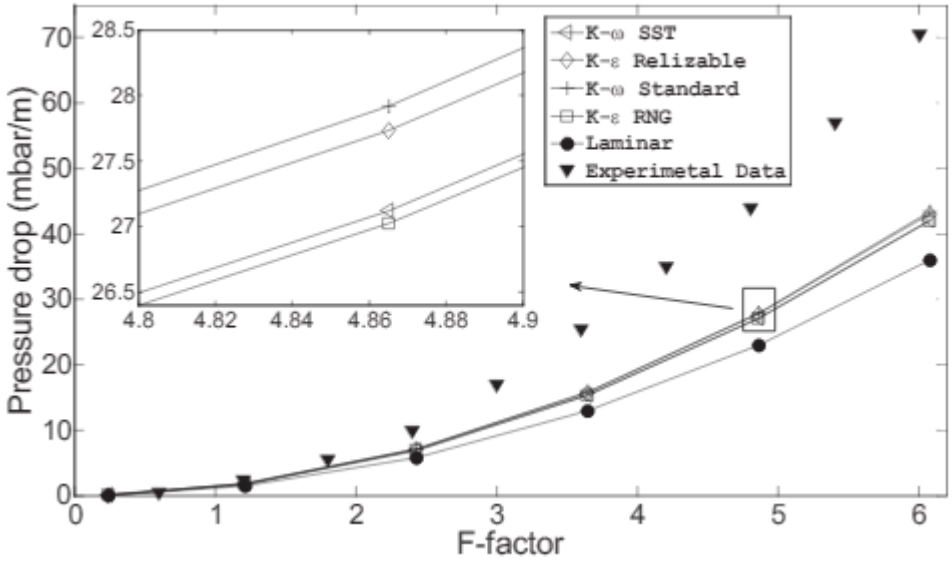

Figure 2.5 : *Pressure drop vs F-Factor in High capacity structured packing simulated for various turbulence models (Amini et al. 2016)*

Wet pressure drop is generally obtained using empirical correlations which are used to correct the dry pressure drop. The wet pressure drop is always higher than the dry pressure drop. The higher value is due the reduction in the area available for gas flow due to the presence of the liquid film which enhances the gas phase velocity locally. Alternatively the wet pressure drop is calculated by the widely accepted procedure (Sebastia-Saez et al. 2014; Li et al. 2016) suggested by Fernandes et al (Fernandes et al. 2009). The procedure involves simulating the wet pressure drop by solving a pseudo-single gas phase simulations using corrected velocity value calculated for the liquid holdup values of the respective structured packing columns. This procedure was adopted in the current thesis for calculating the wet pressure drop for structured packing columns at meso-scale simulations.

The assumption in the Fernandes et al is fully developed film flow which was found inadequate as the liquid maldistribution effects are neglected (Sebastia-Saez et al. 2014) . Sebastia-Saez et al (Sebastia-Saez et al. 2014) found that the wet pressure drop values need to be corrected by appropriately calculating the liquid hold up values, especially in case of liquid maldistribution, in order to find the corrected gas velocity values. They have suggested that the liquid holdup be computed as a function of liquid volume fraction to computational grid cell volume. However the simulations carried by Sebastia-Saez et al (Sebastia-Saez et al. 2014) were confined to structured packing with plane corrugation sheets. In the work carried by Li et al (Li et al. 2016) with wave type

surface textures averaged liquid film thickness was extracted from 2D simulations and used for calculating the wet pressure drop . They haven't considered the procedure suggested Sebastia-Saez et al (Sebastia-Saez et al. 2014) for calculating the liquid hold up using additional computational code.

In conclusion it can be clearly seen from the literature that there is a gap in terms of research at the meso-scale level in terms of including the detailed effect of surface textures on the pressure drop by considering the effects of liquid maldistribution in detail. In this thesis the effect of surface textures on the liquid hold up value are calculated by the procedure suggested by Sebastia-Saez et al (Sebastia-Saez et al. 2014) and pressure drop values were calculated for the REU model. The hold-up was calculated by writing and integrating appropriate code into the existing code of OpenFOAM. Details are given in Chapter 7 and Chapter 8 of this thesis.

2.2.3 Large scale modeling

As explained in previous sections, the liquid holdup play dominant role in the overall performance of structured packing columns. It directly influences the pressure drop which is one of the cost effecting parameters in the post-combustion CCS facilities. The studies in regard to pressure drop have been confined mostly to small and meso-scale due to the computational expenses required utilizing the VOF tracking methods at large scale domains. However there are attempts in the literature to use CFD by representing the gas-liquid flow by Eulerian two fluid model where the two phases are assumed interpenetrating and thus the effect of interface is captured inadequately. In this regard, Fourati et al (Fourati et al. 2012) expanded their study with gamma-ray tomography taking a correlation used by Lappalainen et al (Lappalainen et al. 2009) to predict the variation of the liquid hold-up as a function of the viscosity. Figure 2.6 shows the results obtained in the experimental work from the authors (Fourati et al. 2012).

Each horizontal series of images represents the liquid dispersion found in cross sections of the Mellapak 250X packing at different heights. The liquid load value was kept constant and horizontal series of images were taken for different value of the F-factor. The images from left to right are obtained at equal distance from top to the bottom of the column. It can be seen how the liquid is better distributed at the downstream of the column. In conclusion, the agreement of their simulations with the

experimental work is good but there is still some difference between them. In their discussion the authors state that the dispersion of the liquid within the packing is caused majorly by two mechanisms: capillarity and advection. In general both the effects are neglected in the porous medium approach. As a result, differences exist between the CFD and experimental results. The research reported at large-scale clearly shows the importance of the development of appropriate closures at lower scales.

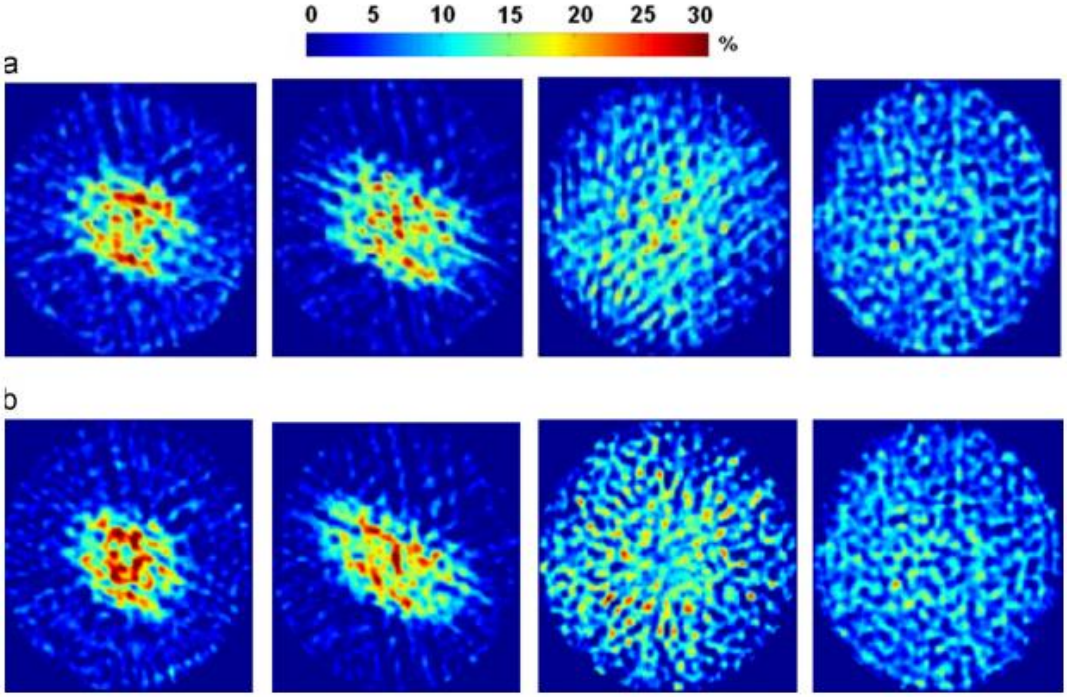

Figure 2.6: *Liquid hold-up maps obtained by tomography for two runs with air and water in Mellapak 250.X (Fourati et al. 2012)*

2.2.4 Interconnection between different scales

The major purpose of utilizing multi-scale approach is to simulate the industrial scale packed bed absorbers. The goal is achieved by deriving the relation between pressure drop and kinetic energy, overall mass transfer rate between gas-liquid phases and rate of CO_2 absorption at small scales and utilizing the outcome as a source terms in the porous medium approach. Many works are carried in this direction (CHEN et al. 2009; Iliuta et al. 2004; Rahimpour et al. 2013).

Some of the noticeable works in this regard are carried by Pham et al (Pham et al. 2015) and Asendrych et al (Asendrych et al. 2013). In both works large scale porous resistance modeling was used effectively for modeling the CO_2 absorption. The effect of liquid phase on pressure drop were included using models developed by other works like Fourati et al (Fourati et al. 2012) , as source terms. The effect of liquid holdup and interfacial area were included using model developed by Tsai et al (Tsai et al. 2009). Species concentration was solved as an additional scalar which does not affect the net momentum of the gas or liquid phase. Their results were able to produce the gas phase outlet concentration with greater accuracy but details like concentration distribution within liquid film region of the bed weren't predicted in detail. The works clearly suggests the necessary of small-scale modeling as a primary requirement for enhancing the accuracy of the large scale modeling.

Another example of interconnection between scales has been presented by Yu et al (Yu et al. 2018). Their work involves simulating the gas liquid flow with mass transfer at lower scales and deriving the liquid holdup and interfacial area. The results were then used in deriving the effective velocity of gas phase in the presence of liquid film, as suggested by Fernandes et al (Fernandes et al. 2009) for calculating the wet pressure drop of packed column .

Apart from this, the large scale simulations are flexible in coupling with 0D or 1D models derived from process simulations. The work of Brinkmann et al (Brinkmann et al. 2014), Fei et al (Fei et al. 2015), and Edge et al (Edge et al. 2013) deal with this co-simulation approach.

2.3 Influence of Surface Texture on Mass Transfer in Structured Packing Columns

Since the aim of the thesis is to study the influence of surface textures on CO_2 absorption, a brief note of the various works carried in this regard are presented here.

One of the most important parameters which can influence the overall performance of the structured packing is the micro texture patterns, often referred as surface roughness, on the corrugated sheets (Yu et al. 2018; Kohrt et al. 2011). Majority of the research till date was confined to study the hydrodynamics of the single phase and two-phase (gas-liquid) flows on micro texture patterns. The patterns in all these investigations were comparable to the texture pattern size of commercial Mellapak series. The first of this kind of investigations about the influence of amplitude of

periodic microstructure on liquid film thickness were carried by Zhao and Cerro (Zhao & Cerro 1992). In their experiments, the film thickness enhancement was studied for Nusselt film thickness to amplitude ratio ranging from 0.1 to 1.

The mass transfer analysis of the texture patterns is very scarce. Kohrt et al. (Kohrt et al. 2011)studied the influence of micro texture on the liquid side mass transfer of CO_2 into silicon oil. The texture patterns used in their investigation were unidirectional transversal waves and bidirectional pyramidal structures of the size comparable to the texture size of Zhao and Cerro (Zhao & Cerro 1992)experiment as shown in Figure 2.7. They found the textures enhanced the mass transfer by almost 80%. Yu et al. (Yu et al. 2018) investigated the mass transfer of O_2 into the water for wavy texture pattern developed by Li et al. (Li et al. 2016) and found the enhancement in the mass transfer by 20%. They have clearly pointed a need for detail CFD based investigations to study the impact of surface roughness on mass transfer.

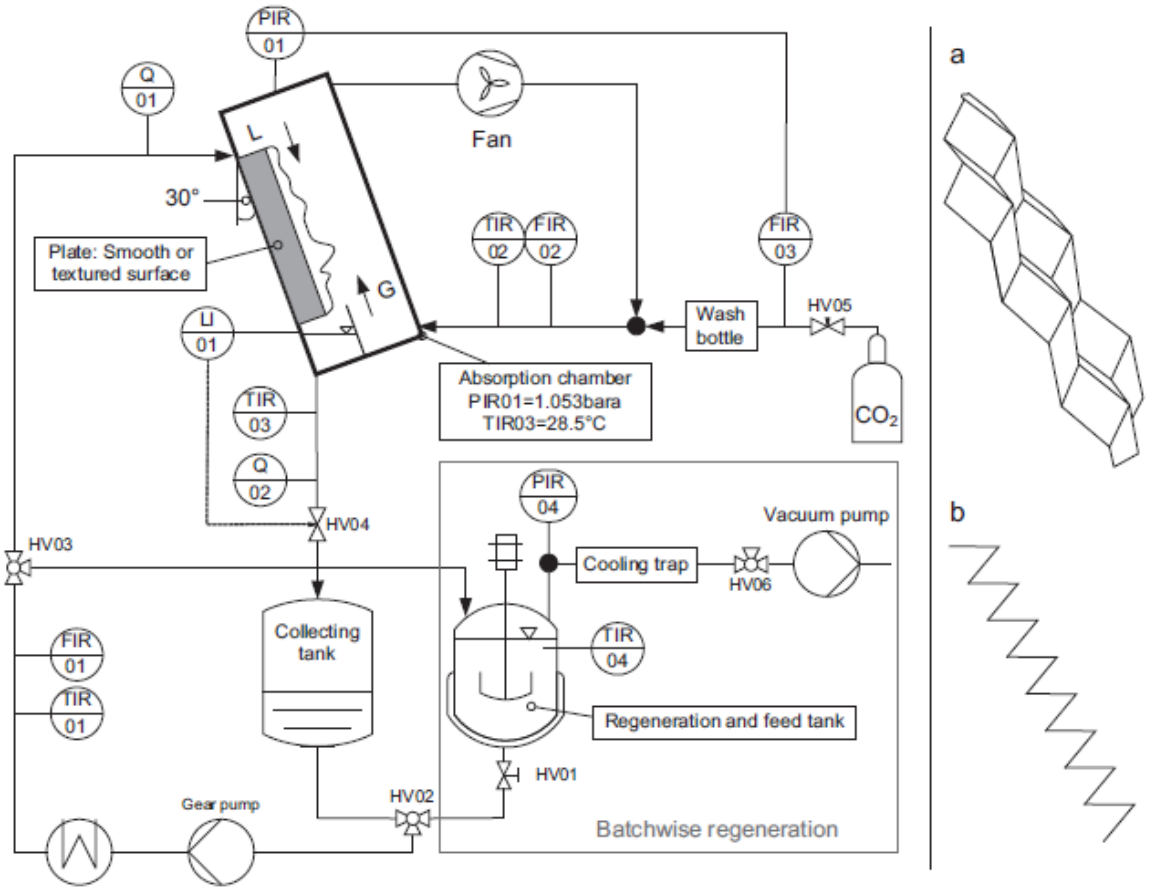

Figure.2.7: *Experimental setup used by Kohrt et al (Kohrt et al. 2011) with* **(a)** *bidirectional (bd-type) and* **(b)** *unidirectional (ud-type) textures*

2.4 CFD Modeling of Physical and Reactive Mass Transfer of CO_2 into MEA

This section briefly introduces various approaches used in CFD modeling of the physical and reactive mass transfer across immiscible phases. The review helps in choosing an appropriate model for effectively modeling the mass transfer across immiscible phases.

Majority of the research in relation to the reactive mass transfer was initially focused on the mass transfer aspects. One of the first investigations in this topic was realized by Ohta and Suzuki (Ohta & Suzuki 1996) who studied the mass transfer from a drop in a solvent extraction process by coupling mass transfer with volume of fluid method (VOF). Later, Sato et al. (Sato et al. 2000) have simulated the three dimensional single droplet flows with mass transfer in continuous phase with different Schmidt numbers using front- capturing method. Davidson and Rudman(Davidson & Rudman 2002) described a volume of fluid (VoF) numerical algorithm for calculating advective and diffusive heat and mass transfer in fluids with interfaces. However, these investigations were restricted to the case where the species concentrations on both sides of the interface are continuous(without considering thermodynamic dissolution equilibrium).More recently, by considering thermo- dynamic equilibrium of chemical species concentration on both sides of the interface, Bothe et al., (Bothe et al. 2004) performed numerical simulations of the mass transfer of oxygen from single bubbles and bubble chains rising in aqueous solutions with volume of fluid method. With the same method, Onea (Onea 2006) studied interfacial mass transfer in a bubble train flow with in square and rectangular mini-channels. The numerical algorithm employed to transport local concentration is based on continuum mechanics. The solubility of chemical species at the interface is determined by Henry's law with constant coefficient. The treatment of jump discontinuity of concentration is computed with special modeling by considering a new scalar. With this procedure, possible numerical difficulties which might appear when concentrations are discontinuous at the interface are avoided. However, a significant drawback of this transformation is that the local diffusive mass flux across the interface is not continue, which makes its calculation difficult in order to obtain the interfacial mass transfer. To satisfy this later condition, the diffusion coefficient of the gas phase is locally replaced by a ratio of diffusivity to Henry's constant in the interface region. This would make the diffusivity in the interface region significantly different from physical diffusion that may product significant differences

with the real case. On the other hand, Yang and Mao (Yang & Mao 2005) simulated mass transfer from a droplet moving in a continuous immiscible liquid with level set method. The concentration field over the computation domain is solved according the one-fluid approach and the jump discontinuity of concentration is computed with a special transformation of the concentration, by considering a new scalar that corresponds to the product of Henry's constant to the concentration of specie in the each phase. The purpose of this transformation is to make the transformed concentration continuous at the interface. However, to satisfy the condition of mass flux continuity at the interface and make the diffusivity in the interface region equal throughout a fluid phase, several parameters as local velocity and diffusivity are transformed. This leads to additional difficulties and make the method complex to use.

At the same time, even though significant efforts have been made to model the interfacial mass transfer, only few numerical studies have considered mass transfer with simultaneous fast chemical reaction, or reactive mass transfer. One of the approaches used in this regard involves modeling reactive mass transfer across the immiscible phases by explicitly adding source terms to the governing equations of VOF approach. Sebastia-Saez *et al* ., (Sebastia-Saez et al. 2014; Sebastia-Saez et al. 2015b; Sebastia-Saez et al. 2013) modeled physical and reactive mass transfer on flat and texture plates by this approach. A similar approach was used by Xu et al., (Xu et al. 2009) for modeling the mass transfer of propane gas into toluene liquid. This kind of approach involves utilization of parameters derived from standard correlations like Higbie (Higbie 1935a) correlation which can under/overestimate the effect of local velocity fluctuations that can influence mass transfer significantly.

Haroun et al (Haroun et al. 2010) proposed a "one fluid formulation" approach which is different from all the previous approaches (Yang & Mao 2005; Onea 2006; Sebastia-Saez et al. 2015b; Bothe et al. 2004). Later on it was used in detailed numerical simulation of (direct numerical simulation, DNS) structured packing sheet also to derive mass transfer and liquid hold up in structured packing element by same group. The group of Haroun used JADIM multiphase software developed by IMFT (Legendre & Magnaudet 1998). Nieves-Remacha et al ., (Nieves-Remacha et al. 2015) implemented this one fluid formulation for simulation of mass transfer in an industrial advanced flow reactor. A similar approach was developed by Marschall et al.(Marschall et al. 2012) and was implemented in OpenFOAM for mass transfer in gas liquid bubble

flow. In Nieves-Remacha(Nieves-Remacha 2014) dissertation thesis, the two formulations of Haroun et al (Haroun et al. 2010) and Marschall et al.(Marschall et al. 2012) were compared and found to be producing same steady state results for various simple test cases. Recently, Wang et al. (Wang et al. 2017) used this approach for simulating the gas liquid mass transfer in wetted wall column. They found the CFD results in reasonable agreement with the experimental values. In the current thesis this "one fluid formulation" was implemented in OpenFOAM to study the influence of surface textures on the reactive mass transfer in structured packing.

2.5 Modeling of Physical and Reactive Mass Transfer of CO_2 into MEA

Since the modeling involves kinetics of CO_2 with MEA (*Mono-Ethanol-Amine*) and the results obtained involve comparison with traditional correlations available in literature, a brief review of the theories available in this regard are presented here. This section is divided into two sections:

1. Physical mass transfer
2. Reaction kinetics

2.5.1 Physical mass transfer

Different approaches have been reported in the literature for the description of the interfacial mass transfer that takes place during the absorption process. All of them assume unidirectional diffusion. The most utilized option in validation of CFD modeling has been the penetration theory due to its suitability to describe transient systems:

- The two-film model (Lewis & Whitman 1924):

  This model assumes that a stagnant film with a finite thickness exists at both sides of the interface, for the liquid and the gas, respectively. Mass transport takes place under steady state conditions within this film via diffusion mechanisms whereas convection is negligible. Outside the film complete mixing of the species occurs, eliminating any concentration gradient within.

- The penetration theory (Higbie 1935b):

  This theory assumes that the diffusion of the gas into the film is an unsteady process by the random motion of the solute molecules. This theory is more suitable for the validation of present simulations, especially for simple cases, since the mass transfer is described as a transient process. A brief

description of mathematical formulation of this theory is described in the mathematical modeling section of this report.

- The surface renewal model (Danckwerts 1979):

  This model was presented as an extension for Higbie's penetration theory and the main difference lies in the fact that the contact time is not the same at every moment, but it follows a distribution function. Perlmutter (Perlmutter 1961) reviewed this theory considering eddy residence time distributions and other aspects such as transient interfaces, changes in the value of the diffusivity near the interface, dead zones in which local laminar flows are developed and multiple capacitance effects.

  In the current thesis Higbie theory is used to compare the results obtained for physical mass transfer analysis.

2.5.2 Reaction kinetics

Investigations about using reactive absorption for removal of pollutants from post combustion exhaust gases had started in the early 19th century (1930). It is a matured technology that can be easily integrated into the existing power plants with a little extra cost (Rochelle 2009). The advantage of reactive absorption lies in effective removal of pollutants which are generally present at low concentrations in the exhaust gases. Even though there is huge research carried for developing new solvents for CO_2 absorption (Perinu et al. 2017; Bernhardsen et al. 2017), reactive absorption by blends of MEA is considered as an attractive option (Mangalapally et al. 2012; von Harbou et al. 2013; Halim et al. 2015; Zhang et al. 2017). Monoethanolamine (MEA) is widely used as the reference to compare new mixtures and solvents (MacDowell et al. 2010).

CO_2-MEA system involves a sequence of finite rate and instantaneous chemical reaction. Out of all the reactions, the formation of carbamite with MEA is considered as the rate controlling step. The carbamite of MEA formed in absorption column is stripped into pure CO_2 and solvent in regeneration column. Thus designing the absorption and regeneration column, a full cycle of removing pollutants from fuel gas, needs the finite rate chemistry to be considered in detail. But from CFD modeling point of view addition of each individual species to modeling equations can add more computational effort. Thus utilizing a condensed form of chemistry with lowest number of possible reactions must be preferred over a detailed chemistry.

Currently there are two familiar theories describing the mechanism of reaction between CO_2 and MEA [Vaidya and Eugeny, 2007]:

- **Zwitterion mechanism**

  The zwitterion mechanism was first introduced by Caplow (Caplow 1968) and reviewed later by Danckwerts (Danckwerts 1979). This mechanism is based on the existence of an intermediate step in which a dipolar molecule called zwitterion is formed. Subsequently, the zwitterion is deprotonated by a base, which can be either water, or the hydroxyl ion or the amine itself. The following reactions describe the formation, i.e. equation (2.1), and the deprotonation of the zwitterion to give the carbamate, i.e. equation (2.2). Both reactions can be expressed as:

  $$CO_2 + RNH_2 \rightarrow RNH_2{}^+COO^- \quad (2.1)$$

  $$RNH_2{}^+COO^- + B \rightarrow RNHCOO^- + BH^+ \quad (2.2)$$

- **Termolecular mechanism**

  The termolecular single-step mechanism skips the intermediate step by which the formation of the zwitterion takes place (Crooks & Donnellan 1989). Therefore, the chemical reaction can be written as:

  $$CO_2 + H_2O^+RNH_2 \rightarrow RNHCOO^- + H_3O^+ \quad (2.3)$$

  Versteeg et al (Versteeg et al. 1996) have supported the formation of zwitterions mechanism, but predicted the first step of the mechanism, i.e. equation (2.1), to be the rate limiting step. Also Versteeg et al (Versteeg et al. 1996) suggested a second order reaction rate for this step. Astarita et al (Giovanni Astarita ,David W. Savage 1983) suggested that the MEA carbamate's stability as given in equation (2.3) is very stable when compared with other intermediate ion formation. Wang et al (Wang et al. 2017)used the single step formation of the carbamate ion formation, similar to equation (2.3) as suggested by Astarita et al (Giovanni Astarita ,David W. Savage 1983), for modeling the reaction of CO_2 with MEA. The overall reaction is given as:

  $$CO_2 + 2RNH_2 \rightarrow RNHCOO^- + RNH_3{}^+ \quad (2.4)$$

In this thesis the single step formulation, equation (2.4), as given by Wang et al (Wang et al. 2017) is used for modeling the reactive mass transfer of CO_2 into MEA.

3. MATHEMATICAL THEORY

In this chapter, based on the project's objectives and the literature review, a description of the applied mathematical models is presented in the form of conservation equations and their source terms. The first section of this chapter describes conservation equations of mass and momentum followed by the interface capturing technique of two-phase laminar flows. The major differences between the interface capturing approaches among the available CFD software is highlighted in this section. The chapter follows a brief introduction to the modeling of the surface tension force acting on the surface of the film in contact with the gas. Since the scope of the thesis also includes meso-scale pressure drop analysis, a brief introduction to the various turbulence models evaluated in regard of structured packing columns is presented and the model used in the current thesis is presented in detail. Finally this section closes with the details of mathematical modeling of one fluid formulation for reactive mass transfer along with the validation of the developed code.

3.1 Two Phase Conservation Equations

Since the information about discretization techniques and associated finite volume theory is a vast and evolving subject area, providing all the details here will result in voluminous enhancement of the thesis. Thus the present thesis is confined to describe theory of high relevance to the present work and further information on the basic finite volume theory and multiphase flow can be found in the relevant open literature and from standard text books (Versteeg & Malaskekera 2007; Yeoh & Tu 2010) .

Two phase flows involve a moving interface between the phases, and the flow domain is divided into two separate regions by this interface. The presence of this interface enhances the complexity of the computational problem. In this thesis a one fluid formulation is used to describe the two phase flow. This one-fluid formulation takes into account the entire fluid flow domain as a single-phase flow field with varying thermo-physical properties across the interface. The single-phase governing equations are solved for each phase with additional source terms such as the surface tension force at the interface and the appropriate boundary conditions. The source terms must be incorporated into the governing equations in order to describe the interaction between

the gas and liquid phases (Jagannath 2015). In the current thesis the governing equations are solved for mass and momentum conservation assuming the operating temperature as constant and fluids flowing to be immiscible and incompressible. Also, Volume of Fluid (VOF) (as described in Section 2.1) method, initially developed by Hirt and Nichols (Hirt & Nichols 1981) is employed to track the interface between the two immiscible phases. A brief overview of the VOF formulation with a description of one-fluid formulation is provided in Section 3.2.

3.2 VOF Formulation

In the conventional VOF method (Hirt & Nichols 1981) , the transport equations for and indicator function, representing the volume of fluid fraction of one phase, is solved along with the mass and momentum conservation equations as given below (Equations 3.1,3.2 & 3.3):

$$\nabla . \mathbf{U} = 0 \tag{3.1}$$

$$\frac{\partial \gamma}{\partial t} + \nabla . (\mathbf{U}\gamma) = 0 \tag{3.2}$$

$$\frac{\partial (\rho \mathbf{U})}{\partial t} + \nabla . (\rho \mathbf{U}\mathbf{U}) = -\nabla p + \nabla . \mathbf{T} + \rho \mathbf{f}_b \tag{3.3}$$

where **U** represents the velocity field shared by the two fluids throughout the computational domain, γ is the phase fraction, **T** is the deviatoric viscous stress tensor $\mathbf{T} = 2\mu\mathbf{S} - 2\mu(\nabla . \mathbf{U})\mathbf{I}/3$, with the mean rate of strain tensor $\mathbf{S} = 0.5[\nabla \mathbf{U} + (\nabla \mathbf{U})^T]$ and $I = \delta_{ij}$, ρ is density, p is pressure, f_b are the body force per unit mass. In VOF formulation the f_b includes the body forces and surface tension forces. The phase fraction γ can take values between the range of [0, 1], with the value of zero and one corresponding to the regions accommodating only one phase. Generally γ=0 is referred as gas and γ=1 is referred as liquid region. The gradients of the phase fraction occur only at the interface region. Since the two immiscible fluids are considered as one effective fluid throughout the domain, the physical properties are calculated as weighted averages of the γ as shown in Equations 3.4 and 3.5. Thus the properties will be equal to the actual values of the pure fluids in the regions of γ with unique value of zero or one and possess mixed values at the vicinity of interface.

$$\rho = \rho_L \gamma + (1 - \gamma)\rho_G \tag{3.4}$$

$$\mu = \mu_L \gamma + (1 - \gamma)\mu_G \tag{3.5}$$

where the subscripts L & G represent the liquid and gas phase respectively. The major challenge in this kind of formulation is the assurance of the conservativeness of the phase fraction and modeling the advection of the phase fraction. Since the velocity field is shared between the two phases and solved by a single momentum equation, it is very difficult to estimate to what extent the advection of the phase fraction is influenced by each phase. Generally the advection of phase fraction is estimated in a two step process. First the phase fraction is advected based upon the net momentum from the grid cells in nearby regions and second the resulting phase fraction distribution is used to estimate the velocity distribution in the computational domain.

From the time of proposal of this VOF method (Hirt & Nichols 1981) for simulating the two phase flow, many variations of the VOF schemes were developed and incorporated into the leading CFD software. They may be divided majorly into two categories: geometric methods involving an explicit reconstruction of the interface from the volume fraction data, and algebraic methods making no such attempt (Roenby et al. 2017). Algebraic VOF schemes are generally much simpler to implement, more efficient and are not restricted to structured meshes. They are, however, founded on much more heuristic considerations and are not as accurate as the geometric VOF schemes (Deshpande et al. 2012) in representing the interface. Geometric VOF schemes, on the other hand, involve complex geometric operations making their implementation cumbersome and their execution slow (Maric et al. 2013; Roenby et al. 2017). They represent the interface accurately but at the same time, they can result in a very high phase fraction gradients across interface which can lead to numerical instabilities for complex geometries (Ahn & Shashkov 2007; Hernández et al. 2008; López et al. 2008; Ivey & Moin 2017; Xie et al. 2014). An integrated method of incorporating the advantages of geometric method into algebraic based algorithms is also developed and is referred as “level set” method (Dianat et al. 2017; Sussman 2003). But conservation of mass across the interface using this method needs usage of high-order schemes which are still under developed (Dianat et al. 2017). All these approaches are great areas of research with their own advantages and limitations.

Since the OpenFOAM involves algebraic VOF scheme and the aim of the current thesis is to utilize this software effectively, we proceed by utilizing the default "interFOAM" module available for simulating two phase flows. As suggested by Deshpande et al (Deshpande et al. 2012) a low time step and fine grid was utilized for simulating the computational domain to avoid the disadvantages of diffusing interface which is usually referred as "spurious currents". In the OpenFOAM an additional term referred as "compression velocity", derived based on the phase fraction conservation of the two phases is added in order to effectively capture the interface (Rusche 2002) . The basic VOF Equation 3.2 was modified to Equation 3.6 as follows:

$$\frac{\partial \gamma}{\partial t} + \nabla.(\mathbf{U}\gamma) + \nabla.[\mathbf{U}_r\gamma(1-\gamma)] = 0 \qquad (3.6)$$

where the Ur represents the relative velocity between the phases. One should note that the compression term, at the end of the Equation 3.6, refers to the term useful in sharpening the interface and it isn't related to compressible flow. The compression term is found active only within the interface region and vanishes at both limits of the phase fraction. Hence it does not affect the solution outside this region. Moreover, if free surface is defined in a theoretical sense as having an infinitesimally small thickness, the (relative) velocity Ur vanishes and the expression reduces to the conventional form.

3.3 Surface Tension Force Modeling

The surface tension forces constitute additional pressure force due to intermolecular attraction between the two phases flowing in a given computational domain and the adhesive force between the fluid and the solid surface. The surface tension force is found to minimize the interfacial area and highly influence the shape of resulting interface in structured packing columns (Sebastia-Saez et al. 2014). The influence of this force must be included in the body force term fb in the equation 3.3. The surface tension force, acting to balance the pressure difference in both the fluids on either side of the interface, is expressed by the Young-Laplace's formula(Wikipedia contributors 2017):

$$\Delta p = p_L - p_G = \kappa\sigma \qquad (3.7)$$

In the above expression, Δp is the pressure drop across the surface, κ is the mean curvature, and σ is the surface tension coefficient, which is defined as the amount of work necessary to create a unit area of free surface. Its value is always positive for

immiscible fluids and determined by the nature of the fluids. The mean curvature κ is defined by:

$$\kappa = \left(\frac{1}{R_G} + \frac{1}{R_L}\right) \tag{3.7}$$

where R_G and R_L are the principal curvature radii in orthogonal directions. Since the pressure is discontinuous at the interface Brackbill et al (Brackbill et al. 1992) proposed a Continuum Surface Model (CSF) to calculate the surface tension force acting normal on the gas liquid interface as a volumetric force . In this model, the pressure is expected to rise within the transitional region between fluids with the same smoothness as the indicator function γ.

In the CSF approach, the interface transitional area is divided into several layers according to the definition of indicator function γ. The surface tension force direction depends on the normal vector on the interface, and its magnitude depends on the interface curvature. The unit normal vector of each layer in the transitional domain is determined by the gradient of the indicator function γ. The interfacial curvature is then expressed in terms of the divergence of the unit normal vector from the interface as shown in the Equation 3.8

$$\kappa = \nabla . \vec{n} \tag{3.8}$$

where the normal vector $\vec{n}$ is defined as $\frac{\nabla\gamma}{|\nabla\gamma|}$. The effect of contact angle is included by correcting the normal vector by including the effect of contact angle θ between the liquid and solid surface as shown in the Equation 3.9:

$$\vec{n} = \vec{n}_{wall}\cos\theta + \vec{t}_{wall}\sin\theta \tag{3.9}$$

where the $\vec{n}_{wall}$ and the $\vec{t}_{wall}$ denotes the normal and tangential vectors to the wall respectively. The resulting additional source term by CSF model is given by Equation 3.10:

$$f_\sigma = \sigma\kappa\Delta\gamma \tag{3.10}$$

where the value of κ is derived from Equations 3.8 &3.9 respectively.

3.4 Pressure Drop Analysis in Structured Packing

Pressure drop constitutes the major part of the overall operational cost of a post combustion CCS facility. The calculation of pressure drop can be divided into two parts as the dry and wet pressure drop. The aim of the literature in regard of pressure drop analysis of structured packing column has been to evaluate the wet pressure drop (Li et al. 2016).

The procedure of calculating the pressure drop involves evaluation of the relation between the pressure drop and kinetic energy in a way similar to Darcy-Weisbach (Brown 2002) equation. The expression derived will be as given in the Equation 3.11:

$$\Delta p = \zeta_{total} \frac{\rho_g v_{g,eff}^2}{2} \tag{3.11}$$

where the ζ total represents the friction factor which is geometric specific and $v_{g,eff}$ is superficial gas velocity. For wet pressure drop the $v_{g,eff}$ is calculated to include the effect of the decrease in the available gas volume using the liquid holdup values as suggested by Fernandes et al (Fernandes et al. 2009) . The modified expression for $v_{g,eff}$ is given by Equation 3.12:

$$v_{g,eff} = \frac{v_g}{\varepsilon(1-h_l)\sin\varphi} \tag{3.12}$$

where the ε represents the voidage of the packed bed in the absence of liquid film, ϕ is the angle of solid surface with respect to the vertical direction. The h_l is called liquid holdup which is defined as the volume of liquid per unit volume of packing. The term ($1-h_l$) in the Equation 3.12 is responsible for including the effect of liquid film on the pressure drop. Since this term is denominator with a negative sign, it can be clearly seen that the effect of hl will be positive on the overall pressure drop i.e., an increase in h_l will result in increase of $v_{g,eff}$ and eventually increase in pressure drop. The most frequently used model to calculate the liquid hold-up inside the packing assumes that the liquid forms a perfectly developed liquid film that fully covers the packing wall. Under these conditions, the liquid hold-up can be calculated as the product of the specific area of the packing A_{spf} and the liquid film thickness δ_l as equation 3.13:

$$h_l = A_{spf}\,\delta_l \tag{3.13}$$

where the δ_l is calculated from the Nuseelt theory (Nusselt 1916) as Equation 3.14:

$$\delta_l = \left(\frac{3\mu_l}{\rho g \cos\varphi}\right)^{\frac{1}{2}} \tag{3.14}$$

Oluji´c et al (Olujić 1999) in their analysis has found that the turbulence in the gas phase contributes to almost 70% of the total pressure drop and it can be modeled by meso-scale analysis using CFD. The other 30% loss in pressure drop, referred as pressure loss due to drag, is due to the sharp bends between the columns and entrance region. These losses can be modeled by considering the full scale models which are computationally expensive. Li et al (Li et al. 2016) suggested to use RNG k-ε turbulence model (Yakhot et al. 1992) based on the works of Raynal et al (Raynal et al. 2013) for evaluating dry and wet pressure drops with reasonable accuracy. In this work the RNG k-ε turbulence model is used for dry and wet pressure drop analysis and an overview of the equations involved are briefed below. Detailed information about various turbulence modeling techniques and their derivations can be found from standard text book (Wilcox 2006).

The RNG model was developed using Re-Normalization Group (RNG) methods by Yakhot et al (Yakhot et al. 1992) to renormalize the Navier-Stokes equations, to account for the effects of smaller scales of motion. It is a modification of the standard k-epsilon (Launder & Spalding 1973) to account all scales of motion on turbulent diffusion. The governing equation for turbulence kinetic energy k is given by Equation 3.15:

$$\frac{\partial}{\partial t}(\rho k) + \frac{\partial}{\partial x_i}(\rho k u_i) = \frac{\partial}{\partial x_j}\left[\left(\mu + \frac{\mu_t}{\sigma_k}\right)\frac{\partial k}{\partial x_j}\right] + P_k - \rho\varepsilon \tag{3.15}$$

where turbulence viscosity μ_t is given by $\mu_t = \rho C_\mu \frac{k^2}{\varepsilon}$ and turbulence production term P_k is calculated as $P_k = -\rho\overline{u_i' u_j'}\frac{\partial u_j}{\partial x_i}$ and subscripts i, j stand for principle axis direction.

The last term ε refers to turblulence dissipation and is calculated by solving Equation 3.16:

$$\frac{\partial}{\partial t}(\rho\varepsilon) + \frac{\partial}{\partial x_i}(\rho\varepsilon u_i) = \frac{\partial}{\partial x_j}\left[\left(\mu + \frac{\mu_t}{\sigma_\varepsilon}\right)\frac{\partial \varepsilon}{\partial x_j}\right] + C_{1\varepsilon}\frac{\varepsilon}{k}P_k - C_{2\varepsilon}^{*}\rho\frac{\varepsilon^2}{k} \quad (3.16)$$

where constant $C_{2\varepsilon}^{*}$ is calculated by the expression $C_{2\varepsilon}^{*} = C_{2\varepsilon} + \frac{C_\mu \eta^3 (1-\frac{\eta}{\eta_0})}{(1+\beta\eta^3)}$. The constant η is estimated as $\eta = \frac{Sk}{\varepsilon}$ where S is given by $S = \left(2S_{ij}S_{ij}\right)^{\frac{1}{2}}$. Other constants in both Equations 3.15 and 3.16 generally possess fixed value as: $C_\mu = 0.09, \sigma_k = 0.7194, \sigma_\varepsilon = 0.7194, C_{\varepsilon 1} = 1.42, C_{\varepsilon 2} = 1.68, \eta_0 = 4.38, \beta = 0.012$.

3.5 Modeling of Reactive Mass Transfer by One Fluid Formulation

The one fluid formulation (Haroun et al. 2010) was implemented as an additional transport equation to model the reactive mass transfer between immiscible phases. The additional equation for the specie transport using this approach is given by Equation (3.17):

$$\frac{\partial \mathrm{C}}{\partial \mathrm{t}} + \nabla.(\vec{\mathrm{v}}\mathrm{C} - \mathrm{D}\nabla\mathrm{C} - \emptyset) - \mathrm{W_i} = 0 \quad (3.17)$$

The one fluid formulation solves a single transport equation for specie concentration across the two phases by treating the concentration as a function of phase fraction. The VOF involves the same approach for defining the flow properties like density and viscosity. The effect of concentration jump at the interface is included using the additional mass flux term ∅ . This additional mass flux is due to the solubility of gaseous specie into the liquid and thus can be calculated using Henry's law. The flux term ∅ modeled to include the solubility is given by the Equation (3.18):

$$\emptyset = -\mathrm{D}\frac{\mathrm{C}(1-\mathrm{H})}{\gamma+\mathrm{H}(1-\gamma)}\nabla\gamma \quad (3.18)$$

where D stands for the effective diffusivity of the specie in the two-phase mixture. The D is calculated as a harmonic average of diffusion of specie in each phase and is given by Equation (3.19):

$$\mathrm{D} = \frac{\mathrm{D_L}\,\mathrm{D_G}}{\gamma \mathrm{D_G} + (1-\gamma)\mathrm{D_L}} \quad (3.19)$$

where the DL and DG represent the diffusion coefficient of specie in liquid and gas phase respectively. The H in equation (3.19) represents the dimensionless Henry's constant for the specie under consideration. It is defined as the ratio of the concentration

of specie in gas (C_G) to the concentration of specie in liquid (C_L) which is $H = C_G/C_L$. Note that the additional flux term $\emptyset$ will have numerical values only at the interface and will be zero within the individual phases. This is because the $\nabla\gamma$ term in Equation (3.18) is essentially zero in grid cells fully occupied by individual phase fraction.

The last term W_i in the Equation (3.17) stands for rate of production of the chemical species. It is modeled as a product of reaction rate constant (r), concentration(C) and phase fraction (γ) as shown in Equation (3.18):

$$W_i = rC\gamma \tag{3.18}$$

The multiplication of the reaction term with the phase fraction γ helps in confining the reaction effect to the desired phase. In the later chapters the values of the constants used in the above equations are selected from open literature based upon the problem under simulation and hence are not re-written here to avoid repetition.

The concentration Equation (3.17) is implemented as an additional equation in the existing code of OpenFOAM module for two phase immiscible flows called *interFOAM*. Additional code was written for effective post processing of the results like: calculating the "film height" from the "bottom wall" over which the fluid is flowing. The code is presented in the **Appendix** at the end of the thesis. The code can be implemented using standard procedure of adding additional code into OpenFOAM as described in tutorial work that was created during the course work of the thesis and available in open literature (Prasad Thummala 2016). Also similar implementation of one fluid formulation can be found in the thesis work of Nieves-Remacha 2014 (Nieves-Remacha 2014) .

3.6 Validation

The term validation is the assessment of the credibility of a simulation model by estimating the degree to which this model is an accurate representation of reality from the perspective of its intended uses (Mehta 1998). The interFOAM module is well verified for flow over inclined plates by Cooke et al (Cooke et al. 2014; Cooke 2016). In their study, Adaptive Mesh Refinement (AMR) was effectively used to model film flow. Even though AMR was useful in predicting the film flow effectively the technique was found inadequate in producing the mass transfer data that is of importance to the

present thesis. The grid density used for simulating full and rivulet film , without AMR, was close to the values proposed by Xu et al (Xu et al. 2009; Hu et al. 2014).

Since the grid independency study for gas-liquid flow is well available in the literature it wasn't repeated here. The focus was confined on validating the additional reactive mass transfer equation (Equation 3.17). Since the validation case for mass transfer and reactive mass transfer studies were scarce, validation was carried for simple cases for which analytical results are available. Also comparison of overall mass transfer coefficient was carried with the available literature, Wang et al (Wang et al. 2017) . The reaction between CO_2-MEA was modeled as pseudo first order reaction (Sebastia-Saez et al. 2015b) and the resulting enhancement in mass flux transfer rate was compared with the theoretical expression of Enhancement factor.

3.6.1. One-Dimensional Mass transfer

As suggested by Haroun et al (Haroun et al. 2010) the one dimensional mass transfer can be validated against an exact numerical solution. The analytical solution is available for one dimensional gas liquid diffusion problem where the two phases aren't flowing. The exact steady-state solution for the concentration along the x-axis is given by:

$$C_L = \frac{C_G^0 - HeC_L^0}{He - \frac{D_L}{D_G}} \frac{x}{e} + C_L^0 \qquad 0 \le x \le e \tag{3.20}$$

$$C_G = \frac{C_G^0 - HeC_L^0}{He\frac{D_G}{D_L} + 1} \frac{x - 2e}{e} + C_G^0 \qquad e \le x \le 2e \tag{3.21}$$

where C denotes concentration, He is Henry's constant, x = e is the location of the gas-liquid interface and the subscripts L and G correspond to the liquid and gas phases, respectively.

3.6.1.1 Computational domain and input parameters

The computational domain is 1-D with a length of 0.001m with liquid phase filling the first half of the volume as shown in Figure 3.1. The initial value of the concentration C is 1 in gas phase and zero in liquid phase as shown in the Figure 3.2. The ratio of diffusivity of the specie in the gas phase to diffusivity of the specie in liquid

phase, D_G/D_L, was 10 and the Henry coefficient of solubility was taken as 0.1. The domain was divided into 300 cells.

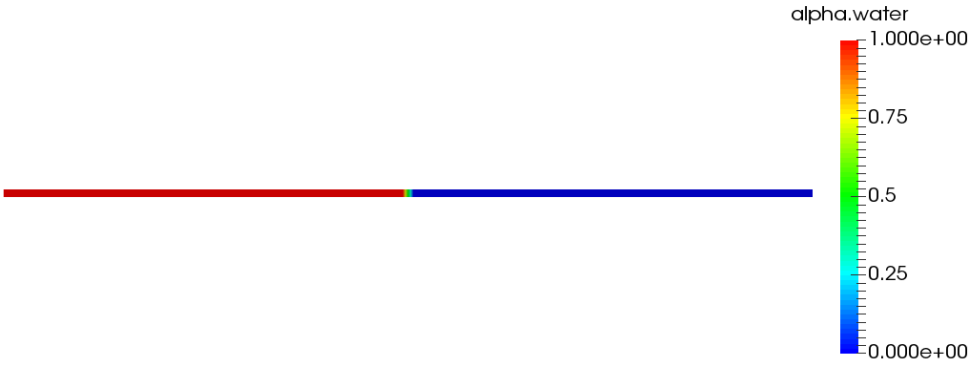

Figure 3.1: *liquid fraction distribution in computational domain for the 1-Dimensional mass transfer problem*

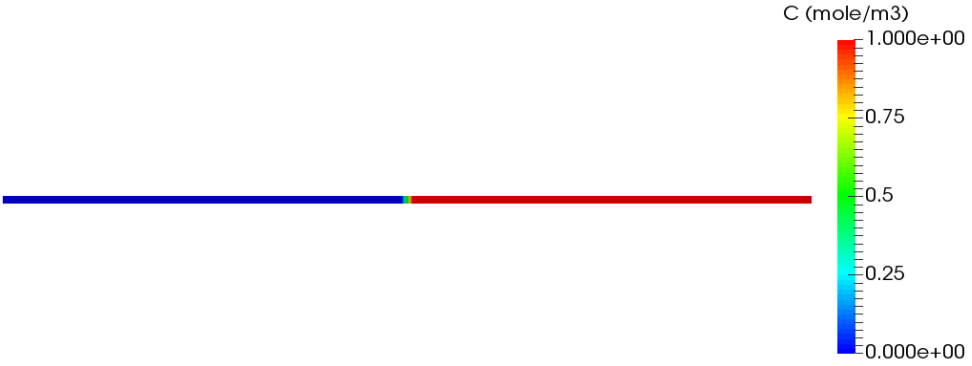

Figure 3.2: *Initial concentration distribution in computational domain for the 1-Dimensional mass transfer problem*

3.6.1.2 Results & discussion

The set up was simulated with a constant time step of 10-5 seconds until steady state was reached. The final concentration distribution in the domain is shown in Figure 3.3. The results were plotted against the analytical expressions give by Equations (3.20 & 3.21) and the resulting plot is shown in Figure 3.4. From the results it can be clearly seen that there is a very good agreement between the simulated and analytical solutions, verifying the correct implementation of the method. The method was also able to capture the discontinuity in species concentration at the interface region, with a good resolution of the concentration.

Figure 3.3: *Final concentration distribution in computational domain for the 1-Dimensional mass transfer problem*

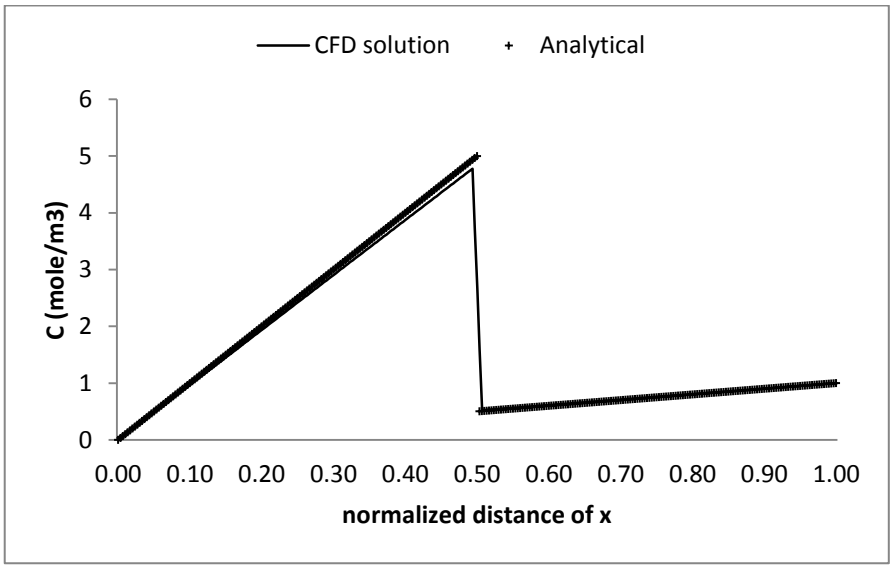

Figure 3.4: *Final concentration distribution plotted against analytical solution for the 1-Dimensional mass transfer problem*

3.6.2. Overall mass transfer coefficient

Because of the algebraic method of interface reconstruction in OpenFOAM the resulting interface will be diffused over a minimum of three computational grid cells. This diffused interface will make the identification of the location of the cell with highest concentration, on the liquid side due to solubility, difficult unless DNS is used (Marschall et al. 2012). At the same time because the overall mass balance is attained while using the one fluid formulation, there is possibility to obtain overall and averaged mass transfer coefficient using this method.

In the work of Wang et al (Wang et al. 2017), the one fluid formulation was effectively used to simulate a wetted wall column (counter current gas liquid flow) and the resulting overall mass transfer coefficient was compared with the experimental results consisting of a total of fourteen different conditions. According to authors, the simulation results were over or under estimating the experimental values but are still in good agreement with experiments when compared with two film theory. In the current thesis, two cases (case 3 and case 5) of their work were simulated and compared with the results.

3.6.2.1 Computational domain and input parameters

A simplified geometry arrangement, as shown in Figure 3.5, was used in the current simulation to calculate the counter current gas liquid overall mass transfer. The height of the domain is 100mm with 1mm liquid inlet and 4 mm gas inlet. The liquid and gas inlet velocities and other input parameters are evaluated from the work of Wang et al (Wang et al. 2017) and are given in the Table 3.1. Mesh density was used as suggested by Wang et al (Wang et al. 2017).

As mentioned by authors a clear difference between the predicted results and experimental results exist, but in very close approximation. This kind of deviations from the experimental values on using CFD were observed by Xu et al (Xu et al. 2009), Yu et al (Yu et al. 2006) and Sebastia-saez (SEBASTIA-SAEZ 2016) thesis work.

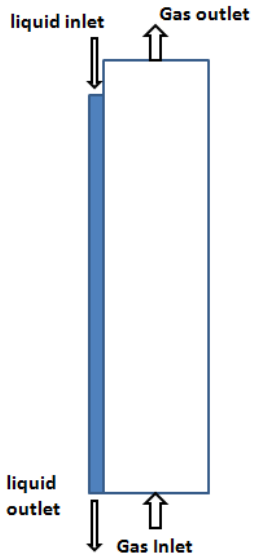

Figure 3.5: *Computational domain to calculate the overall mass transfer coefficient*

Table 3.1*: Input parameters used in calculation of the overall mass transfer coefficient*

	Units	Case 3	Case 5
liquid Density	kg/m^3	1024	1022
liquid Kinematic Viscocity	m^2/s	1.83E-06	1.79E-06
Diffusivity in liquid	m^2/s	6.88E-09	6.50E-09
gas Density	kg/m^3	1.42	1.2987
gas Kinematic Viscocity	m^2/s	1.20E-05	1.48E-05
Diffusivity in gas	m^2/s	1.20E-05	1.48E-05
Henry constant		2.17E+00	1.79E+00
Liquid inlet velocity	m/s	2.30E-01	1.25E-01
Gas inlet velocity	m/s	0.0516	0.0577

3.6.2.2 Results & discussion

The results of the simulations are shown in Table 3.2:

Table 3.2: *Overall mass transfer coefficient simulated in this work compared with Wang et al., (2017)*

Overall mass transfer coefficient, K_L	**This work**	**Wang et al (2017)**
Case 3	3.00E-08	3.73E-08
Case 5	2.40E-08	2.82E-08

In order to understand the advantages and limitations along with tackling the high mesh density requirement found during this study, a detailed analysis was carried and is briefed in Chapter 4. Hence details of deriving input parameters from correlations for the above work and grid independency study can be found in detail in Chapter 4.

3.6.3. Reactive mass transfer

Because of the high concentrations of the MEA used in industrial reactors the reaction between CO_2-MEA are generally simulated as a pseudo first order reaction (Sebastia-Saez et al. 2015b). The overall reaction, as described in Chapter 2, can be written as:

$$CO_2 + 2RNH_2 \rightarrow RNHCOO^- + RNH_3{}^+$$

where R stands for MEA i.e., R= CH_2CH_2OH. The rate of reaction for this reaction is calculated from the expression given by Ali (Ali 2005) Equation (3.22):

$$\ln r = 20.54 - 5612.91/T \qquad (3.22)$$

where reaction rate constant *r* (m^3/mol.s) is included in the mass transfer equation by expression given in Equation (3.18). The temperature in the current simulation is kept constant at 298.15 K and the value of *r* was obtained as 5.5522 (m^3/mol.s).

The computational domain simulated for the reactive mass transfer is similar to the domain used in section 3.6.2. The concentration of the CO_2 at the gas inlet was 10% and liquid solvent concentration of MEA was 30% (wt %). These values are generally used in industrial post combustion CCS operations. The properties of gas and liquid are given in Table 3.2.

In general the Hatta number (Ha) which compares the reaction and the solute diffusion rate is used to indicate whether the reaction takes place either in the bulk phase or only in the gas–liquid interface. A higher Ha implies that the chemical reaction is more dominant with respect to the physical absorption process whereas the opposite occurs when its value is low.

Table 3.2: Input parameters used in calculation of reactive mass transfer

	Units	
liquid Density	kg/m^3	1013
liquid Kinematic Viscocity	m^2/s	2.49E-06
Diffusivity in liquid	m^2/s	7.76E-10
gas Density	kg/m^3	1.21
gas Kinematic Viscocity	m^2/s	1.45E-05
Diffusivity in gas	m^2/s	1.45E-05
Henry constant		1.54E+00
Liquid inlet velocity	m/s	0.4
Gas inlet velocity	m/s	0.1

The Ha number is given by the expression in Equation (3.23) (Sebastia-Saez et al. 2015b):

$$Ha = \frac{\sqrt{r[MEA]D_{CO_2,l}}}{k_l} \tag{3.23}$$

where *r* is rate constant, [MEA] is concentration of MEA in liquid and k_l is liquid side mass transfer coefficient without reaction. In the current simulation k_l was calculated from the CO_2 concentration values at interface and liquid side outlet. The interface value was estimated theoretically using solubility law as the gas side mass transfer

coefficient is negligible in these reactive systems (Sobieszuk & Pohorecki 2010). The Ha value was estimated from Equation (3.22) as 27.994.

As described by Kale et al (Kale et al. 2013) when the Ha is greater than 10, the Enhancement factor (E) that is given by expression in Equation (3.24) for pseudo first order reaction (Sebastia-Saez et al. 2015b) approximately becomes equal to Ha number i.e., E≈Ha.

$$E = \frac{Ha}{\tanh(Ha)} \tag{3.24}$$

This was verified in the current simulation by calculating the Enhancement factor as the ratio of the amount of absorption with and without reaction. The values were easily obtained by overall balance of CO_2 concentration at all gas and liquid inlet and outlets of the computational domain. The Enhancement factor value obtained from current CFD simulation was 27.4, which was very close to the value of Ha which is 28, confirming the validity of the implemented code.

The validation work carried in this section also gives an insight that the reactive mass transfer can be readily estimated using the physical mass transfer information by simply multiplying with Ha number. Thus in order to reduce the computational resources here after in the coming chapters, emphasis was given to the simulation of physical mass transfer.

4. INVESTIGATING THE ADVANTAGES AND LIMITATIONS OF MODELING PHYSICAL MASS TRANSFER OF CO_2 ON FLAT PLATE BY ONE FLUID FORMULATION IN OPENFOAM

CO_2 is the main greenhouse gas that is causing an increase in average surface temperature of earth and need to be captured at the source to reduce its impact on the environment. The main sources of CO_2 emission are power plants, industrial processes and domestic consumption of fuels. Nearly 40% of this total CO_2 emission originates from industries (Aaron & Tsouris 2005). Hence, technologies required to capture the CO_2 gas at the source need to be developed. Several technologies have been developed in this regard and out of them the absorption of CO_2 by MEA (*mono ethyl amine*) solvent is one of the most preferred technique (Luis 2016). CO_2 absorption into MEA is majorly carried using packed bed reactors. Various kinds of reactors like bubble column, stirred tank and packed bed reactor are available for effective utilization of absorption phenomena. Among them, the availability of high interfacial area for mass transfer at low pressure drop makes the packed bed reactors preferable for gas liquid absorption process.

The packed bed reactors facilitate high interfacial areas using either structured packing or random packing. Structured packing are found to give higher mass transfer rates (Pham et al. 2015; Li et al. 2014; Aroonwilas et al. 2003; Aroonwilas et al. 2001) . The efficiency of a structured packing depends majorly upon micro level interactions between gas liquid immiscible phases next to packing surface. Hence understanding the micro-level mass transfer helps in developing better design and effective utilization of packed bed reactors (Kohrt et al. 2011; Fischer et al. 2003).

Computational fluid dynamics (CFD) is an effective tool in understanding the dynamics of multi-phase flows in complex geometries. CFD reduces the overall number of experiments and allow access to velocity, temperature and other scalar and vector fields of interest at any location of the geometry, which otherwise is very difficult to be accessed by experimental techniques (Sebastia-Saez et al. 2013). A detailed overview of utilizing CFD as an effective tool in modeling absorption in packed bed can be found the recent article published by Haroun and Raynal (Haroun & Raynal 2016).

The micro level analysis of structured packing essentially involves modeling of multiphase fluid dynamics as immiscible phase flow where the fluids are not

interpenetrating. The immiscible two phase flow is generally modeled using Volume of Fluid (VOF) approach and results are comparable to experimental values derived using particle image velocimetry techniques (Hoffmann et al. 2004). The mass transfer across these immiscible fluids is modeled majorly in two different ways. One approach involves the modeling of mass transfer across the immiscible phases by explicitly adding source terms to the governing Eq.s of VOF approach. Sebastia-Saezl et al. (Sebastia-Saez et al. 2015b; Sebastia-Saez et al. 2014; Sebastia-Saez et al. 2013) modeled physical and reactive mass transfer on flat and texture plates by this approach. The geometry in their work was same as that of Hoffmann et al. (Hoffmann et al. 2004) and similar approach was used by Xu et al. (Xu et al. 2009) for modeling the mass transfer of propane gas into toluene liquid.

Another approach for modeling the mass transfer across immiscible phases is familiarly known as "one fluid approach" or ''continuous specie transfer (CST)'' approach. This approach was proposed and validated by Haroun et al. (Haroun et al. 2010). Later on it was used in detailed numerical simulation of (direct numerical simulation, DNS) structured packing sheet also to derive mass transfer and liquid hold up in structured packing element by same group. The group of Haroun used JADIM multiphase software developed by IMFT (Legendre & Magnaudet 1998). Nieves-Remacha et al. (Nieves-Remacha et al. 2015) implemented this one fluid formulation for simulation of mass transfer in an industrial advanced flow reactor. A similar approach was developed by Marschall et al. (Marschall et al. 2012) and was implemented in OpenFOAM (Jasak & Weller 1995; Rusche 2002) for mass transfer in gas liquid bubble flow. In Nieves-Remacha (Nieves-Remacha 2014) dissertation thesis, the two formulations of Haroun et al. (Haroun et al. 2010) and Marschall et al. (Marschall et al. 2012) were compared and found to be producing same steady state results for various simple test cases. Recently, Wang et al. (Wang et al. 2017) used this approach for simulating the gas liquid mass transfer in wetted wall column. They found the CFD results in reasonable agreement with the experimental values.

The aim of this chapter is to discuss the advantages and limitations of utilizing *one fluid formulation* for modeling the physical mass transfer of CO_2 in OpenFOAM CFD software. The one fluid formulation was implemented as an additional transport equation in the existing code of OpenFOAM CFD software and a separate procedure for reducing the overall computational time is proposed. The physical absorption of CO_2

was studied using N_2O analogy. A comparison of liquid side mass transfer coefficient value derived from the simulations with the standard theoretical correlation proposed by Higbie (Higbie 1935a) is carried to study the aim. The investigations were carried for operating parameters such as flow rate, concentration of MEA and angle of inclination of plate. The simulation domain is two dimensional (2D) and the gas-liquid flow is counter current.

4.1 Modeling and Analysis

The simulations are carried using "*interFoam*" module available as part of open source software OpenFOAM. The theory and governing equations of the two phase modeling is described in section 3.1to 3.3. The one fluid formulation developed by Haroun et al.(Haroun et al. 2010) was implemented for modeling the mass transfer between immiscible phases. The governing equation (Eq. 3.17) is described in section 3.5 without source term W_i , as the current study is about the physical mass transfer.

4.2 Input Parameters

The physical mass transfer of CO_2 was modeled using surrogate N_2O gas. This kind of approach was used in many studies involving physical mass transfer of CO_2 and is known as N_2O analogy. The N_2O analogy avoids the effect of reaction, between CO_2 and MEA, on absorption. An excellent review of using N_2O analogy in the context of CO_2 capturing analysis can be found in Monteiro & Svendsen (Monteiro & Svendsen 2015) . The simulations were carried at isothermal conditions at a temperature of 298 K. The CO_2 loading on MEA solvent for current investigation was fixed at 20%. It was chosen so that the current studies can be used as a preliminary work for reactive mass transfer. In reactive mass transfer, the value of CO_2 concentration dissolved in MEA will highly influence the equilibrium partial pressure on the gas side of the interface and for CO_2 loading less than 30% this influence was found negligible by Aronu et al. (Aronu et al. 2011) and Wang et al. (Wang et al. 2017). The solvent properties are chosen based on the concentration of MEA (% wt) which in our study vary between 10 to 40%.

In the current simulation, pure N_2O gas was used on gas side. The gas density values were calculated using ideal gas law and viscosity values were taken from open literature for pure N_2O. The N_2O diffusivity within gas medium is taken equal to that of

kinematic viscosity. The diffusivity value of N_2O in the solvent is calculated from correlation proposed by Versteeg and van Swaal (Versteeg & van Swaal 1988) as shown in Eq. (4.1).

$$D_{N_2O} = 5.07\ x\ 10^{-6} \exp\left(-\frac{2371}{T}\right) \left(\frac{\mu_{water}}{\mu_{soln}}\right)^{0.8} \quad (4.1)$$

where the μ_{water} and μ_{soln} are viscosities of pure water and carbonated solvents respectively. Properties like viscosity and density of carbonated solvents were taken from Weiland et al. (Weiland et al. 1998) and surface tension values were taken from Fu et al. (Fu et al. 2012).The Henry constant values were calculated from the Eqs (4.2, 4.3 & 4.4) proposed by Penttila et al. (Penttilä et al. 2011). The units of Henry constant in their work is

$$H_{N_2O,water} = \exp\left(158.245 - \frac{9048.596}{T} - 20.86.ln(T) - 0.00252.T\right) \quad Pa.m^3/mol \quad (4.2)$$

$$H_{N_2O,MEA} = -9172.5 + 39.598.\mathrm{T} \quad Pa.m^3/mol \quad (4.3)$$

$$H_{N_2O,solvent} = H_{N_2O,water}\mathrm{x_{water}} + H_{N_2O,MEA}\mathrm{x_{MEA}} + \mathrm{A_1}\,[\mathrm{x_{water}x_{MEA}}][1 - \frac{\mathrm{T}}{\mathrm{A_2}}]\exp\,[-\mathrm{A_3}.\mathrm{x_{MEA}}] \quad (4.4)$$

where in the Eq. (4.4) the A_1, A_2 and A_3 are constants with values of 3524641.533, 324.718 and 13.219 respectively. The x_{water} and x_{MEA} represent the mole fraction of water and MEA in the solvent. The calculated Henry constant values with units, as mentioned in Eq. (4.2), are then converted into dimensionless Henry constant by using Eq. (4.5)

$$H_{N_2O,dimless} = \frac{H_{N_2O,solvent}}{RT} \quad (4.5)$$

where R is the universal gas constant with value 8.314 $Pa.m^3.mole^{-1}.K^{-1}$ and T is temperature in K. The contact angle value for solvent was taken as fixed at 40^0 as given in Wang et al. (Wang et al. 2017).

The ranges of values used in our simulations are as tabulated in Table 4.1. Units of all the variables used in the current simulations have SI units.

Table 4.1: *Modeling input parameters*

Parameter	**Value/Range**	**Units**
Operating temperature	298	K
MEA mass fraction	[0.1, 0.4]	g of MEA/g solvent
CO_2 loading	0.2	Mole of CO_2/mol of MEA
Inlet N_2O mole fraction	1	Dimensionless
Liquid Reynolds number , Re_L	[83,249]	Dimensionless
Gas Reynolds number, Re_G	200	Dimensionless
Henry coefficient	[1.42,1.8]	Dimensionless
N_2O Diffusivity in solvent	[5E-10,9.98E-10]	m^2/s
Surface tension	0.0673	N/m
Solvent contact angle	40^0	Degree
Gas Inlet concentration	40.896	$mole/m^3$

4.3 Geometry, Mesh and Boundary conditions

The current study was carried on 2D (two dimensional) geometry. The geometry under simulation is shown in Figure 4.1. The liquid enters the computational domain through a 1mm inlet and leaves through a 1mm outlet. The gas enters counter currently through a 4mm inlet and leaves through a 4mm outlet. The height of the plate on which the liquid flows is 50 mm and the height of the gas chamber is 55mm. Through preliminary investigations we found that the height of gas chamber needs to be more than the liquid plate height in order to capture the mass transfer effects near liquid entrance regions. In our simulation we used a 10% additional height for gas chamber (55mm) when compared to liquid plate height (50 mm) and found this geometry giving accurate results.

Generic boundary conditions available in OpenFOAM were used in this simulation and are listed in Table 4.2. A comprehensive work for setting up a two dimensional investigation in OpenFOAM using generic boundary conditions can be found in Tong et al. 2013 (Tong et al. 2013), for further reading.

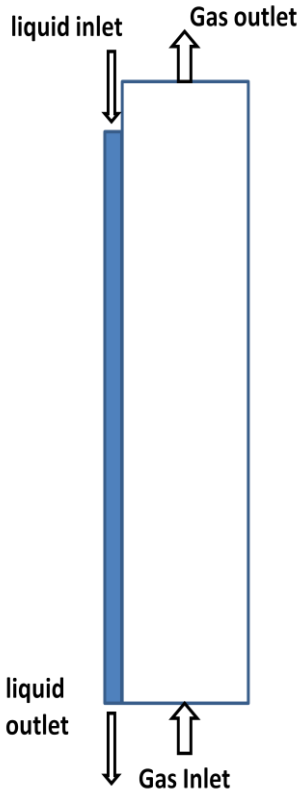

Figure 4.1: *Overall geometry under simulation for counter current gas-liquid flow*

Table 4.2: *Boundary conditions*

Boundary name	**U** (Velocity)	**p** (pressure)	**α** (phase fraction)	**C** (concentration)
Liquid inlet	surfaceNormalFixedValue	zeroGradient	FixedValue 1	zeroGradient
Liquid outlet	zeroGradient	zeroGradient	zeroGradient	zeroGradient
Gas inlet	surfaceNormalFixedValue	zeroGradient	FixedValue 0	FixedValue
Gas outlet	zeroGradient	totalPressure p0 0;	zeroGradient	zeroGradient
Wall on the liquid side	zeroGradient	zeroGradient	constantAlphaContactAngle $\theta = 40^0$	zeroGradient
Wall on the gas side	zeroGradient	zeroGradient	zeroGradient	zeroGradient

In their investigation of counter current gas liquid mass transfer Xu(2009) found that to capture the mass transfer effect with reasonable accuracy a mesh size of 0.07h, where h is the film thickness, is required. Since the average film thickness in our study

is 0.4 mm the minimum size of mesh required was 0.028mm. But through our preliminary investigations to find the grid independency, we found that a mesh size of 0.00625mm (approx. 0.015h) is required in order to capture the mass transfer effectively. The requirement of higher mesh refinement can be due to the one fluid formulation used in our study which involves modeling of the very low diffusivity of gas in the liquid solvent. The lower diffusivity confines the gas concentration layer to regions near interface. A similar observation of high mesh refinement was made by Cooke (Cooke 2016). In the remaining gas side geometry, a uniform mesh size of 0.0125mm in the horizontal direction was used. Further refinement in this region wasn't affecting the final solution of concentration field, which can be due to the higher diffusivity of gas. In order to reduce the computational time, the size of 0.0125mm was used in the gas side of domain. In the direction of height, a size of 0.1mm was used. A snapshot of refined mesh is given in Figure 4.2. The final mesh size was approximately 0.3 million hexahedra cells. The details of grid independency are presented in next section.

4.4 Grid Independency

The grid independence study was aimed to find out the minimum number of nodes after which an increase in the number of nodes wouldn't affect the concentration measured at the outlet significantly. The study was carried for MEA weight percentage of 30%, at Re_L of 125 and Re_G of 200. The resulting graph (Fig 4.3) of liquid outlet concentration as a function of number of nodes clearly shows that a number of 160 nodes (6.25μm) in the liquid inlet region of 1mm are sufficient to capture the outlet concentration as invariable of grid size:

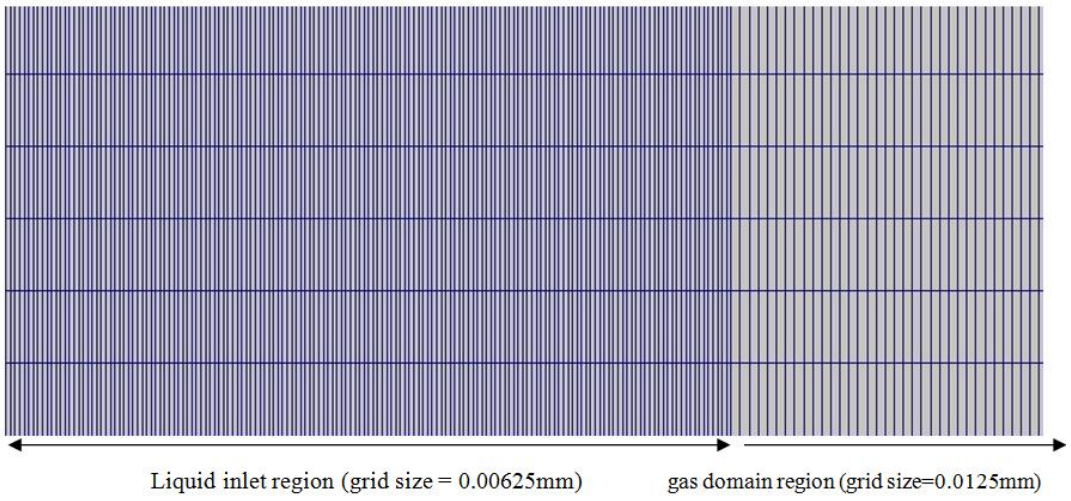

Figure 4.2: *Mesh size distribution in the domain*

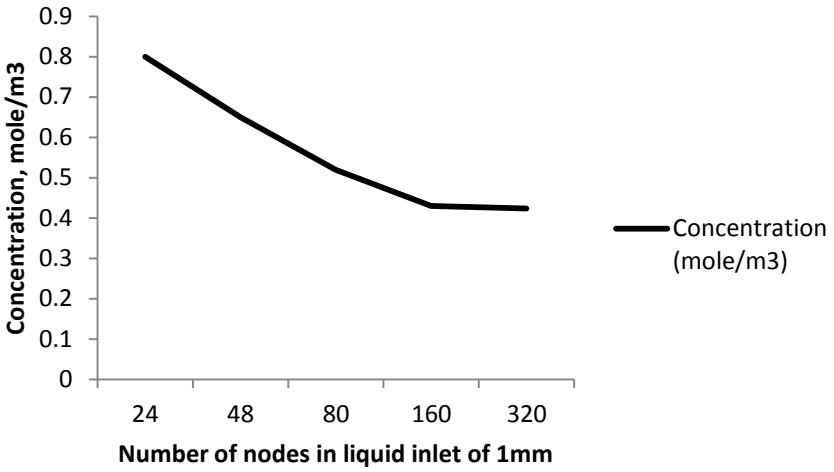

Figure 4.3: *Concentration at liquid outlet as a function of number of nodes in liquid inlet*

4.5 Solver Setting and Analysis of Results

Higher order vanLeer scheme available in OpenFOAM was used to solve the continuity, momentum and concentration Eq.s. The tolerance of 10^{-14} was used as convergence criteria. All the flow Eq.s were solved transiently until steady state flow field was achieved. An adjustable time step was used with a maximum Courant number of 0.9. In order to reduce the simulation time, the flow field was solved initially on a coarse mesh with 0.028mm in the film thickness region. Later this flow field was mapped on refined mesh with 0.00625mm and further simulated transiently until steady state flow field was achieved. The concentration Eq. was then solved independently on the resulting flow field with a fixed time step of 10^{-5}s, until steady state was achieved. This procedure has resulted in reducing the overall computational time from several days to hours without compromising the quality of the model. Note that this suggested procedure is suitable for problems involving steady state solutions and may not be suitable for obtaining transient solutions which are highly dependent on initial conditions. Despite the suggested procedure to reduce the computation time, the time to obtain result for one flow condition that is from solving flow field on coarse mesh to solving concentration Eq. was not less than 30 hours in total on a Dell workstation (DELL PRECISION T7810 (v2)) with 2 Intel Xeon E5-2630 v3 processors (16 core).

On obtaining the concentration values at steady state, the liquid side mass transfer coefficient is calculated from the simulation results using the Eq. (4.6)

$$k_L = F/\Delta C \tag{4.6}$$

where F is the mass flux at the gas -liquid interface per unit area and ΔC is the difference between the concentration at the interface and bulk liquid. The results are compared with theoretical correlation proposed by Higbie (Higbie 1935a) as Eq. (4.7)

$$k_L = 2\sqrt{\frac{D_L}{\pi\tau}} \tag{4.7}$$

where τ is the time of exposure calculated using an expression in Eq. (4.8) reported by Haroun et al.(Haroun et al. 2012):

$$\tau = L/|v_i| \tag{4.8}$$

where L is the length of the plate and v_i is the interfacial velocity

The interfacial velocity is calculated using Nusselt (Nusselt 1916) theory which is valid for laminar flows. The Nusselt expression (Eq. 4.9) predicts the liquid velocity within the liquid film region as a function of distance from the plate surface. The expression also includes the effect of inclination of the plate with respect to the horizontal surface.

$$v = \frac{\rho_L g \delta^2 \sin(\beta)}{2\mu_L}\left[1 - \left(\frac{z}{\delta}\right)^2\right] \tag{4.9}$$

4.6 Results and Discussion

4.6.1 Comparing the effect of flow rate

The counter current gas flow reduces and flattens the liquid surface velocity and the maximum liquid velocity can occur at a different position than that of interface. This kind of flow filed instabilities at micro scale near the interface can enhance the mass transfer by multitude, even in laminar flow conditions (Yu et al. 2006). Hence a study of influence of liquid flow rate is of prime importance in understanding the mass transfer under counter current flow conditions. In this study, the effect of liquid flow rate on absorption of gas was studied at gas phase Reynolds number of Re_G = 200 and

for liquid phase Reynolds number of 83 <Re_L<249. This Re_G was the minimum value used in Yu et al. (Yu et al. 2006) experiments of counter current gas liquid absorption. Also, it was found in the Yu et al. (Yu et al. 2006) experiments that the gas phase velocity has little influence on the interface liquid velocity and hence the effect of varying gas phase velocity wasn't studied in our investigations. The liquid and gas Reynolds numbers are defined as:

$$Re_L = \frac{d_L u_L \rho_L}{\mu_L} \tag{4.10}$$

$$Re_G = \frac{d_G u_G \rho_G}{\mu_G} \tag{4.11}$$

The liquid side mass transfer coefficient, k_L (with units mole/Pa.s.m^2) is calculated using Eq. (4.6) where the flux value F is calculated based on overall mass consumption at steady state. The mass conservation inherently states that the amount of N_2O dissolved through gas liquid interface is equal to the amount of N_2O removed by solvent at liquid outlet. This amount of N_2O removed at outlet when divided by interfacial area gives the mass flux value, F, in mole/m^2-s. The resulting liquid side mass transfer coefficient is then compared to Higbie (Higbie 1935a) correlation for various Re_L and results are presented in Figure 4.4.

The results agree very well with Higbie penetration theory at low Re_L and deviate at higher Re_L. The deviation at higher Re_L can be due to the influence of surface instabilities whose effects aren't included in the Higbie (Higbie 1935a) model as mentioned in Yu et al. (Yu et al. 2006). The deviations in the velocity profile at the liquid outlet from the Nusselt film profile can be seen in Figure 4.5 (a , b, c &d).Also, it can be due to the small size of geometry and parameters used from experimental data published in open literature. Since the current model is promising by accurately predicting the mass transfer coefficient values at low Re_L, it may be used by coupling with studies involving DNS to develop new correlations for higher Re_L and this will be part of our future work.

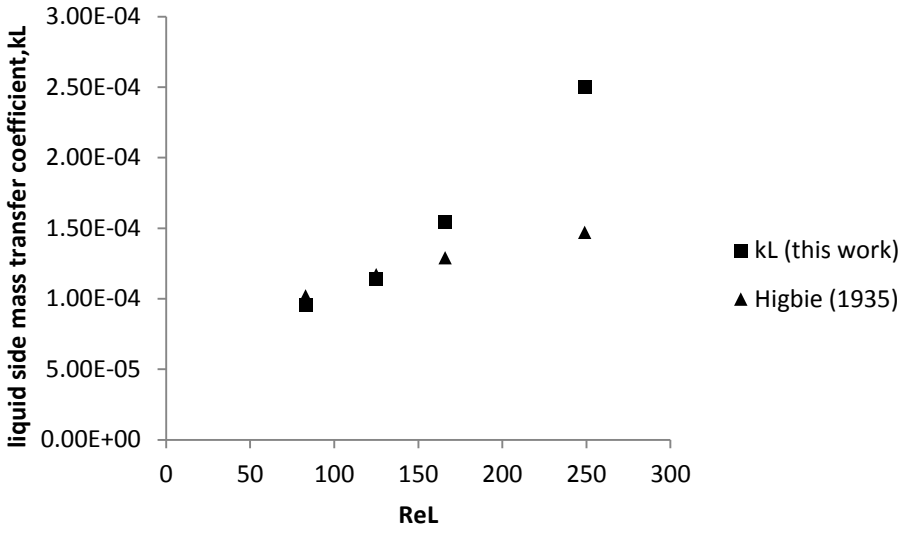

Figure 4.4: *Liquid side mass transfer coefficient is compared to Higbie (1935) correlation for varying* Re_L

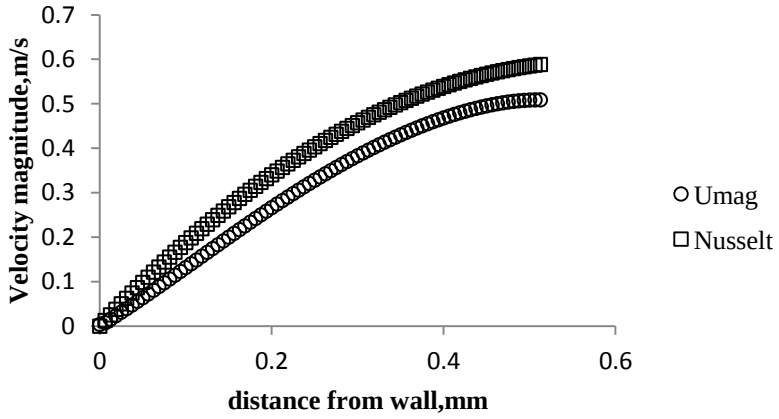

Figure 4.5(a): *Comparison of velocity profile with Nusselt (1916) laminar profile at* Re_L *= 83 at* Re_G *=200*

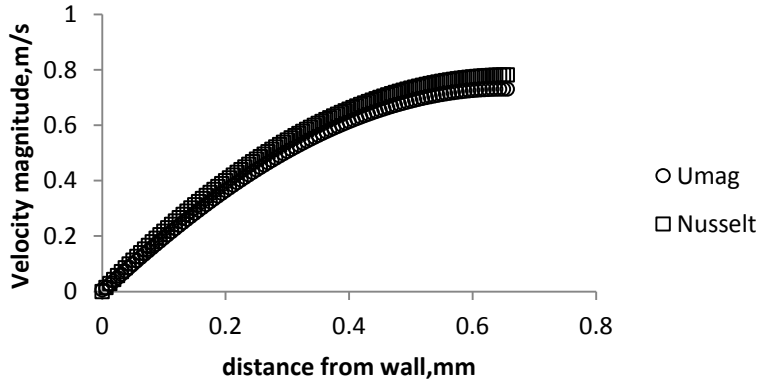

Figure 4.5(b): *Comparison of velocity profile with Nusselt (1916) laminar profile at* Re_L *= 125 at* Re_G *=200*

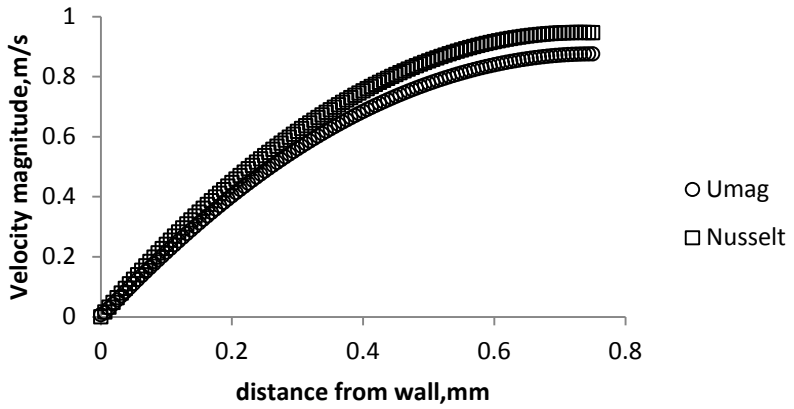

Figure 4.5(c): *Comparison of velocity profile with Nusselt (1916) laminar profile at Re_L = 166 at Re_G =200*

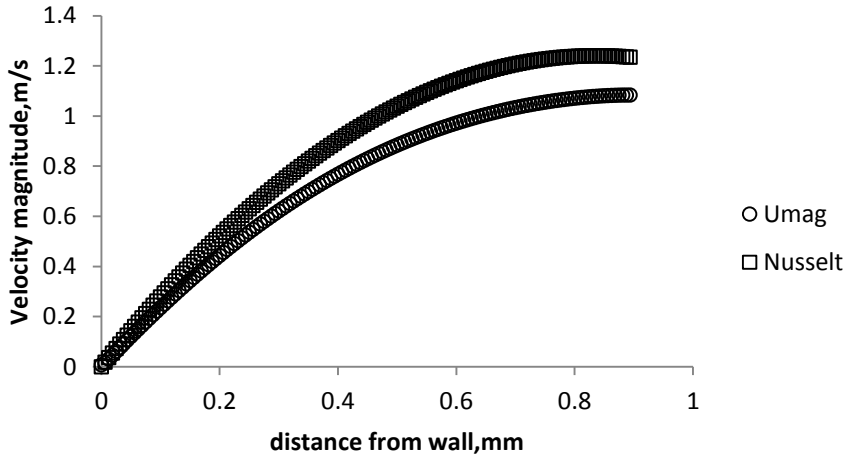

Figure 4.5d: *Comparison of velocity profile with Nusselt (1916) laminar profile at Re_L = 249 at Re_G =200*

4.6.2 Comparing the influence of MEA concentration

Since at Re_L of 125 the Higbie (Higbie 1935a) model was accurately approximating the liquid side mass transfer coefficient for solvent with MEA mass fraction of 30%, as explained in the previous section, the current study was carried at Re_L of 125. The influence of MEA mass fraction in the liquid solvent on the liquid side mass transfer coefficient has been studied for four values of: 10%, 20%, 30% and 40% respectively. The results are as shown in Figure 4.6.

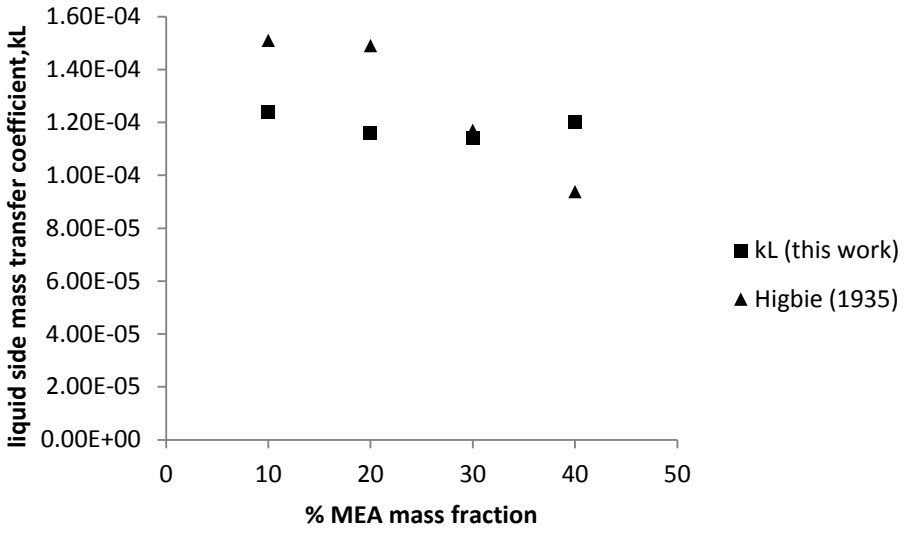

Figure 4.6: *Comparison of liquid side mass transfer coefficient obtained from this work with Higbie(1935) for varying MEA concentration*

For MEA mass fraction less than 30% the Higbie (Higbie 1935a) model over estimates and for mass fraction of 40% underestimates the liquid side mass transfer coefficient. Also for MEA mass fraction of 30% the Higbie (Higbie 1935a) model accurately estimates the liquid side mass transfer coefficient. This kind of behavior was observed by Sebastia-Saez et al. (Sebastia-Saez et al. 2015b) . Such variations occurs presumably due to the variation of liquid properties like kinematic viscosity and density of the solvent based on the MEA mass fraction. Hence it is safe to say that, using this approach a better estimate of physical mass transfer can be obtained than theoretical models. Since the MEA mass fraction is an important parameter influencing the chemical absorption rate (Meldon & Morales-Cabrera 2011) the current approach is suggested for estimating the enhancement factor and studies involving the design of CO_2 reactors.

4.6.3 Comparing the influence of angle of inclination of plate to the horizontal plane

In the two previous sections the film was flowing downward on a vertical plate. But in practice corrugated sheets are used for designing packed beds. These packed beds are generally made of metal sheets of steel and have corrugated textures with an angle of 45^0 or 60^0 between the corrugations respectively (Kohrt et al. 2011). In this study, the influence of the plate inclination on the liquid side mass transfer coefficient was also investigated for inclinations of 45^0 and 60^0 at Re_L of 83 for solvent with MEA mass

fraction of 30%. Figure 4.7 shows simulation domain of an inclined plate in our simulation. The results are shown in Figure 4.8. The liquid side mass transfer coefficient is exactly approximated by Higbie (Higbie 1935a) model. Hence it is concluded that the current model allows the modeling of physical mass transfer in counter current flow on corrugated sheets, which are used to increase the available surface area per unit volume of the packed bed, accurately.

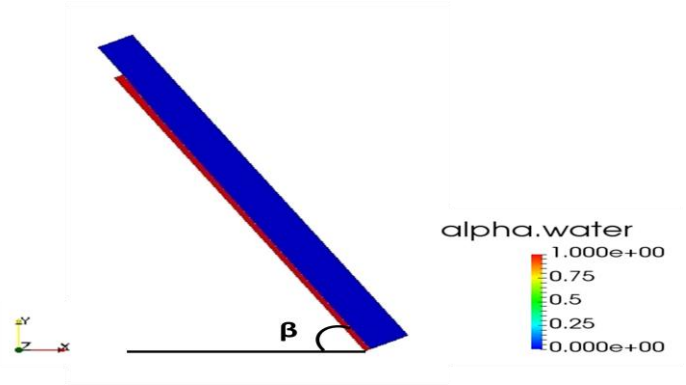

Figure 4.7: *Domain inclined to the horizontal plane by an angle of β*

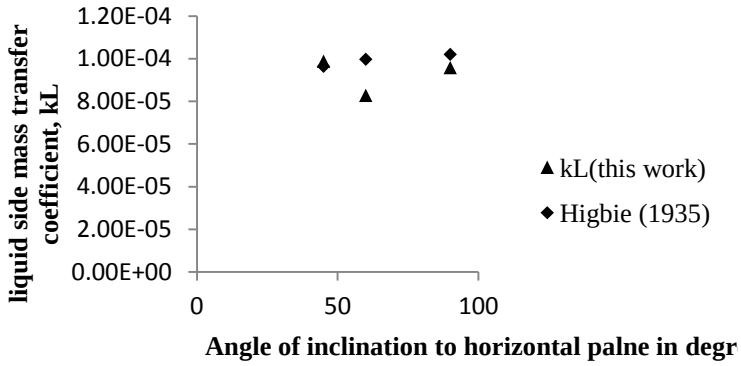

Figure 4.8: Comparison of liquid side mass transfer coefficient obtained from this work with Higbie (1935) at different inclinations of flat plate

4.7 Conclusions

In this study we implement and analyze the advantages and limitations of one fluid formulation approach for CO_2 physical mass transfer into MEA. The domain considered is a flat plate and gas liquid flow is counter current. The analysis was carried for operating parameters like liquid phase Reynolds number in the range of 83 $<Re_L<249$, MEA mass fraction in the range of 0.1 to 0.4 and for the angle of inclination of flat plate varying between 45 to 90^0 respectively.

The results clearly show that the model effectively captures the deviation in liquid side mass transfer coefficient due to the surface instabilities which are significant at higher Reynolds numbers. The effect of liquid properties which vary with the mass fraction of MEA in the solvent are also predicted with greater accuracy. These effects are generally neglected in the standard correlations. The model also shows that the standard Higbie correlation is well suitable for modeling the flows at low Reynolds number.

The grid independent studies show that a size of 6.25μm is required in the interface region for effectively using this approach. The requirement of this high mesh resolution results in high computational resource time. In order to reduce the overall computational time we adopted a sequential procedure of solving the concentration equation independently on the desired flow field. Also the time required for obtaining the flow field was further reduced by first solving the flow field on a coarse mesh and mapping the result on refined a mesh. This procedure was found to reduce the overall computational time from days to hours. However it should be noted that the suggested procedure is suitable for problems involving steady state solutions and may not be suitable for obtaining transient solutions which are highly dependent on initial conditions.

In conclusion, it can be said that the CFD modeling of mass transfer by one fluid formulation is proven to be a promising approach and an alternative to experimentation .The higher accuracy of this approach is due to the consideration of the effect of thermodynamic properties like diffusion and solubility on mass transfer coefficient instead of using derived values from correlations. Hence future CFD investigations of micro structure impact on CO_2 mass transfer can be carried using this approach and our suggested procedure can be adopted for reducing the simulation time effectively.

5. MODELING OF SURFACE TEXTURE INFLUENCE ON CO_2 MASS TRANSFER INTO MEA BY OPENFOAM

Structured packing columns, also referred as ordered packing columns, are widely used in separation processes involving removal of pollutant gases like CO_2 from industrial emissions. They are found to give higher mass transfer rates and any kind of development in their design can help in enhancing the industrial energy savings (Schultes & Chambers 2007). In view of their importance, several investigations were carried in the last decades to find the optimal designing and operating parameters (Li et al. 2014; Pham et al. 2015; Aroonwilas et al. 2001; Aroonwilas et al. 2003).

One of the most important parameters which can influence the overall performance of the structured packing is the micro texture patterns, often referred as surface roughness, on the corrugated sheets (Yu et al. 2018; Kohrt et al. 2011). Majority of the research till date was confined to study the hydrodynamics of the single phase and two-phase (gas-liquid) flows on micro texture patterns. The patterns in all these investigations were comparable to the texture pattern size of commercial Mellapack 250Y. The first of this kind of investigations about the influence of amplitude of periodic microstructure on liquid film thickness were carried by Zhao and Cerro (Zhao & Cerro 1992). In their experiments, the film thickness enhancement was studied for Nusselt film thickness to amplitude ratio ranging from 0.1 to 1.

Since the experimental analysis is time-consuming and doesn't provide the flow field details, CFD was found as an attractive technique for analysis of hydrodynamics of micro-structured patterns(Xu et al. 2014; Hoffmann et al. 2004; Huang et al. 2015). Szulczewska et al. (Szulczewska et al. 2003) studied the hydrodynamics of countercurrent gas-liquid flow in a 2D domain of Meallpack 250Y with surface textures. Valluri et al. (Valluri et al. 2005) studied liquid film flow on 2D sinusoidal surfaces and Li et al. (Li et al. 2016) have studied the hydrodynamics of wave patterned textures in 2D. Li et al. (Li et al. 2016) also extended their studies to investigate the effective wetted area in 3D.

To the author's best knowledge the mass transfer analysis of the texture patterns is very scarce. Kohrt et al. (Kohrt et al. 2011) studied the influence of micro texture on the liquid side mass transfer of CO_2 into silicon oil. The texture patterns used in their investigation were unidirectional transversal waves and bidirectional pyramidal

structures of the size comparable to the texture size of Zhao and Cerro (Zhao & Cerro 1992) experiment. They found the textures enhanced the mass transfer by almost 80%. Yu.et al. (Yu et al. 2018) investigated the mass transfer of O_2 into the water for wavy texture pattern developed by Li et al. (Li et al. 2016) and found the enhancement in the mass transfer by 20%. They have pointed a need for detail CFD investigations to study the impact of surface roughness on mass transfer. To sum up, there is a need to evaluate the influence of the micro structures on the mass transfer of CO_2 into MEA (monoethanolamine).

In this chapter, the influence of micro structures on the mass transfer of CO_2 into 30% MEA solvent was carried for countercurrent gas-liquid flow condition. The mass transfer studies were initially carried for commercial Mellapack 250 Y structure and the studies were then extended to structures with different amplitudes and patterns. The simulations were carried at fixed flow rates of gas and liquid, keeping the geometry structure size as the only variable, in order to compare the impact of the geometry on the mass transfer. The flow rates were chosen to keep the gas-liquid flow essentially laminar to avoid the influence of turbulence mixing on the overall mass transfer. Important design parameter was detected and suggestions were made for developing new designs based on this parameter. The effect of CO_2-MEA reaction on mass transfer was not considered in the current study as the change in the liquid solvent concentration is insignificant at micro-scale analysis (Sebastia-Saez et al. 2015b). To the author's best knowledge there is no detail CFD study investigating the impact of various texture pattern design parameters impact on gas-liquid mass transfer. This is the first attempt in that direction.

5.1. Modeling and Analysis

The theory, mathematical background and methodology for deriving the input parameters are similar to the methodology in the previous Chapter 4. The only difference in the current investigation is that the operating temperature was fixed at 298K and the liquid solvent considered was 30% MEA without CO_2 loading. The values used in our simulations are as tabulated in Table 5.1.

Table 5.1: *Input parameter values*

Parameter	**Value/Range**	**Units**
Operating temperature	298	K
MEA mass fraction	0.3	g of MEA/g solvent
CO_2 loading	0	Mole of CO_2/mol of MEA
Inlet N_2O mole fraction	1	
Liquid Reynolds number , Re_L	30	
Gas Reynolds number, Re_G	21	
Henry coefficient	1.54	Dimensionless
N_2O Diffusivity in solvent	7.76E-10	m^2/s
Gas Inlet concentration	1	Normalized, Dimensionless
Surface Tension of MEA	0.065	N m-1

5.2 Geometry, Mesh, and Boundary Conditions

The current study was carried on 2D (two dimensional) geometry. The overall geometry under simulation is shown in Figure 5.1. The domain is inclined at an angle (β) of 60^0 to the horizontal plane (the angle at which commercial corrugated sheets are inclined generally).The liquid enters the computational domain through a 1mm inlet and leaves through a 1mm outlet. The gas enters counter currently through a 4mm inlet and leaves through a 4mm outlet. The height of the plate on which the liquid flows is 35 mm and the height of the gas chamber is 45mm. Through preliminary investigations, we found that the height of gas chamber needs to be more than the liquid plate height in order to capture the mass transfer effects near liquid entrance regions. In our simulation we used a 10 mm additional height for gas chamber (45mm) when compared to liquid plate height (30 mm) and found this geometry giving accurate results. Generic boundary conditions available in OpenFOAM were used in this simulation as listed in Table 5.2.

The texture plates investigated are placed at the center of the domain and spread over 15mm. The base width (λ) and amplitude 2A were varied and tested for three different combinations as shown in Figure 5.2. The investigations were carried initially for commercial Mellapack 250Y geometry with triangular and wave structure followed by altering the $2A/\lambda$ ratio. An additional investigation was also carried for texture having a flat surface between consecutive peaks.

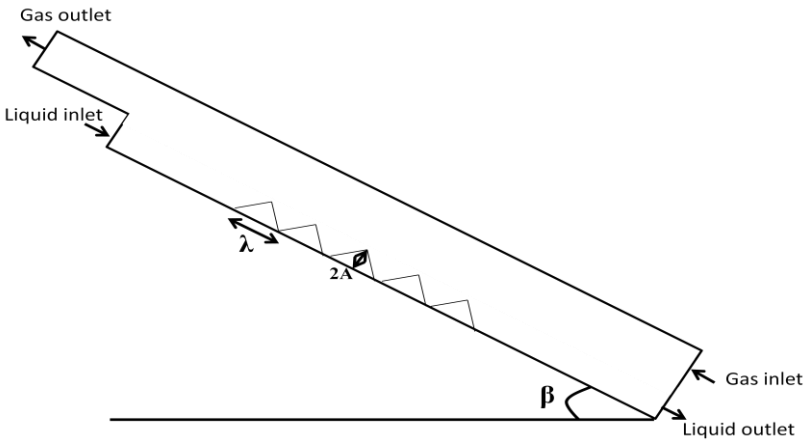

Figure 5.1: *Overall geometry with textures inclined at an angle of β (=60^0) to the horizontal plane*

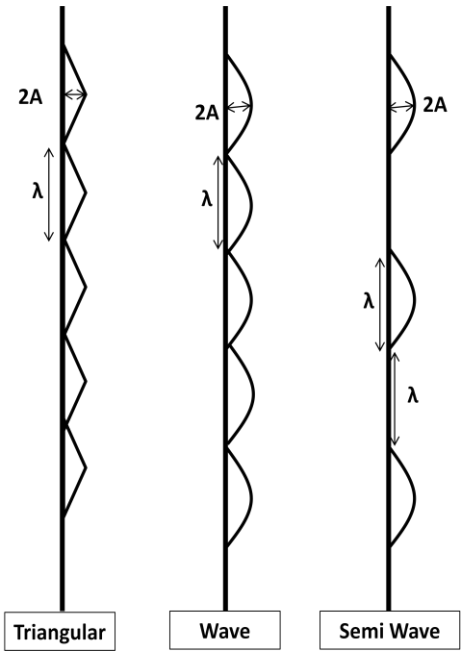

Figure 5.2: *Texture patterns investigated*

Table 5.2: *Boundary conditions*

Boundary	**U**	**p**	**α**	**C**
Liquid inlet	surfaceNormalFixedValue	zeroGradient	FixedValue 1	zeroGradient
Liquid outlet	zeroGradient	zeroGradient	zeroGradient	zeroGradient
Gas inlet	surfaceNormalFixedValue	zeroGradient	FixedValue 0	FixedValue
Gas outlet	zeroGradient	totalPressure p0 0;	zeroGradient	zeroGradient
Wall	zeroGradient	zeroGradient	zeroGradient	zeroGradient

In their investigation of counter current gas-liquid mass transfer Xu et al.(Xu et al. 2009) found that to capture the mass transfer effect with reasonable accuracy a mesh size of 0.07h, where h is the film thickness, is required. Since the average film thickness in our study is 0.4 mm the minimum size of the mesh required was 0.028mm. But through our preliminary investigations to find the grid independency, we found that a mesh size of 0.00625mm (approx. 0.015h) is required in order to capture the mass transfer effectively. The requirement of higher mesh refinement can be due to the one fluid formulation used in our study which involves modeling of the very low diffusivity of gas in the liquid solvent. The lower diffusivity confines the gas concentration layer to regions near the interface. A similar observation of high mesh refinement was made by Cooke (Cooke 2016). In the remaining gas side geometry, a uniform mesh size of 0.0125mm in the horizontal direction was used. Further refinement in this region wasn't affecting the final solution of concentration field, which can be due to the higher diffusivity of the gas. In order to reduce the computational time, the size of 0.0125mm was used in the gas side of the domain. In the direction of height, a size of 0.1mm was used. A snapshot of refined mesh for individual texture is shown in Figure 5.3. The final mesh size was approximately 0.3 million hexahedra cells.

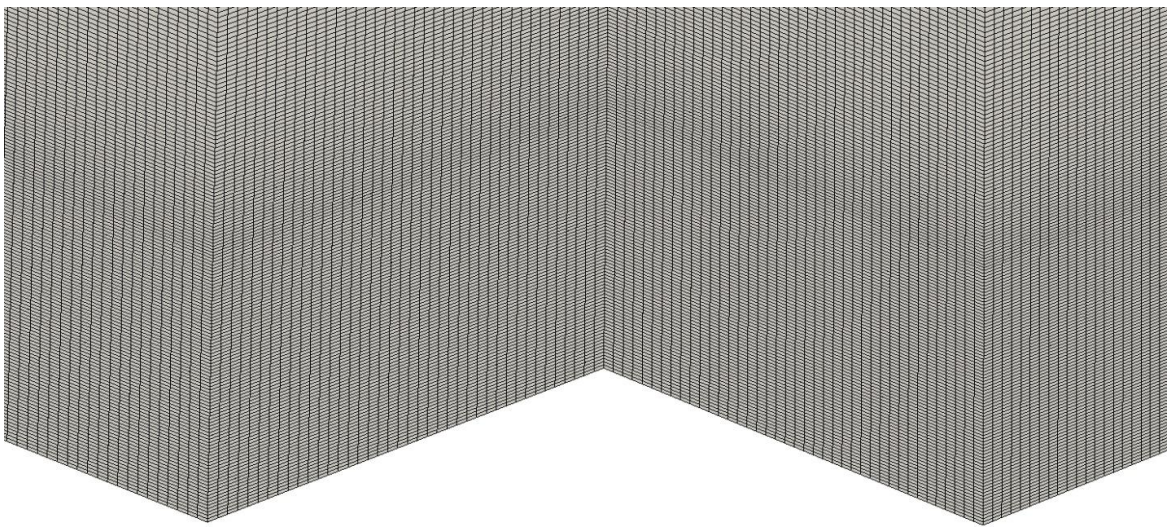

Figure 5.3: *Refined mesh on triangular texture patterns investigated*

5.3 Solver Setting and Analysis of Results

The solver settings and methodology for the analysis of the results used in Chapter 4 are effectively used for this investigation. Also and additional user defined code was written for post processing of liquid film height from the iso-surface of the solvent volume fraction (α=0.5).

5.4 Results and Discussion

5.6.1 Effect of texture geometry: wave vs triangular

All the simulations were carried at a fixed liquid and gas Reynolds number of Re_L = 30 and Re_G = 21. At these low Reynolds numbers the flow field is safely assumed laminar. Also, the evaluation at fixed Reynolds number allows investigation of geometry effect on mass transfer in detail by avoiding the influence of other flow parameters like pressure drop and turbulence. The liquid side Re_L was chosen such that the Nusselt film thickness (equation 21) at this flow rate was 0.4mm.

The effect of texture type was studied for two generally used texture types: wave and triangular. The $2A/\lambda$ ratio for both the textures was fixed at 0.2, which is similar to the $2A/\lambda$ of surface textures in commercial Mellapack 250Y structured columns. The λ value is 3 mm for both the textures. The film thickness on the two surfaces is as shown in **Figure 5.4a, 5.4b**.

From Figure 5.4(a) and Figure 5.4(b), it can be clearly seen that the resulting film thickness doesn't vary highly from Nusselt film thickness (equation 21) of 0.4mm. But the mass flux, liquid side mass transfer coefficient and the mass fraction of CO_2 at the solvent outlet, as given in Table 5.3, for wave pattern are found to be higher than the values generated by triangular pattern with same $2A/\lambda$ ratio. This enhancement in mass transfer can be due to the formation of waves with higher amplitude of value $\approx$ 0.6mm in the wave patterned texture when compared with the triangular texture having wave amplitudes of $\approx$ 0.5mm. Hence it can be concluded that the amplitude of the wave plays a dominant role in the mass transfer process and wave patterns must be preferred over triangular texture patterns for attaining higher mass transfer rates.

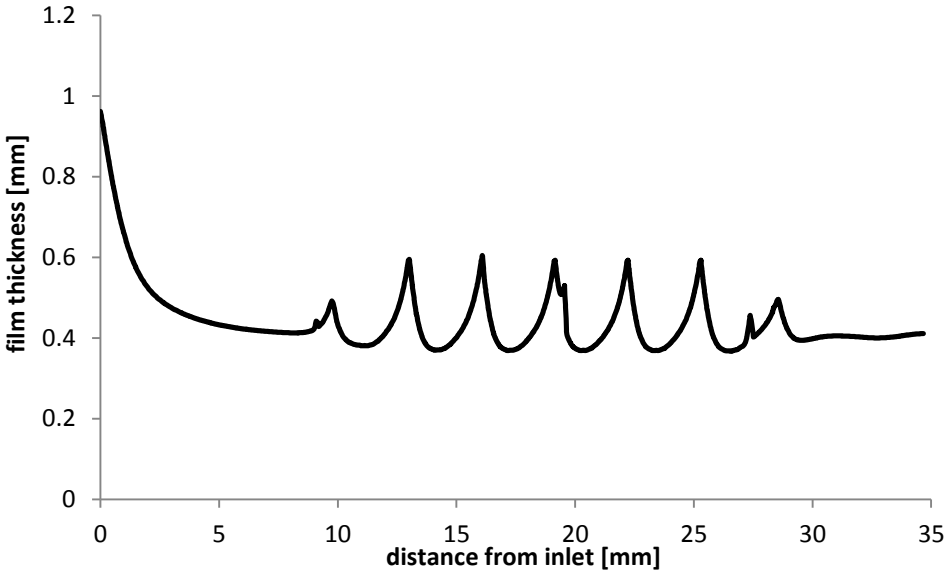

(a)

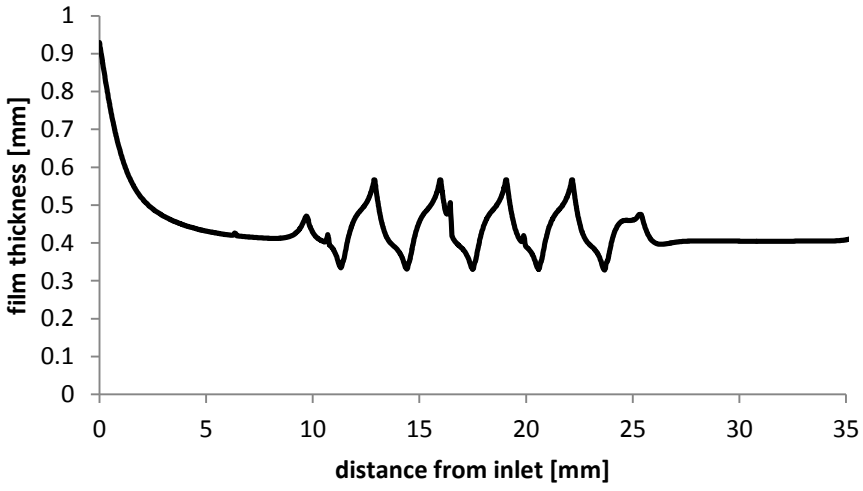

(b)

Figure 5.4(a), 5.4(b): *Film thickness over wave and triangular texture patterns*

5.6.2 Effect of having a flat surface between consecutive peaks

A flat surface between consecutive peaks can help in reducing the liquid holdup by avoiding solvent accumulation in the valley region between consecutive peaks. This can effectively enhance the utilization of solvent. Keeping this observation in view we have analyzed mass transfer over a wave patterned texture separated by a flat surface of length equal to 1mm. The geometry is referred in our work as "Semi wave" and is shown in Figure 5.3. The resulting film thickness distribution over the plate is shown in Figure 5.5.

From Figure 5.5 it can be seen that the resulting film thickness isn't varying significantly from Nusselt film thickness. But the mass flux, liquid side mass transfer coefficient and the mass fraction of CO_2 at the solvent outlet, as shown in Table 5.3, were found less when compared to texture without the flat surface between the peaks. It can be due to the decrease in wave amplitude which for this texture pattern was ≈ 0.4mm.

Table 5.3: *Mass flux, liquid side mass transfer coefficient and CO_2 mass fraction at solvent outlet for different texture patterns*

Texture Pattern	**2A/λ ratio**	**λ in mm**	**F x 10^5** [mol/m^2-s]	**k_L x 10^5** [mol/Pa.s.m^2]	**CO_2 mass fraction at solvent outlet**
Plane	-	-	3.58	5.65	0.029
Triangular	0.2	3	9.4	15.6	0.0745
Triangular	0.1	3	7.7	12.6	0.06
Wave	0.2	3	9.76	16.3	0.084
Double triangle	0.2	1.5	9.77	16.3	0.084
Semi wave	0.2	3	8.52	14	0.07

5.6.3 Effect of 2A/λ ratio

The 2A/λ ratio was altered in this study by varying three amplitude (2A) values of 0.3, 0.6 and 0.9mm by retaining the λ value of 3mm. The intermediate value of 2A = 0.6mm and λ=3mm corresponds to commercial Mellapack 250-Y, as discussed in previous sections. For amplitude value of 0.9mm the film was found break into droplets by entering the gas side tangentially. This is not desirable in reactors as it can lead to the carryover of the solvent by gas. The resulting film thickness distribution is shown in Figure 5.6.

The resulting film thickness is having a thickness of ≈ 0.4mm without noticeable amplitude. The corresponding values of mass flux, liquid side mass transfer coefficient and CO_2 mass fraction at solvent outlet , as shown in Table 5.3, were found less when compared with standard Mella pack configuration. From this, it can be concluded that the amplitude of the wave plays a dominant role in the designing of texture patterns.

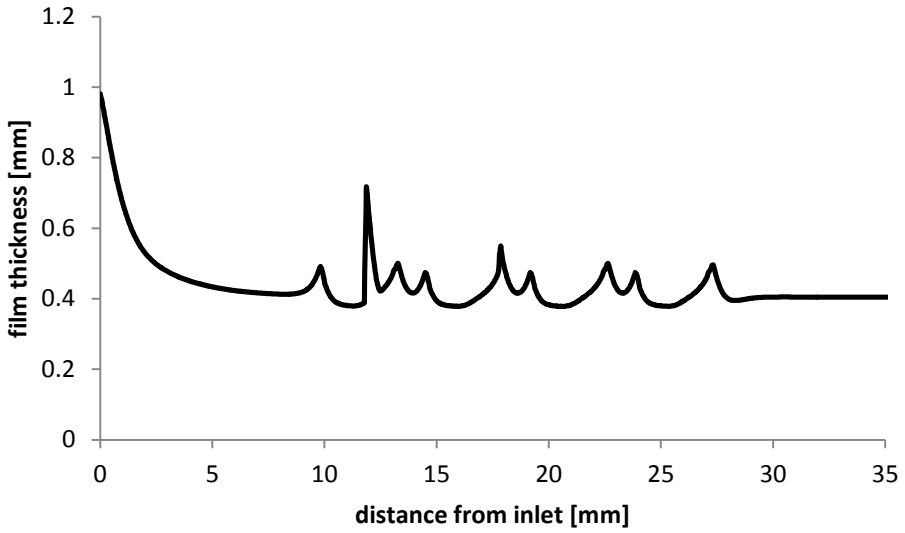

Figure 5.5: *Film thickness over semi wave texture pattern*

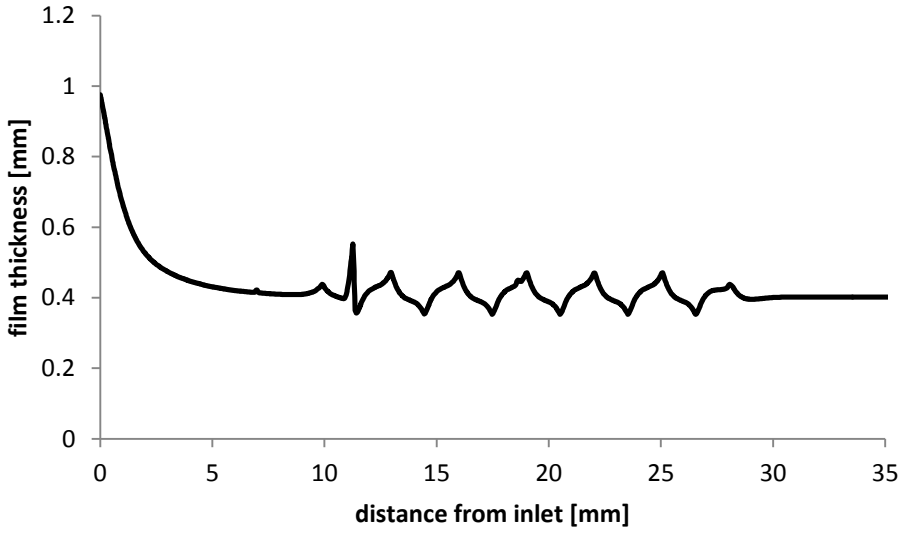

Figure 5.6: *Film thickness over texture pattern with 2a/λ ratio of 0.2 and 2A=0.3mm*

5.6.4 Effect of increasing number of textures

In the section, we investigate the effect of increasing the number of textures by retaining the 2A/λ ratio. The textures under consideration have 2A value of 0.3mm and λ value of 1.5mm. This has resulted in 'two triangular' textures in the same area of a single texture of Mella pack 250-Y. For ease, we refer this texture as "double triangle" in this article. The resulting film thickness distribution is shown in Figure 5.7.

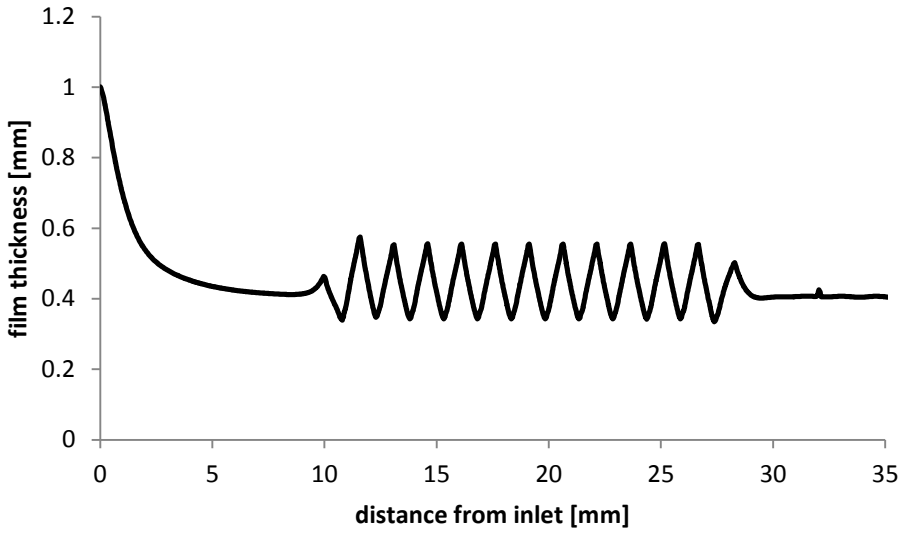

Figure 5.7: *Film thickness over double triangle texture pattern*

From the film thickness distribution, it is evident that the amplitude of the wave generated by this pattern with lesser 2A of 0.3mm and same 2A/λ is comparable in size to the wave amplitude generated by 0.6mm. The corresponding values of mass flux, liquid side mass transfer coefficient and the CO_2 mass fraction at solvent outlet, as shown in Table 3, were found to have values closer to the values generated by wave pattern with 2A values of 0.6. It can be due to the increased number of wave peaks generated by this pattern. Hence it can be safely said that the amplitude of resulting wave and number of waves generated will have direct influence over the amount of mass transfer possible by a texture pattern.

5.7 Conclusions

In this chapter, surface texture patterns influence on the physical mass transfer of CO_2 into MEA solvent was studied in detail. The study was carried by implementing *one fluid formulation* for specie transfer across immiscible phases in OpenFOAM. The mass transfer studies were initially carried for commercial Mellapack 250 Y structure and then studies were extended to structures with different amplitudes and patterns. All the simulations were carried at a fixed liquid and gas Reynolds number of $Re_L = 30$ and $Re_G = 21$. The following important observations were drawn:

1. One of the most important design parameters in the design of surface texture is 2A/λ. The value of this parameter must be less than 0.2 which otherwise will result in the breakage of the liquid film by directing the solvent to flow to gas

region resulting in the formation of solvent droplets which can eventually be carried away by gas.

2. The amplitude of the waves generated in the plane surface region was comparable to the Nusselt film thickness region but found varying by 50% in the region of textures.
3. The wave pattern texture is found to be effective when compared with the triangular texture pattern. Hence future research can be based on this kind of patterns
4. The amplitude of resulting wave and the number of waves were found to influence the mass transfer significantly

In conclusion, a surface texture with continuous wave pattern with reduced size and having amplitude to base ratio of 0.2 is suggested for better mass transfer in structured packing columns. A detailed three-dimensional study of the patterns based on these observations is carried and results are presented in the next chapters.

6. EFFECT OF SURFACE TEXTURES ON INTERFACIAL AREA

From chapters 4 and 5, it can be clearly seen that the computational mesh required to capture the details of mass transfer in the film region is very high by using the one fluid formulation. Also it was clearly found in the study by Haroun et al (Haroun et al. 2014) that the interfacial area contributes to 80% of the total mass transfer and hence the designing of the structured packing must focus on enhancing the effective interfacial area. Keeping this observation in view and using the designing parametric observations of Chapter 5, in this chapter the influence of surface textures on the interfacial area was studied in detail and also a new surface texture was proposed that is found to produce high interfacial area at low liquid flow rate.

Iso and Chen (Iso & Chen 2011) in their study about the influence of surface textures had found that the surface textures contribute significantly in enhancing the interfacial area. They have studied the influence of textures for the liquid film generated for water flowing on a flat plate in a domain filled with air. The size of the geometry was similar to the geometry of Hoffmann et al (Hoffmann et al. 2006). Sebastia-Saez (Sebastia-Saez et al. 2014) studied the influence of textures on interfacial area and also the oxygen absorption rate. They have insisted on detail investigation in this regard. The boundary condition for inlet of liquid was chosen as 0.4 mm in height along the width of the plate. This kind of inlet boundary condition was used by Xu et al (Xu et al. 2014) who studied the effect of counter current gas liquid flow on the flat plate.

6.1 Effect of Surface Textures on Interfacial Area

As the interfacial area on flat plate was well studied for water by (Xu et al. 2014; Sebastia-Saez et al. 2014) along with grid independency studies, in this study the effect of surface texture on the interfacial area was carried for MEA solvent. MEA 30% (wt %) was chosen as the solvent flowing over the plate as it is the amine solvent preferably used in industries. The properties were taken from the references mentioned in Chapter 4 and 5. The plane and texture geometry was chosen similar to the geometry of the works of Iso and Chen (Iso & Chen 2011). The mesh density used was similar to the works of Xu et al (Xu et al. 2014) with having a minimum of 8 nodes in film region. The boundary conditions were similar to the works of Iso and Chen (Iso & Chen 2011). The results are as shown in **Figure 6.1**.

The interface area on the flow was observed to achieve a quasi steady value (oscillating with less than 2% deviation for every times step) within 0.25s for plane and 2s for textured plates; all the simulations in this study were carried for 5s. From the results it can be clearly seen that the surface textures spread the solvent over the flat plate and hence enhance the available interfacial area. Also it can be observed that a full film is formed at low Reynolds number of 32 by MEA solvent which can be due to the high viscosity of the amine solvent. The film height function written as part of the thesis is found effective in visualizing the film height distribution across the plate surface. Followed by this a new texture was proposed in this thesis as shown in the Figure 6.2. The new texture was proposed on the observation of keeping the $2A/\lambda$ less than 0.2 based on the observations of Chapter 5.

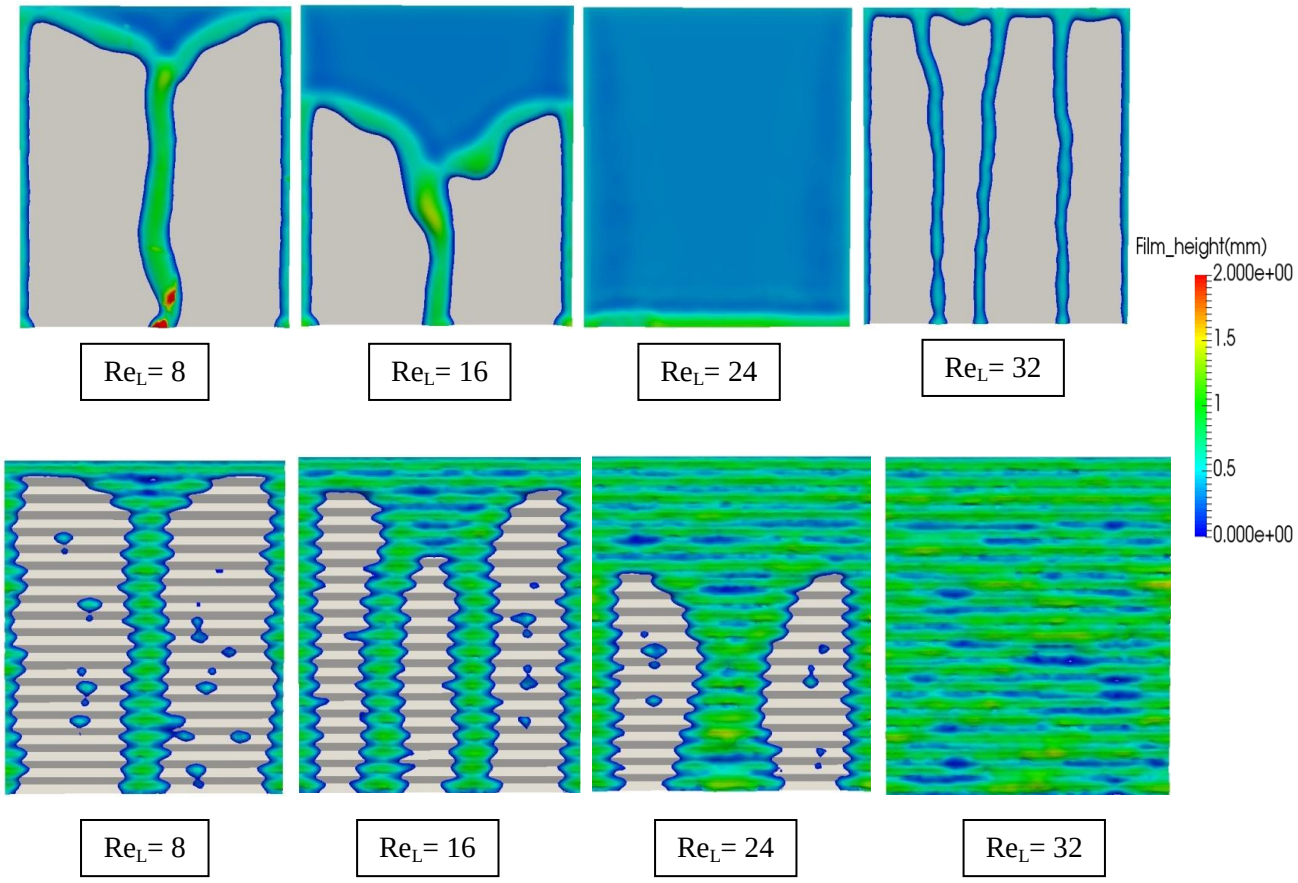

Figure 6.1: *30% MEA flow over Flat and textured plate at Re of 8, 16, 24 and 32*

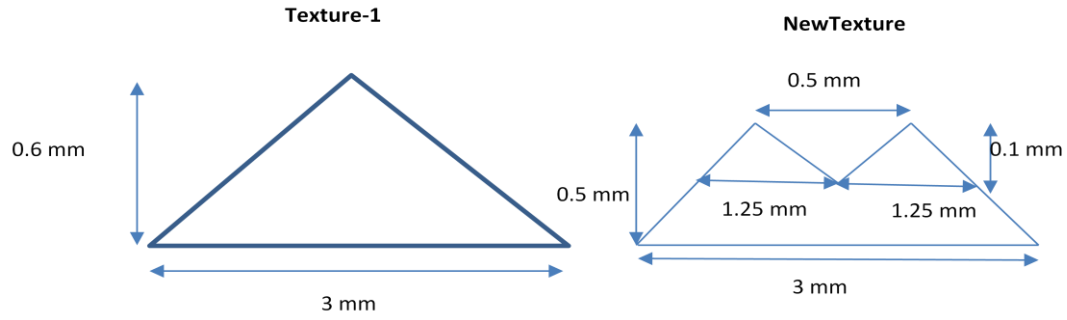

Figure 6.2: *Texture-1 similar to the texture used by Iso and Chen (2011) and the New texture developed in the present work on the right side.*

The new texture proposed was then tested starting from low Reynolds numbers. This is to verify whether the proposed texture will be effectively producing interfacial area at low Reynolds number or not. As the design was effectively based on the parameters derived in Chapter 5, the flat plate with proposed texture was able to produce a full film on entire flat plate at a Reynolds number of 16 as shown in Figure 6.3.

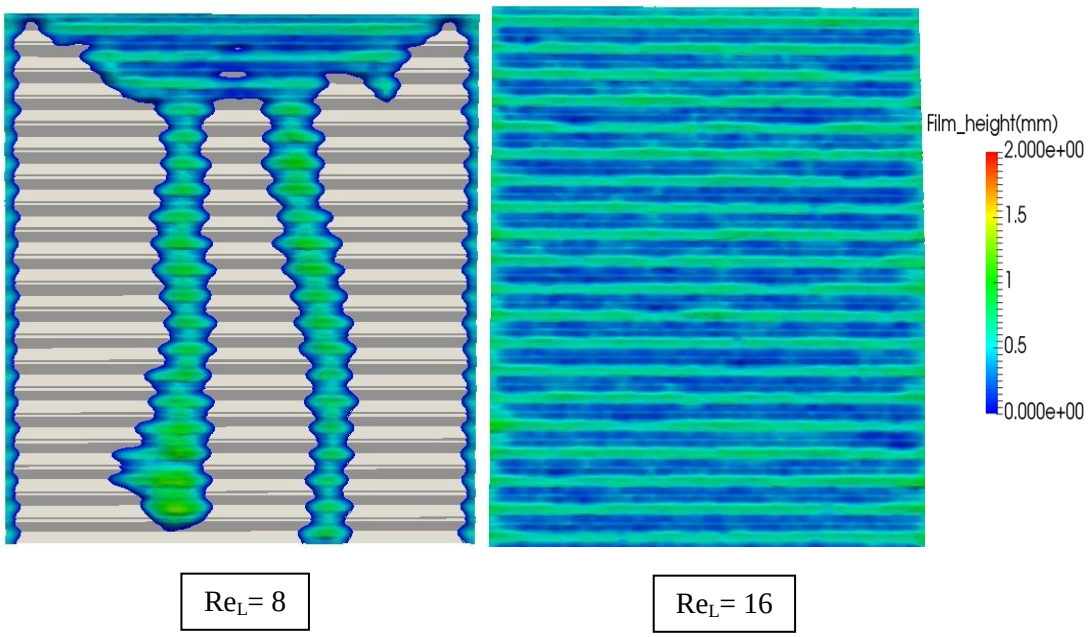

Figure 6.3: *MEA 30% solvent flow over the proposed new texture at Re_L of 8, 16.*

Wetted area plays an important role in the overall performance of the structured packing. Wetted area is defined as the ratio of the interfacial area to the plate area. It is used as a parameter to measure the effectiveness of the structured packing. The resulting wetted area for the plane and the two textured geometries (similar to Iso and Chen (Iso

& Chen 2011) and new pattern in proposed in the current thesis) is plotted against Re_L in Figure 6.4. It can be seen that the proposed surface texture produces a wetted area ratio of 1.0 at low Re_L of 16.

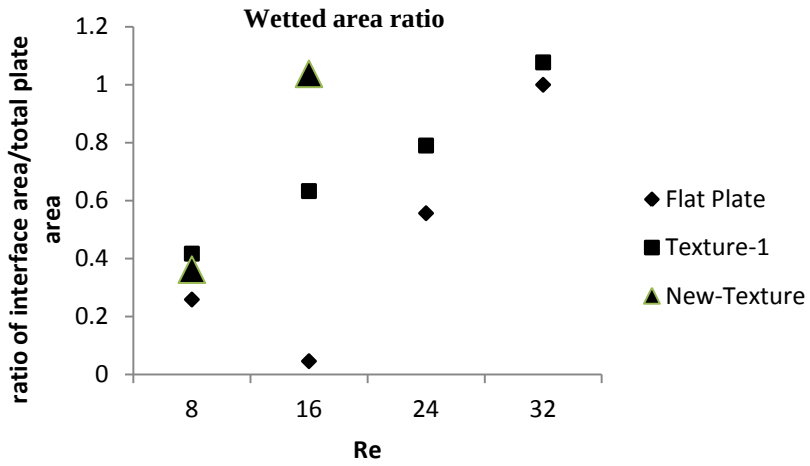

Figure 6.4: *Wetted area vs Re_L for MEA 30% for plane and surface textures.*

A part from the wetted area liquid hold up also plays an important role in determining the effective utilization of structured packing (Aferka et al. 2011). Liquid holdup can be defined as the volume of stationary liquid that exists in the form of a film on the surface of the packing or is present in voids, dead spots, and phase boundaries in the bed of packing within a column during the period in which the liquid phase descends at a constant rate onto the surface of the bed (Zakeri et al. 2012a). Using the additional code developed and implemented in this thesis (**Appendix**) the liquid hold up was calculated for plane and the two surface textures described in Figure 6.2. The results are as given in Figure 6.5:

From the results in Figure 6.5, it can be seen that the proposed new surface texture doesn't enhance the liquid hold up significantly when compared with the Texture-1 at Re_L of 16 but at the same time produces full film at Re_L of 16 as shown in Figure 6.3.

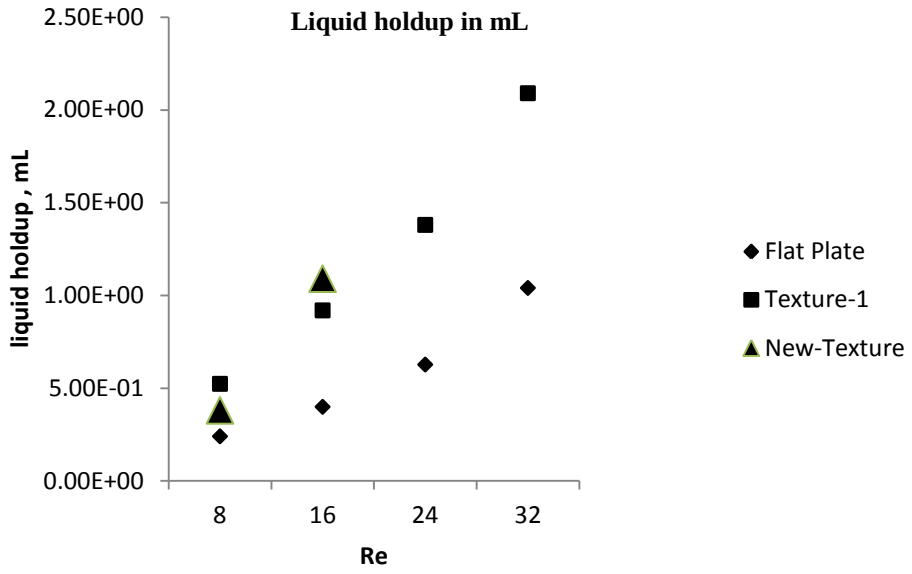

Figure 6.5: *Liquid hold up vs Re_L for MEA 30% for plane and surface textures*

6.2 Experimental Qualitative Verification of Effect of Surface Texture on Wetted Area

The proposed texture design was experimentally verified for observing the influence of texture of wetted area for selected flow rates. The flow rates were selected in a way that at these flow rates channel flow occurs on plane surface. This kind of analysis will be useful to understand the spreading phenomenon produced by surface textures.

6.2.1 Experimental setup

Since MEA requires very low flow rate (<120 ml/min), expensive and can react with coloring agent, water was chosen as working fluid for ease of experiment. Water was used at atmospheric conditions (20^0C) and the overall setup is as shown in **Figure 6.6 (a)**. Continuous and controlled flow was achieved by Longer® Gear Pump (Model WT 3000). The flow rates chosen for this work were 450, 550 and 600 mL/min. These flow rates were chosen after repeating experiments twice by adjusting flow rate carefully, starting with high flow rate of 800 mL/min (full film condition) and decreasing by 10 mL/min every instant, and allowing the flow to settle to achieve steady state. Methyl blue was used as a coloring agent. The plane and textured plates were made with Aluminium from a local firm in Turkey. No special arrangement was made

at inlet of the plate. The flow on the plates is open to atmosphere and is under the influence of gravity and surface tension forces. The plates, as shown in **Figure 6.6(b),** were having an extension of 20mm upstream and downstream to allow the liquid to form film at the entrance of the textured region surface. All the walls except the metal plate were made of PVC transparent plates. The experiment differs from the experiments carried by Hoffmann et al (Hoffmann et al. 2006) (for a flat plate) and and Iso and Chen (Iso & Chen 2011) (flat and textured plate), in terms of the material of construction (which is aluminum in this study) and the side walls (made up of PVC in this study). CFD simulations were carried for the channel flow conditions of 450 mL/min using water as working fluid with density 1000 kg/m^3, γ=10^{-6} m^2/s and surface tension of 0.07 N/m. The contact angle with the wall was fixed as 70^0. The computational domain and boundary conditions were same to that used for the MEA solvent simulations in the section 6.1. The simulations were carried for a time of 1s.

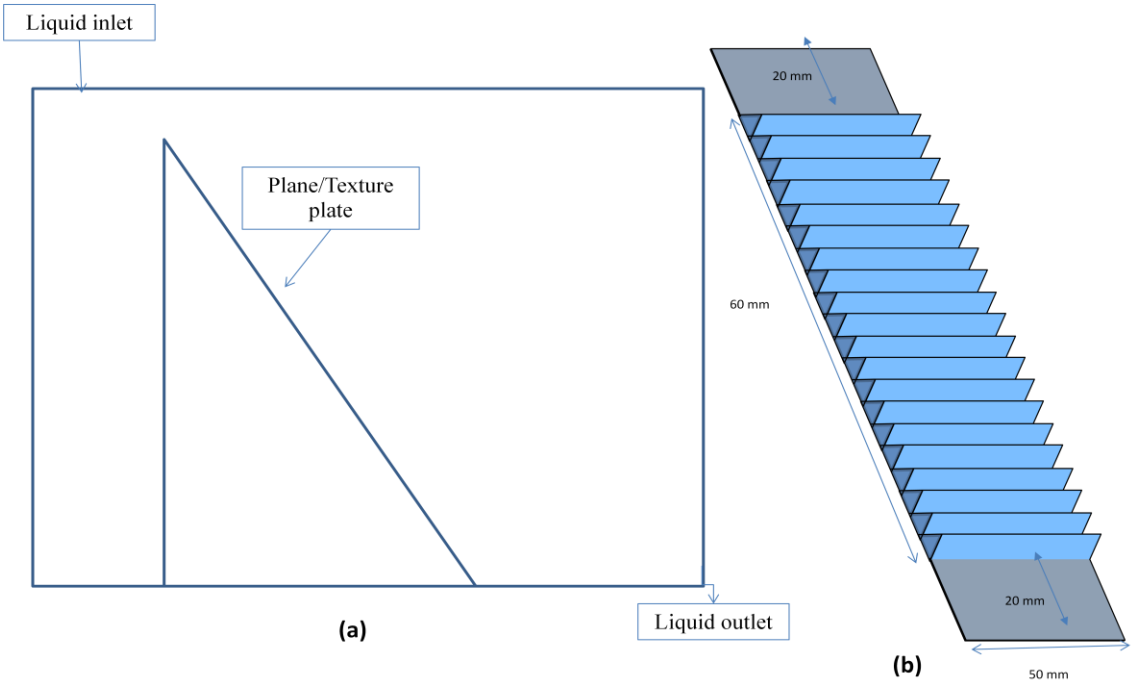

Figure 6.6: *Overall experimental setup of flat and textured plate investigation*

6.2.2 Results

The resulting flow patterns at these experimental flow rates are as shown in Figure 6.7, Figure 6.8 and Figure 6.9. The resulting flow patterns on the experiment were compared to the CFD simulations in Figure 6.10, Figure 6.11 ad Figure 6.12. The textured plate area in the middle of the plate section, which is the exact size of the computational domain, was used to compare the CFD simulation results (contours of iso-surface of volume fraction, α=0.5).

A clear enhancement in wetted area was found and was highlighted for ease of identification. It can be clearly seen from the results that the proposed texture produces enhanced wetted area even at low flow rate (450 mL/min) when compared with the plane and the surface texture that was used in the previous experiments by Iso and Chen (Iso & Chen 2011). CFD simulations results are in close approximation of the experimental results produced for the flat plate. But for the textured plates, the experimental flow patterns were found to have asymmetry distribution of the film where as CFD simulations found to result in symmetry fluid film. The asymmetry in experimental results can be due to the metal surface finishing of the textured plates whereas the symmetry nature of the film in the CFD results can be due to the treatment of the plates as perfectly finished without roughness.

6.3 Conclusions

From the works of this chapter it is evident that a new design of surface texture utilizing the proposed design suggestions in Chapter 5, like the one developed in this chapter, can significantly enhance the available wetted area (gas-liquid interfacial area) and eventually lead to enhanced mass transfer.

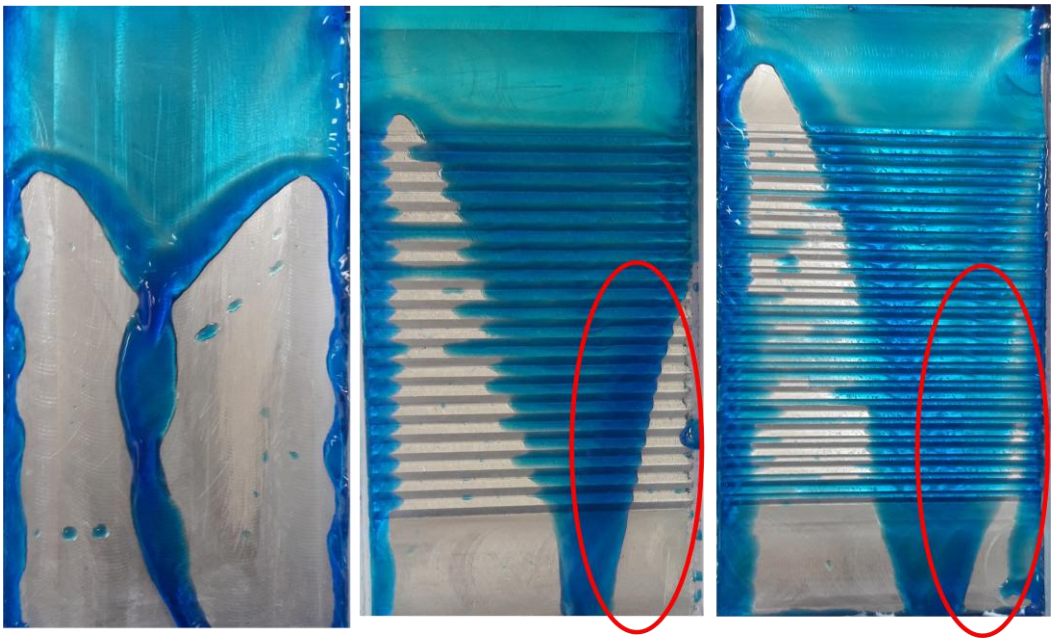

Figure 6.7: *Flow pattern generated by water at a flow rate of 450 mL/min on (a) plane, (b) Iso and Chen(2011) and (c) new texture pattern proposed in this thesis*

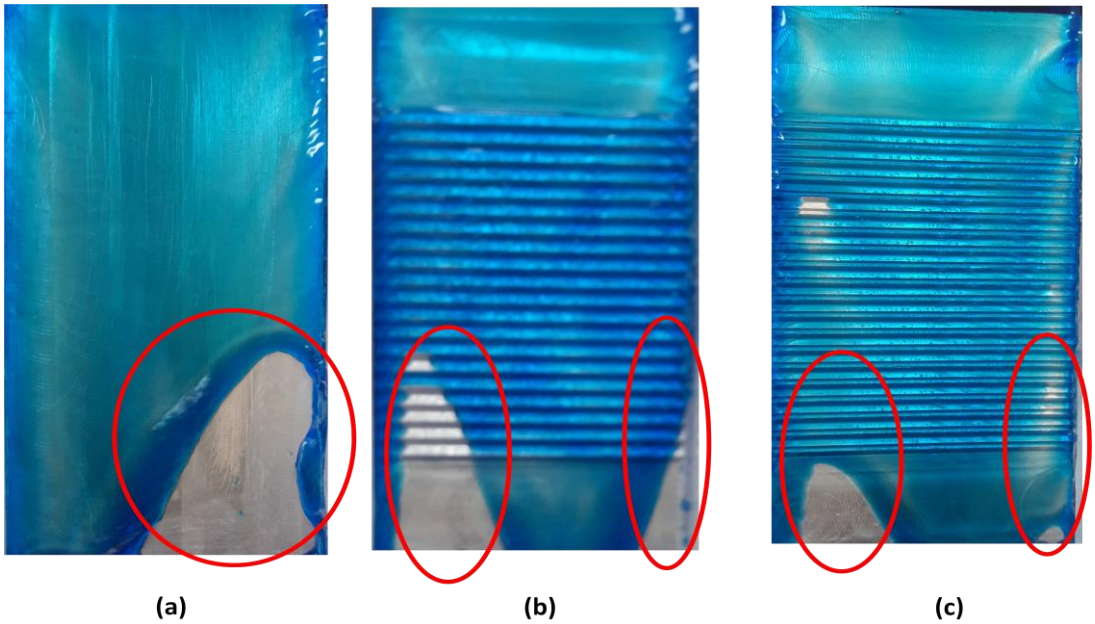

Figure 6.8: *Flow pattern generated by water at a flow rate of 550 mL/min on (a) plane, (b) Iso and Chen (2011) and (c) new texture pattern proposed in this thesis*

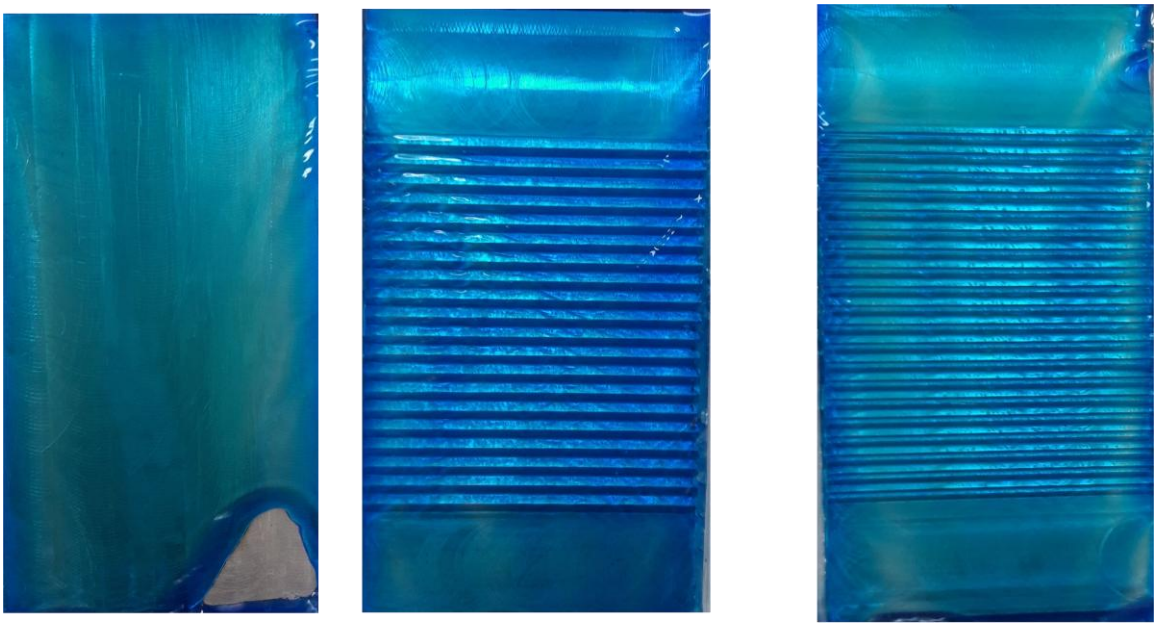

Figure 6.9: *Flow pattern generated by water at a flow rate of 600 mL/min on (a) plane, (b) Iso and Chen (2011) and (c) New texture pattern proposed in this thesis*

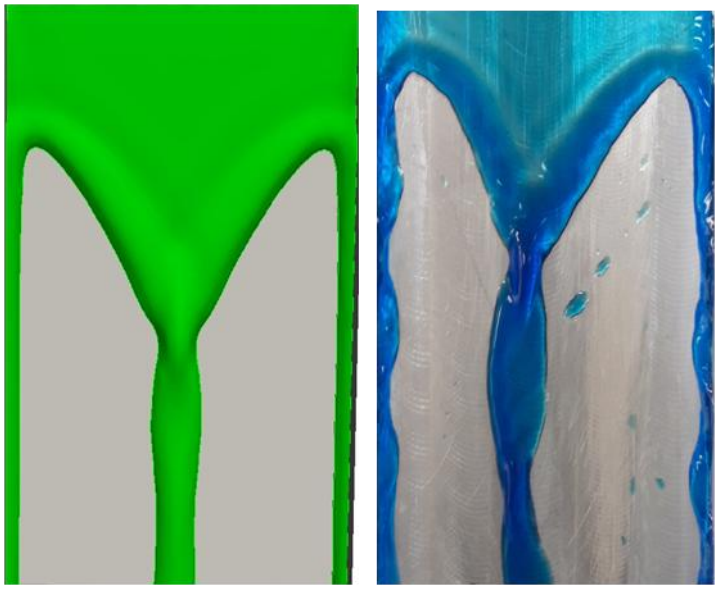

Figure 6.10. *CFD and experiment results at 450 mL/min for a plane surface*

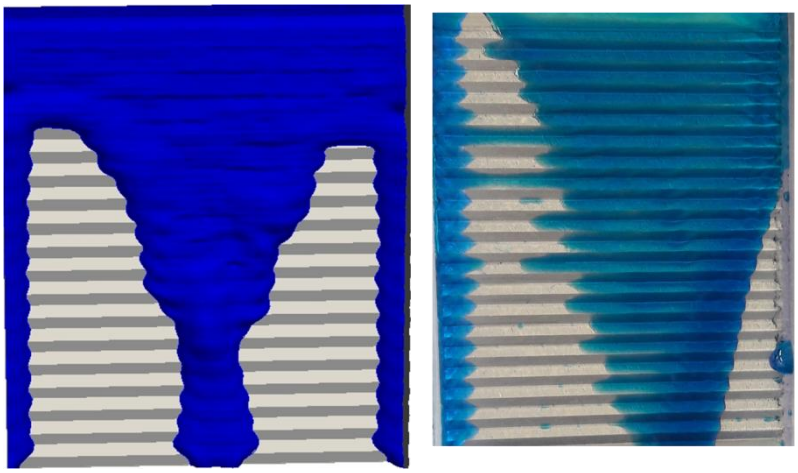

Figure 6.11: *CFD and experiment results at 450 mL/min for a textured plate surface whose geometry is similar to Iso and Chen (2011)*

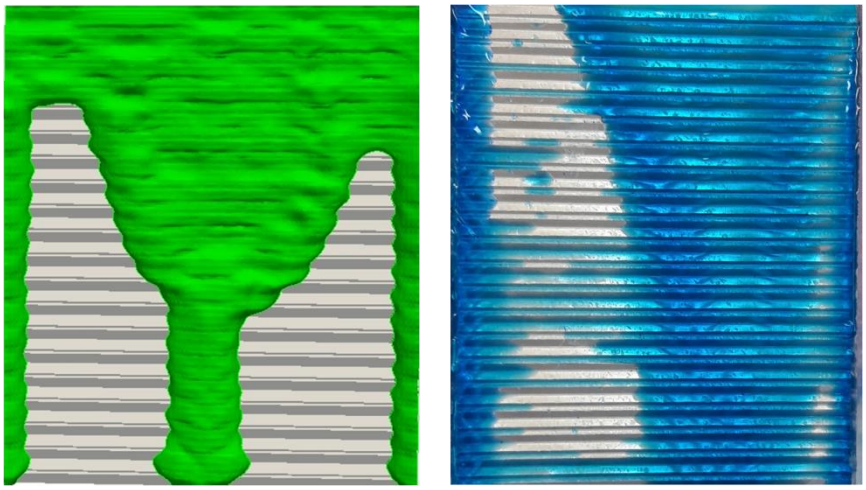

Figure 6.12: *CFD and experiment results at 450 mL/min for a textured plate surface developed in this work*

7. MESO-SCALE MODELING OF PRESSURE DROP IN PACKED COLUMNS WITH SURFACE TEXTURES

The aim of the meso-scale analysis in the literature has always been to calculate the pressure drop that constitutes the major part of the overall operational cost of a post combustion CCS facility (Li et al. 2016). The calculation of pressure drop can be divided into two parts as the dry and wet pressure drop. In this chapter the effect of surface textures on the pressure drop is presented in detail for MEA 30% solvent with determining the wet pressure drop as main objective.

7.1 Overall Description of Geometry and Modeling Approach

As outlined in Chapter 3, the procedure of calculating the pressure drop involves evaluation of the relation between the pressure drop and kinetic energy in a way similar to Darcy-Weisbach (Brown 2002) equation. For calculating the wet pressure drop, the procedure suggested by Fernandes et al (Fernandes et al. 2009), pseudo single phase approach is used. The approach involves the calculation of effective gas velocity which includes the effect of the decrease in the available gas volume using the liquid holdup. The liquid holdup is calculated by the user code developed as part of the thesis (**Appendix**). RNG k-ε turbulence model (Yakhot et al. 1992) was used for modeling turbulence effects as suggested by Li et al (Li et al. 2016).

The geometry considered was of height of 82mm with a width of 96mm having three consecutive corrugations of size of that of commercial Mellapak 250-X . Meso-scale analysis using three consecutive corrugations was proven preferable by works of Li et al (Li et al. 2016). The Mellapak 250-X corrugations have a base of 22.6 mm and a height of 11.3 m (Haroun et al. 2014). The corrugations are considered with plane as well as with the textures as described in Chapter 6. The overall geometry is as shown in Figure 7.1.The mesh density for calculating the liquid holdup was similar to the work in Chapter 6. For pressure drop analysis, the mesh was sufficiently refined on all the walls in order to maintain the y+ less than 5 (well less than 4) in order to accurately capture the turbulent pressure losses by using RNG k-ε turbulence model. The gas was flowing in bottom up direction.

As a first step, the effect of dry and wet pressure drops for plane corrugations were calculated using CFD and results were compared with the experimental works of Zakari et al (Zakeri et al. 2012b) who carried the effect pressure drop calculations for

MEA 30% on Sulzer Mellapak 2X packing. Then the analysis was extended to geometry with both the textures (Texture-1 and New-Texture) described in Chapter 6.

7.2 Dry and Wet Pressure Drop of Plane Geometry

As a first step liquid holdup was determined as for liquid load of $5m^3/m^2$-h and $25m^3/m^2$-h using the procedure described in Chapter 6 as 0.0447 and 0.1. The results for dry pressure drop (without liquid load) and wet pressure drop are shown in Figure 7.2

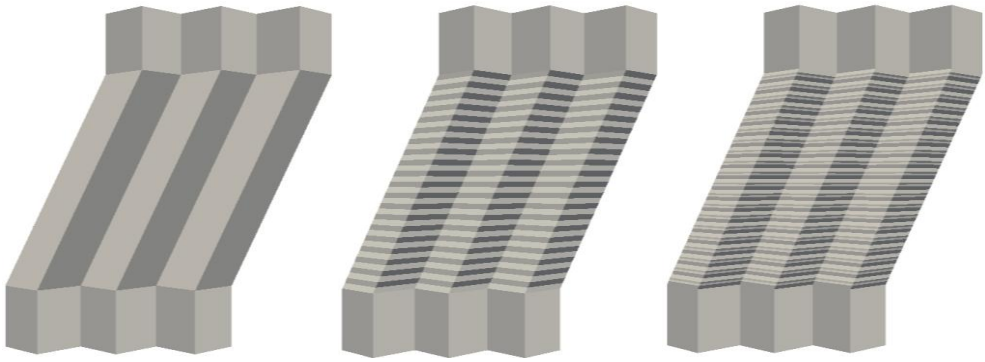

(a) (b) (c)

Figure 7.1: *Geometry with three Mellapack-250X corrugations with (a) plane (b) Texture1 and (c) New texture developed in this thesis*

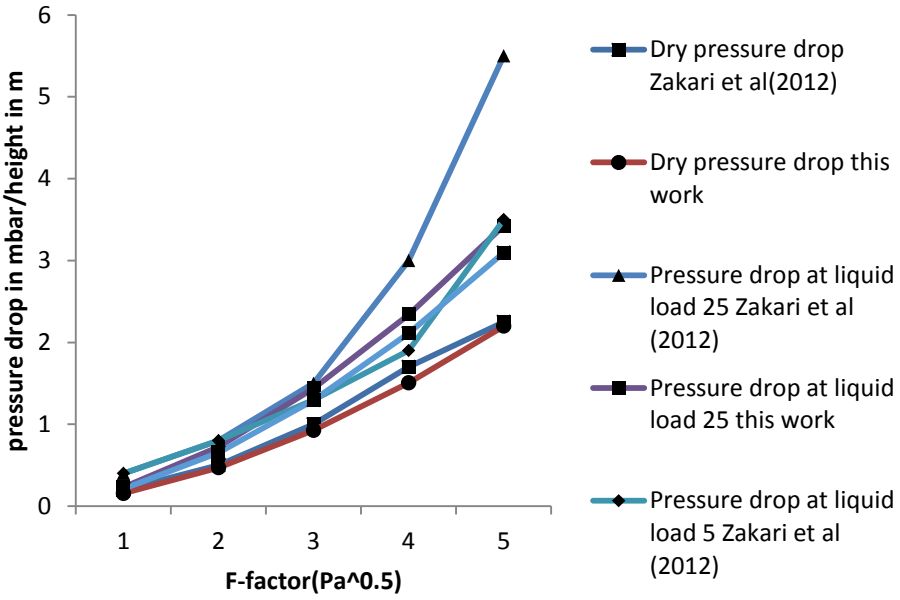

Figure 7.2: *Dry and wet pressure drop of Mellapack-250X corrugations with plane surface compared with the results of Zakari et al (2012)*

From Figure 7.2 it can be clearly seen that the non-linear dependency of pressure drop with kinetic energy (F-factor) is clearly captured by current simulations. The results closely follow the experimental results at lower liquid loads and deviate at higher liquid loads which can be due to the differences in the geometry under simulation and other modeling and experimental deviations. This kind of deviations are found inevitable when simulations are compared with experimental results (Sebastia-Saez et al. 2015a).

7.3 Comparison of Dry and Wet Pressure Drop of Plane, Texture-1 & New-texture

Adopting a similar procedure of Section 7.1, the dry and wet pressure drops were calculated for liquid load of $5m^3/m^2$-h and $25m^3/m^2$-h for all geometries shown in Figure 7.1. The resulting liquid holdup values are summarized in Table 7.1 and the resulting plot of pressure drop vs F-factor is shown in Figure 7.3, Figure 7.4 and Figure 7.5.

From the Figure 7.3, Figure 7.4 and Figure 7.5, it can be clearly seen that the textures result in higher pressure drop when operated at same liquid load and F-factor. It is due to the resistance offered by the surface textures to the flow. But in practice the geometries with textured packing, as detailed in Chapter 6, are operated at low liquid loads as they produce higher interfacial areas at low liquid loads. At low liquid loads texture geometries produce lesser pressure drop when compared with the plane geometries operated at high liquid loads to produce same interfacial area.

Table 7.1: *Liquid hold up values at different liquid loads*

liquid load (m^3/m^2-h)	Plane	Texture-1	New-Texture
5	0.0447	0.034	0.0311
25	0.1	0.0963	0.0651

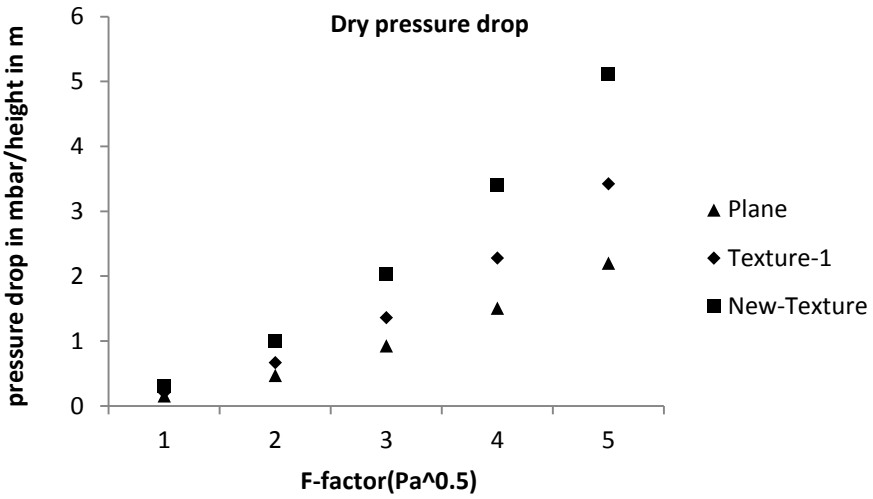

Figure 7.3: *Dry pressure drop of Mellapack-250X corrugations with plane and texture geometries*

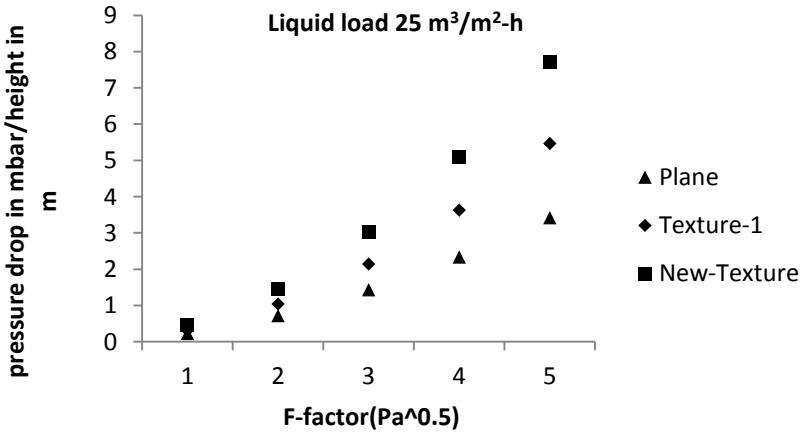

Figure 7.4: *Wet pressure drop of Mellapack-250X corrugations at liquid load of 25 m^3/m^2-h with plane and texture geometries*

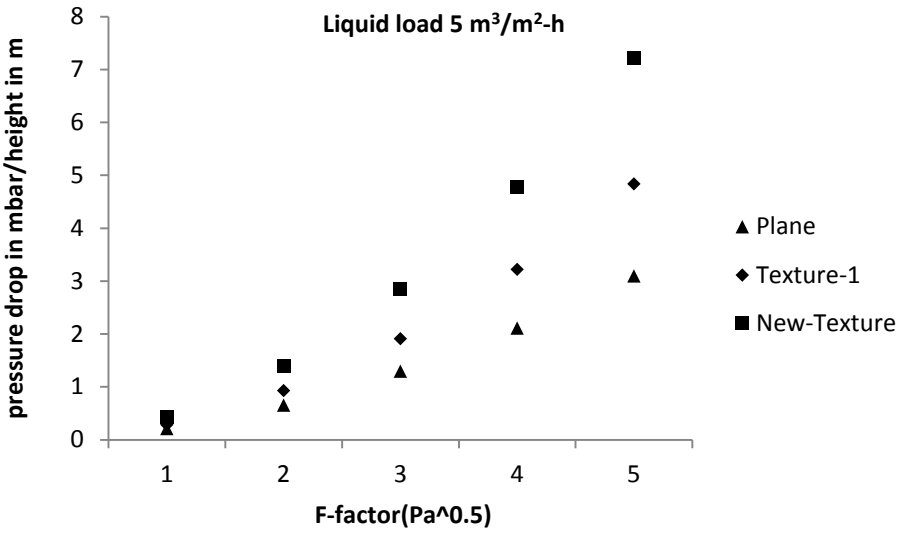

Figure 7.5: *Wet pressure drop of Mellapack-250X corrugations at liquid load of 5m^3/m^2-h with plane and texture geometries*

7.4 Conclusions

From detailed analysis of dry and wet pressure drop under the influence of surface textures carried in this chapter it can be concluded that addition of textures will lead to increase in pressure drop. But since the textures effectively spread the fluid resulting in higher interfacial area, geometries with surface textures can be operated at low liquid loads which can eventually reduce the operating cost in terms of pressure drop. CFD is found an effective tool in understanding this phenomena in detail and hence carrying a detailed CFD analysis can help in deciding the design for desired gas liquid flows.

8. FINAL REMARKS

This thesis deals in detail about the influence of structured packing surface texture on CO_2 absorption. Simulations were carried using OpenFOAM (open source CFD software). Even though OpenFOAM is a general purpose CFD code, it allows additional code to be implemented using C++ language for deriving the results that aren't available in default software.

8.1 Contributions to Knowledge:

The contributions of the present thesis are listed as follows:

1. This thesis discuss the most reliable approach called *one fluid formulation* for modeling the mass transfer across immiscible phases and suggests methods to overcome limitations found during its implementation in OpenFOAM. Also a procedure is suggested to reduce the overall computational resource required for simulating the system of equations.
2. The additional functions implemented helps users to derive correct values of liquid hold up, film height distribution and interfacial area through developed additional functions
3. This thesis proposes a best practice of keeping "amplitude to base ratio of a texture <0.2".
4. A new texture was developed based on the suggested amplitude to base ratio and verified by both CFD and experiment for its effectiveness of producing higher wetted area (gas liquid interfacial area) when compared with existing commercial packing textures.
5. This thesis derives the pressure drop by considering detailed surface texture geometry at meso-scale for the first time.

8.2 Summary of Results:

Surface texture patterns on the structured packing elements are found to highly influence the efficiency of the post combustion carbon capture and storage process. The importance of surface textures and need of detailed investigations were highlighted in the literature section of the thesis. As discussed in literature, the surface texture patterns are of micro scale and demand detail investigations at this scale. OpenFOAM (open source CFD software) was effectively used for this purpose.

The study was initiated by carrying a detailed investigation of approaches useful in modeling the mass transfer. The most effective approach, one fluid formulation, was implemented and verified in Chapter 3. Advantages, limitations and possible solutions to overcome these limitations were discussed in detail in Chapter 4. It was concluded that modeling of mass transfer by one fluid formulation is a promising approach and an alternative to experimentation.

The study was then extended derive the design parameters of surface texture patterns which can influence the physical mass transfer of CO_2 into MEA solvent in Chapter 5. The mass transfer studies were initially carried for commercial Mellapack 250 Y structure and then studies were extended to structures with different amplitudes and patterns. One of the most important design parameters in the design of surface texture was found as $2A/\lambda$ (where 2A represent the amplitude and λ the base size of the texture pattern). A value of $2A/\lambda$ being less than 0.2 is proposed for future designs. Also increasing the number of waves was found to influence the mass transfer in similar manner of the texture having higher size at same $2A/\lambda$ ratio. These observations have shown a potential of designing new texture.

A new texture pattern was proposed in Chapter 6. The pattern was found to produce full film, maximum interfacial area, at low flow rates when compared with the available commercial texture patterns. The pattern was also experimentally verified. The thesis was then extended to study the influence of texture patterns on pressure drop using established methods in Chapter 7.

Overall OpenFOAM (open source CFD software) was effectively utilized in investigating the influence of surface texture patterns on the CO_2 absorption and other parameters, like wetted area and pressure drop, of significant importance. Design rules were suggested and a new texture pattern was developed based on these rules and was found to be effective in terms of experiment and by CFD.

8.3 Future Work:

Potential areas of expanding the current research were found during this work and are listed below for perusal of the scientific community.

1. The “diffusive interface” region due to the VOF formulation in interFOAM module needs to be developed to produce a sharp interface using coarse mesh.

Even though there are new advancements in recent times like “iso-advection” algorithm a lot need to be done in this domain.

2. Even though modeling reactive mass transfer can be achieved using “one fluid formulation” the higher mesh requirement is a limitation that needs to be developed to produce reliable results on coarse mesh utilizing least computational resources.
3. The surface textures developed in this thesis are verified at micro-scale and proven effective. But in order to commercially utilize the outcome commercially, a pilot and full scale experiment need to be carried.
4. Discrepancies during scale up are a potential area of research both in terms of CFD and experiment.
5. Impact of wave patterns generated by textures on mass transfer in turbulent flow conditions can be a potential research as there isn’t detailed research outcome available in this regard.

REFERENCES

[1] Aaron, D. & Tsouris, C., 2005. Separation of CO_2 from Flue Gas: A Review. *Separation Science and Technology*, 40(1–3), pp.321–348. Available at: http://www.tandfonline.com/doi/abs/10.1081/SS-200042244.

[2] Aferka, S. et al., 2011. Tomographic measurement of liquid hold up and effective interfacial area distributions in a column packed with high performance structured packings. *Chemical Engineering Science*, 66(14), pp.3413–3422.

[3] Ahn, H.T. & Shashkov, M., 2007. Multi-material interface reconstruction on generalized polyhedral meshes. *Journal of Computational Physics*, 226(2), pp.2096–2132.

[4] Ali, S.H., 2005. Kinetics of the reaction of carbon dioxide with blends of amines in aqueous media using the stopped-flow technique. *International Journal of Chemical Kinetics*, 37(7), pp.391–405.

[5] Amini, Y., Karimi-Sabet, J. & Esfahany, M.N., 2016. Experimental and Numerical Simulation of Dry Pressure Drop in High-Capacity Structured Packings. *Chemical Engineering and Technology*, 39(6), pp.1161–1170.

[6] Armstrong, L.M., Gu, S. & Luo, K.H., 2013. Dry pressure drop prediction within Montz-Pak B1-250.45 packing with varied inclination angles and geometries. *Industrial and Engineering Chemistry Research*, 52(11), pp.4372–4378.

[7] Aronu, U.E. et al., 2011. Solubility of CO2in 15, 30, 45 and 60 mass% MEA from 40 to 120°C and model representation using the extended UNIQUAC framework. *Chemical Engineering Science*, 66(24), pp.6393–6406.

[8] Aroonwilas, A. et al., 2003. Mathematical modelling of mass-transfer and hydrodynamics in CO2absorbers packed with structured packings. *Chemical Engineering Science*, 58(17), pp.4037–4053.

[9] Aroonwilas, A., Tontiwachwuthikul, P. & Chakma, A., 2001. Effects of operating and design parameters on CO2 absorption in columns with structured packings. *Separation and Purification Technology*, 24(3), pp.403–411.

[10] Asendrych, D., Niegodajew, P. & Drobniak, S., 2013. CFD modelling of CO2 capture in a packed bed by chemical absorption. *Chemical and Process Engineering - Inzynieria Chemiczna i Procesowa*, 34(2), pp.269–282.

[11] Bernhardsen, I.M. et al., 2017. Performance of MAPA Promoted Tertiary Amine Systems for CO2 Absorption: Influence of Alkyl Chain Length and Hydroxyl Groups. In *Energy Procedia*. pp. 1682–1688.

[12] Biliyok, C. & Yeung, H., 2013. Evaluation of natural gas combined cycle power plant

for post-combustion CO2 capture integration. *International Journal of Greenhouse Gas Control*, 19, pp.396–405.

[13] Boccardo, G. et al., 2015. Validation of a novel open-source work-flow for the simulation of packed-bed reactors. *Chemical Engineering Journal*, 279, pp.809–820.

[14] Bothe, D. et al., 2004. Direct numerical simulation of mass transfer between rising gas bubbles and water. *Bubbly Flows: Analysis, Modelling and Calculation*, pp.159–174. Available at: http://apps.webofknowledge.com.gate6.inist.fr/full_record.do?product=UA&search_mode=GeneralSearch&qid=1&SID=N1WZwAVMXiUl7fGzniS&page=1&doc=1.

[15] Brackbill, J.U., Kothe, D.B. & Zemech, C., 1992. Brackbill A continuum method for modeling surface tension 1992.pdf. *Journal of Computational Physics*, 100(2), pp.335–354.

[16] Brinkmann, U., Janzen, A. & Kenig, E.Y., 2014. Hydrodynamic analogy approach for modelling reactive absorption. *Chemical Engineering Journal*, 250, pp.342–353.

[17] Brown, G.O., 2002. The History of the Darcy-Weisbach Equation for Pipe Flow Resistance. In *Environmental and Water Resources History*. pp. 34–43. Available at: http://ascelibrary.org/doi/abs/10.1061/40650%282003%294.

[18] Caplow, M., 1968. Kinetics of Carbamate Formation and Breakdown. *Journal of the American Chemical Society*, 90(24), pp.6795–6803.

[19] CHEN, J. et al., 2009. CFD Simulation of Flow and Mass Transfer in Structured Packing Distillation Columns. *Chinese Journal of Chemical Engineering*, 17(3), pp.381–388.

[20] Cooke, J.J. et al., 2014. Adaptive mesh refinement of gas-liquid flow on an inclined plane. *Computers and Chemical Engineering*, 60, pp.297–306.

[21] Cooke, J.J., 2016. *Modelling of reactive absorption in gas-liquid flows on structured packing*. UNIVERSITY OF SOUTHAMPTON.

[22] Crooks, J.E. & Donnellan, J.P., 1989. Kinetics and mechanism of the reaction between carbon dioxide and amines in aqueous solution. *Journal of the Chemical Society, Perkin Transactions 2*, (4), p.331. Available at: http://xlink.rsc.org/?DOI=p29890000331.

[23] Danckwerts, P. V., 1979. The reaction of CO2 with ethanolamines. *Chemical Engineering Science*, 34(4), pp.443–446.

[24] Davidson, M.R. & Rudman, M., 2002. Volume-of-fluid calculation of heat or mass transfer across deforming interfaces in two-fluid flow. *Numerical Heat Transfer, Part B: Fundamentals*, 41(3–4), pp.291–308.

[25] Deshpande, S.S., Anumolu, L. & Trujillo, M.F., 2012. Evaluating the performance of the two-phase flow solver interFoam. *Computational Science & Discovery*, 5(1),

p.14016. Available at: http://stacks.iop.org/1749-4699/5/i=1/a=014016?key=crossref.48e889e2d1a207d9665630feb80f2a41.

[26] Dianat, M., Skarysz, M. & Garmory, A., 2017. A Coupled Level Set and Volume of Fluid method for automotive exterior water management applications. *International Journal of Multiphase Flow*, 91, pp.19–38.

[27] Ding, H. et al., 2015. CFD simulation and optimization of winpak-based modular catalytic structured packing. *Industrial and Engineering Chemistry Research*, 54(8), pp.2391–2403.

[28] Edge, P.J. et al., 2013. Integrated fluid dynamics-process modelling of a coal-fired power plant with carbon capture. *Applied Thermal Engineering*, 60(1–2), pp.242–250.

[29] Fei, Y. et al., 2015. Evaluation of the potential of retrofitting a coal power plant to oxy-firing using CFD and process co-simulation. *Fuel Processing Technology*, 131, pp.45–58.

[30] Fernandes, J. et al., 2009. Application of CFD in the study of supercritical fluid extraction with structured packing: Wet pressure drop calculations. *Journal of Supercritical Fluids*, 50(1), pp.61–68.

[31] Fischer, L., Bühlmann, U. & Melcher, R., 2003. Characterization of high-performance structured packing. *Chemical Engineering Research and Design*, 81(1), pp.79–84.

[32] Fluent Inc., 2011. ANSYS Fluent 14.0 UDF manual. *Knowledge Creation Diffusion Utilization*, 15317(November), p.566. Available at: http://www1.ansys.com/customer/content/documentation/121/fluent/flwb.pdf.

[33] Fourati, M., Roig, V. & Raynal, L., 2012. Experimental study of liquid spreading in structured packings. *Chemical Engineering Science*, 80, pp.1–15.

[34] Fu, D. et al., 2012. Experiments and model for the surface tension of carbonated monoethanolamine aqueous solutions. *Science China Chemistry*, 55(7), pp.1467–1473. Available at: http://link.springer.com/10.1007/s11426-012-4641-7.

[35] Giovanni Astarita ,David W. Savage, A.B., 1983. *Gas Treating with Chemical Solvents*,

[36] Haelssig, J.B. et al., 2010. Direct numerical simulation of interphase heat and mass transfer in multicomponent vapour-liquid flows. *International Journal of Heat and Mass Transfer*, 53(19–20), pp.3947–3960.

[37] Halim, H.N.A., Shariff, A.M. & Bustam, M.A., 2015. High pressure CO<inf>2</inf> absorption from natural gas using piperazine promoted 2-amino-2-methyl-1-propanol in a packed absorption column. *Separation and Purification Technology*, 152, pp.87–93.

[38] von Harbou, I., Mangalapally, H.P. & Hasse, H., 2013. Pilot plant experiments for two new amine solvents for post-combustion carbon dioxide capture. *International Journal of Greenhouse Gas Control*, 18, pp.305–314.

[39] Haroun, Y., Legendre, D. & Raynal, L., 2010. Volume of fluid method for interfacial reactive mass transfer: Application to stable liquid film. *Chemical Engineering Science*, 65(10), pp.2896–2909.

[40] Haroun, Y. & Raynal, L., 2016. Use of Computational Fluid Dynamics for Absorption Packed Column Design. *Oil and Gas Science and Technology*, 71(3).

[41] Haroun, Y., Raynal, L. & Alix, P., 2014. Prediction of effective area and liquid hold-up in structured packings by CFD. *Chemical Engineering Research and Design*, 92(11), pp.2247–2254.

[42] Haroun, Y., Raynal, L. & Legendre, D., 2012. Mass transfer and liquid hold-up determination in structured packing by CFD. *Chemical Engineering Science*, 75, pp.342–348.

[43] Henry Z. Kister, 1992. *Distillation Design*,

[44] Hernández, J. et al., 2008. A new volume of fluid method in three dimensions - Part I: Multidimensional advection method with face-matched flux polyhedra. *International Journal for Numerical Methods in Fluids*, 58(8), pp.897–921.

[45] Higbie, R., 1935a. The Rate of Absorption of a Pure Gas Into a Still Liquid During Short Periods of Exposure. *Transactions of American Institute of Chemical Engineers*, (31), pp.365–389.

[46] Higbie, R., 1935b. The rate of absorption of a pure gas into a still liquid during short periods of time. *Transactions of the American Institute of Chemical Engineers*, 31, pp.365–389.

[47] Hirt, C.W. & Nichols, B.D., 1981. Volume of fluid (VOF) method for the dynamics of free boundaries. *Journal of Computational Physics*, 39(1), pp.201–225.

[48] Hoffmann, A. et al., 2006. Detailed investigation of multiphase (gas-liquid and gas-liquid-liquid) flow behaviour on inclined plates. *Chemical Engineering Research and Design*, 84(2 A), pp.147–154.

[49] Hoffmann, A. et al., 2004. Fluid dynamics in multiphase distillation processes in packed towers. *Computer Aided Chemical Engineering*, 18(C), pp.199–204.

[50] Hosseini, S.H. et al., 2012. Computational fluid dynamics studies of dry and wet pressure drops in structured packings. *Journal of Industrial and Engineering Chemistry*, 18(4), pp.1465–1473.

[51] Hu, J. et al., 2014. Numerical simulation of carbon dioxide (CO2) absorption and interfacial mass transfer across vertically wavy falling film. *Chemical Engineering Science*, 116, pp.243–253.

[52] Huang, J. et al., 2015. Hydrodynamics of layered wire gauze packing. *Industrial and Engineering Chemistry Research*, 54(17), pp.4871–4878.

[53] Iliuta, I., Petre, C.F. & Larachi, F., 2004. Hydrodynamic continuum model for two-phase flow structured-packing-containing columns. *Chemical Engineering Science*, 59(4), pp.879–888.

[54] IPCC, 2005. *IPCC special report on carbon dioxide capture and storage*,

[55] Iso, Y. et al., 2013. Numerical and experimental study on liquid film flows on packing elements in absorbers for post-combustion CO2 capture. In *Energy Procedia*. pp. 860–868.

[56] Iso, Y. & Chen, X., 2011. Development of Numerical Prediction of Liquid Film Flows on Packing Elements in Absorbers. *IHI Engineering Review*, 44(2), pp.1–8. Available at: http://ihins.ihi.co.jp/var/ezwebin_site/storage/original/application/72d421f60a35c7985f2ddca0b768e0f2.pdf.

[57] Ivey, C.B. & Moin, P., 2017. Conservative and bounded volume-of-fluid advection on unstructured grids. *Journal of Computational Physics*, 350, pp.387–419.

[58] Jagannath, R.M., 2015. *Two-Phase CFD Simulation of Turbulent Gas-Driven Liquid Film Flows on Heated Walls*.

[59] Janzen, A. et al., 2013. Investigation of liquid flow morphology inside a structured packing using X-ray tomography. *Chemical Engineering Science*, 102, pp.451–460.

[60] Jasak, H. & Weller, H., 1995. Interface tracking capabilities of the inter-gamma differencing scheme. *Unknown*, (2), pp.1–9. Available at: http://powerlab.fsb.hr/ped/kturbo/OpenFOAM/docs/InterTrack.pdf.

[61] Kale, C., G??rak, A. & Schoenmakers, H., 2013. Modelling of the reactive absorption of CO2 using mono-ethanolamine. *International Journal of Greenhouse Gas Control*, 17, pp.294–308. Available at: http://dx.doi.org/10.1016/j.ijggc.2013.05.019.

[62] Kohrt, M. et al., 2011. Texture influence on liquid-side mass transfer. *Chemical Engineering Research and Design*, 89(8), pp.1405–1413.

[63] Lappalainen, K., Manninen, M. & Alopaeus, V., 2009. CFD modeling of radial spreading of flow in trickle-bed reactors due to mechanical and capillary dispersion. *Chemical Engineering Science*, 64(2), pp.207–218.

[64] Launder, B.E. & Spalding, D.B., 1973. Mathemtical Models of Turbulence. *Journal of Applied Mathematics and Mechanics*, 53(6), p.424.

[65] Lautenschleger, A., Olenberg, A. & Kenig, E.Y., 2015. A systematic CFD-based method to investigate and optimise novel structured packings. *Chemical Engineering Science*, 122, pp.452–464.

[66] Legendre, D. & Magnaudet, J., 1998. The lift force on a spherical bubble in a viscous linear shear flow. *Journal of Fluid Mechanics*, 368, p.S0022112098001621. Available

at: http://www.journals.cambridge.org/abstract_S0022112098001621.

[67] Lewis, W.K. & Whitman, W.G., 1924. Principles of Gas Absorption. *Industrial and Engineering Chemistry*, 16(12), pp.1215–1220.

[68] Li, Q. et al., 2016. Hydrodynamics of novel structured packings: An experimental and multi-scale CFD study. *Chemical Engineering Science*, 143, pp.23–35.

[69] Li, W. et al., 2014. Mass Transfer Coefficients for CO 2 Absorption into Aqueous Ammonia Using Structured Packing. *Industrial & Engineering Chemistry Research*, 53(14), pp.6185–6196. Available at: http://dx.doi.org/10.1021/ie403097h.

[70] López, J. et al., 2008. A new volume of fluid method in three dimensions - Part II: Piecewise-planar interface reconstruction with cubic-Bézier fit. *International Journal for Numerical Methods in Fluids*, 58(8), pp.923–944.

[71] Luis, P., 2016. Use of monoethanolamine (MEA) for CO2capture in a global scenario: Consequences and alternatives. *Desalination*, 380, pp.93–99.

[72] Luo, Y., Yang, H. & Lu, L., 2014. CFD simulation of the liquid flow on structured packing in the liquid desiccant dehumidifier. In *Energy Procedia*. pp. 180–183.

[73] MacDowell, N. et al., 2010. An overview of CO2 capture technologies. *Energy & Environmental Science*, 3(11), p.1645. Available at: http://xlink.rsc.org/?DOI=c004106h.

[74] Mangalapally, H.P. et al., 2012. Pilot plant study of four new solvents for post combustion carbon dioxide capture by reactive absorption and comparison to MEA. *International Journal of Greenhouse Gas Control*, 8, pp.205–216.

[75] Maric, T., Marschall, H. & Bothe, D., 2013. voFoam-A geometrical Volume of Fluid algorithm on arbitrary unstructured meshes with local dynamic adaptive mesh refinement using OpenFOAM. *arXiv preprint arXiv:1305.3417*, pp.1–30. Available at: http://arxiv.org/abs/1305.3417.

[76] Marschall, H. et al., 2012. Numerical simulation of species transfer across fluid interfaces in free-surface flows using OpenFOAM. *Chemical Engineering Science*, 78, pp.111–127.

[77] Mehta, U.B., 1998. Credible Computational Fluid Dynamics Simulations. *AIAA Journal*, 36(5), pp.665–667. Available at: http://arc.aiaa.org/doi/10.2514/2.431.

[78] Meldon, J.H. & Morales-Cabrera, M.A., 2011. Analysis of carbon dioxide absorption in and stripping from aqueous monoethanolamine. *Chemical Engineering Journal*, 171(3), pp.753–759.

[79] Min, J.K. & Park, I.S., 2011. Numerical study for laminar wavy motions of liquid film flow on vertical wall. *International Journal of Heat and Mass Transfer*, 54(15–16), pp.3256–3266.

[80] Monteiro, J.G.M.S. & Svendsen, H.F., 2015. The N2O analogy in the CO2capture context: Literature review and thermodynamic modelling considerations. *Chemical Engineering Science*, 126, pp.455–470.

[81] Mores, P. et al., 2012. CO2capture in power plants: Minimization of the investment and operating cost of the post-combustion process using MEA aqueous solution. *International Journal of Greenhouse Gas Control*, 10, pp.148–163.

[82] Nawrocki, P.A., Xu, Z.P. & Chuang, K.T., 1991. Mass transfer in structured corrugated packing. *The Canadian Journal of Chemical Engineering*, 69(6), pp.1336–1343.

[83] Nieves-Remacha, M.J., 2014. *Microreactor Technology: Scale-up of Multiphase Continuous Flow Chemistries*. Available at: http://hdl.handle.net/1721.1/91068.

[84] Nieves-Remacha, M.J., Kulkarni, A.A. & Jensen, K.F., 2015. OpenFOAM Computational Fluid Dynamic Simulations of Single-Phase Flows in an Advanced-Flow Reactor. *Industrial and Engineering Chemistry Research*, 54(30), pp.7543–7553.

[85] Nusselt, W., 1916. Die Oberflächenkondensation des Wasserdampfes. *Z. Ver. Deut. Ing.*, 60, pp.541–546.

[86] Ohta, M. & Suzuki, M., 1996. Numerical analysis of mass transfer from a free motion drop in a solvent extraction process. *Solvent Extraction Research and Development*, 1996(3).

[87] Olujić, Ž., 1999. Effect of column diameter on pressure drop of a corrugated sheet structured packing. *Chemical Engineering Research and Design*, 77(6), pp.505–510.

[88] Olujić & Jansen, H., 2015. Large-diameter experimental evidence on liquid (mal)distribution properties of structured packings. *Chemical Engineering Research and Design*, 99, pp.2–13.

[89] Onea, A.A., 2006. *Numerical simulation of mass transfer with and without first order chemical reaction in two-fluid flows*. University of Karlsruhe.

[90] Owens, S.A. et al., 2013. Computational Fluid Dynamics Simulation of Structured Packing. *Industrial & Engineering Chemistry Research*, 52(5), pp.2032–2045. Available at: http://pubs.acs.org/doi/abs/10.1021/ie3016889.

[91] Özkan, F. et al., 2016. Numerical investigation of interfacial mass transfer in two phase flows using the VOF method. *Engineering Applications of Computational Fluid Mechanics*, 10(1), pp.100–110.

[92] Penttilä, A. et al., 2011. The Henry's law constant of N2O and CO2in aqueous binary and ternary amine solutions (MEA, DEA, DIPA, MDEA, and AMP). *Fluid Phase Equilibria*, 311(1), pp.59–66.

[93] Perinu, C. et al., 2017. CO2 Capture by Aqueous 3-(Methylamino)propylamine in Blend with Tertiary Amines: An NMR Analysis. In *Energy Procedia*. pp. 1949–1955.

[94] Perlmutter, D.D., 1961. Surface-renewal models in mass transfer. *Chemical Engineering Science*, 16(3–4), pp.287–296. Available at: http://linkinghub.elsevier.com/retrieve/pii/0009250961800390.

[95] Petre, C.F. et al., 2003. Tailoring the pressure drop of structured packings through CFD simulations. In *Computational Fluid and Solid Mechanics 2003*. pp. 1087–1091.

[96] Pham, D.A. et al., 2015. Porous media Eulerian computational fluid dynamics (CFD) model of amine absorber with structured-packing for CO2 removal. *Chemical Engineering Science*, 132, pp.259–270. Available at: http://www.sciencedirect.com/science/article/pii/S0009250915002699.

[97] Prasad Thummala, P., 2016. Description of reactingTwoPhaseEulerFoam solver with a focus on mass transfer modeling terms. In *CFD with OpenSource Software*. Available at: http://www.tfd.chalmers.se/~hani/kurser/OS_CFD_2016.

[98] Rahimpour, M.R. et al., 2013. Investigation of natural gas sweetening process in corrugated packed bed column using computational fluid dynamics (CFD) model. *Journal of Natural Gas Science and Engineering*, 15, pp.127–137.

[99] Raynal, L. & Royon-Lebeaud, A., 2007. A multi-scale approach for CFD calculations of gas-liquid flow within large size column equipped with structured packing. *Chemical Engineering Science*, 62(24), pp.7196–7204.

[100] Raynal, S. et al., 2013. An experimental study on fish-friendly trashracks - Part 2. Angled trashracks. *Journal of Hydraulic Research*, 51(1), pp.67–75.

[101] Rix, A. & Olujic, Z., 2008. Pressure drop of internals for packed columns. *Chemical Engineering and Processing: Process Intensification*, 47(9–10), pp.1520–1529.

[102] Rochelle, G.T., 2009. Amine Scrubbing for CO2 Capture. *Science*, 325(5948), pp.1652–1654.

[103] Roenby, J. et al., 2017. A New Volume-of-Fluid Method in Openfoam. *VII International Conference on Computational Methods in Marine Engineering, MARINE 2017*, (February), pp.1–12.

[104] Rusche, H., 2002. *Computational Fluid Dynamics of Dispersed Two-Phase Flows at High Phase Fractions*. Available at: http://portal.acm.org/citation.cfm?doid=1806799.1806850.

[105] Said, W., Nemer, M. & Clodic, D., 2011. Modeling of dry pressure drop for fully developed gas flow in structured packing using CFD simulations. *Chemical Engineering Science*, 66(10), pp.2107–2117.

[106] Sato, T., Jung, R.-T. & Abe, S., 2000. Direct simulation of droplet flow with mass transfer at interface. *Journal of Fluids Engineering*, 122(3), pp.510–516. Available at: http://cat.inist.fr/?aModele=afficheN&cpsidt=790730.

[107] Schultes, M. & Chambers, S., 2007. How to Surpass Conventional and High Capacity Structured Packings with Raschig Super-Pak. *Chemical Engineering Research and Design*, 85(1 A), pp.118–129.

[108] Sebastia-Saez, D. et al., 2013. 3D modeling of hydrodynamics and physical mass transfer characteristics of liquid film flows in structured packing elements. *International Journal of Greenhouse Gas Control*, 19, pp.492–502.

[109] Sebastia-Saez, D. et al., 2015a. Meso-scale CFD study of the pressure drop, liquid hold-up, interfacial area and mass transfer in structured packing materials. *International Journal of Greenhouse Gas Control*, 42, pp.388–399.

[110] Sebastia-Saez, D. et al., 2015b. Micro-scale CFD modeling of reactive mass transfer in falling liquid films within structured packing materials. *International Journal of Greenhouse Gas Control*, 33, pp.40–50.

[111] Sebastia-Saez, D. et al., 2014. Micro-scale CFD study about the influence of operative parameters on physical mass transfer within structured packing elements. *International Journal of Greenhouse Gas Control*, 28, pp.180–188.

[112] SEBASTIA-SAEZ, D.J., 2016. *CFD MODELLING OF POST-COMBUSTION CARBON CAPTURE WITH AMINE SOLUTIONS IN STRUCTURED PACKING COLUMNS*. CRANFIELD UNIVERSITY.

[113] Sobieszuk, P. & Pohorecki, R., 2010. Gas-side mass transfer coefficients in a falling film microreactor. *Chemical Engineering and Processing: Process Intensification*, 49(8), pp.820–824.

[114] Stéphenne, K., 2014. Start-up of world's first commercial post-combustion coal fired ccs project: Contribution of shell cansolv to saskpower boundary dam iccs project. In *Energy Procedia*. pp. 6106–6110.

[115] Sun, B. et al., 2013. A new multi-scale model based on CFD and macroscopic calculation for corrugated structured packing column. *AIChE Journal*, 59(8), pp.3119–3130.

[116] Sussman, M., 2003. A second order coupled level set and volume-of-fluid method for computing growth and collapse of vapor bubbles. *Journal of Computational Physics*, 187(1), pp.110–136.

[117] Szulczewska, B., Zbicinski, I. & Górak, A., 2003. Liquid Flow on Structured Packing: CFD Simulation and Experimental Study. *Chemical Engineering & Technology*, 26(5), pp.580–584. Available at: http://dx.doi.org/10.1002/ceat.200390089.

[118] Tong, Z. et al., 2013. Experimental and numerical investigation on gravity-driven film flow over triangular corrugations. *Industrial and Engineering Chemistry Research*, 52(45), pp.15946–15958.

[119] Tsai, R.E. et al., 2009. Influence of viscosity and surface tension on the effective mass transfer area of structured packing. In *Energy Procedia*. pp. 1197–1204.

[120] Valluri, P. et al., 2005. Thin film flow over structured packings at moderate Reynolds numbers. *Chemical Engineering Science*, 60(7), pp.1965–1975.

[121] Versteeg, G.F., VAN DIJCK, L.A.J. & VAN SWAAIJ, W.P.M., 1996. on the Kinetics Between Co 2 and Alkanolamines Both in Aqueous and Non-Aqueous Solutions. an Overview. *Chemical Engineering Communications*, 144(1), pp.113–158. Available at: http://www.tandfonline.com/doi/abs/10.1080/00986449608936450.

[122] Versteeg, G.F. & van Swaal, W.P.M., 1988. Solubility and Diffusivity of Acid Gases (CO2, N2O) in Aqueous Alkanolamine Solutions. *Journal of Chemical and Engineering Data*, 33(1), pp.29–34.

[123] Versteeg, H.K. & Malaskekera, W., 2007. *An Introduction to Computational Fluid Dynamics*,

[124] Viebahn, P., Daniel, V. & Samuel, H., 2012. Integrated assessment of carbon capture and storage (CCS) in the German power sector and comparison with the deployment of renewable energies. *Applied Energy*, 97, pp.238–248.

[125] Wang, C. et al., 2017. Hierarchical calibration and validation for modeling bench-scale solvent-based carbon capture. Part 1: Non-reactive physical mass transfer across the wetted wall column. *Greenhouse Gases: Science and Technology*, 7(4), pp.706–720.

[126] Wehinger, G.D. et al., 2013. Numerical simulation of vertical liquid-film wave dynamics. *Chemical Engineering Science*, 104, pp.934–944.

[127] Weiland, R.H. et al., 1998. Density and viscosity of some partially carbonated aqueous alkanolamine solutions and their blends. *Journal of Chemical and Engineering Data*, 43(3), pp.378–382.

[128] Wielage, K., 2005. *Analysis of Non-Newtonian and Two-Phase Flows*. Paderborn University.

[129] Wikipedia contributors, 2017. Young-Laplace equation. *Wikipedia*. Available at: https://en.wikipedia.org/w/index.php?title=Special:CiteThisPage&page=Young–Laplace_equation&id=775196728.

[130] Wilcox, D.C., 2006. Turbulence Modeling for CFD (Third Edition). *DCW Industries*, (1), p.2006. Available at: http://www.amazon.com/Turbulence-Modeling-CFD-Third-Edition/dp/1928729088.

[131] Xie, B., Ii, S. & Xiao, F., 2014. An efficient and accurate algebraic interface capturing method for unstructured grids in 2 and 3 dimensions: The THINC method with quadratic surface representation. *International Journal for Numerical Methods in Fluids*, 76(12), pp.1025–1042.

[132] Xu, Y. et al., 2014. Detailed investigations of the countercurrent multiphase (gas-liquid and gas-liquid-liquid) flow behavior by three-dimensional computational fluid dynamics simulations. *Industrial and Engineering Chemistry Research*, 53(18), pp.7797–7809.

[133] Xu, Y.Y. et al., 2009. Computational Approach to Characterize the Mass Transfer between the Counter-Current Gas-Liquid Flow. *Chemical Engineering & Technology*, 32(8), pp.1227–1235. Available at: http://doi.wiley.com/10.1002/ceat.200900099.

[134] Yakhot, V. et al., 1992. Development of turbulence models for shear flows by a double expansion technique. *Physics of Fluids A*, 4(7), pp.1510–1520.

[135] Yang, C. & Mao, Z.-S., 2005. Numerical simulation of interphase mass transfer with the level set approach. *Chemical Engineering Science*, 60(10), pp.2643–2660. Available at: http://linkinghub.elsevier.com/retrieve/pii/S0009250904009601.

[136] Yang, W. et al., 2015. Mass transfer performance of structured packings in a CO2 absorption tower. *Chinese Journal of Chemical Engineering*, 23(1), pp.42–49. Available at: http://www.sciencedirect.com/science/article/pii/S1004954114001852.

[137] Yeoh, G.H. & Tu, J., 2010. *Computational Techniques for Multiphase Flows*,

[138] Yildirim, Ö. et al., 2012. Reactive absorption in chemical process industry: A review on current activities. *Chemical Engineering Journal*, 213, pp.371–391.

[139] Yu, D. et al., 2018. Experimental and CFD studies on the effects of surface texture on liquid thickness, wetted area and mass transfer in wave-like structured packings. *Chemical Engineering Research and Design*, 129, pp.170–181.

[140] Yu, L.M., Zeng, A.W. & Yu, K.T., 2006. Effect of interfacial velocity fluctuations on the enhancement of the mass-transfer process in falling-film flow. *Industrial and Engineering Chemistry Research*, 45(3), pp.1201–1210.

[141] Zakeri, A., Einbu, A. & Svendsen, H.F., 2012a. Experimental investigation of liquid holdup in structured packings. *Chemical Engineering Research and Design*, 90(5), pp.585–590.

[142] Zakeri, A., Einbu, A. & Svendsen, H.F., 2012b. Experimental investigation of pressure drop in structured packings. *Chemical Engineering Science*, 73, pp.285–298.

[143] Zhang, R. et al., 2017. The Comparison of CO2 Absorption Performance between DEAPA (3-Diethylaminopropylamine) and Blends of MEA-MDEA. In *Energy Procedia*. pp. 1877–1882.

[144] Zhao, L. & Cerro, R.L., 1992. Experimental characterization of viscous film flows over complex surfaces. *International Journal of Multiphase Flow*, 18(4), pp.495–516.

[145] Zheng, X. et al., 2013. Three-dimensional computational fluid dynamics modeling of two-phase flow in a structured packing column. *Chinese Journal of Chemical*

Engineering, 21(9), pp.959–966.

[146] Zivdar, M., Haghshenas Fard, M. & Prince, R.G.H., 2006. Evaluation of pressure drop and mass-transfer characteristics of a structured packing for production and separation of food flavours Part I: Pressure drop characteristics. *Food and Bioproducts Processing*, 84(3 C), pp.200–205.

APPENDIX

The code for one fluid formulation is implemented in OpenFOAM by modifying the interFOAM source code. Only the modifications made in the original code are highlighted here. Detail instructions of implementing a new code into OpenFOAM are available from a tutorial course work carried as part of the thesis (Prasad Thummala 2016) .

A.1. Modifications made to interFOAM.C main script:

The interFOAM solver was copied to user directory and was renamed as interFOAM_R (R standing for reaction-user can name it anyway).In the interFOAM_R folder the main interFOAM.C file was renamed as CO2_R.C and the species equation was written and included as a separate header file:CO2.H. Also the post processing file to calculate the film height, liquid hold up and interfacial area was included as a separate header file:post.H .Since the specie equation was solved on a steady flow field to reduce the computational time, the pimple loop was disabled in the main CO2_R.C file. The modified part of the CO2_R.C with CO2.H is given below:

```
while (runTime.run())
    {
        #include "readTimeControls.H"

        if (LTS)
        {
            #include "setRDeltaT.H"
        }
        else
        {
            #include "CourantNo.H"
            #include "alphaCourantNo.H"
            #include "setDeltaT.H"
        }

        runTime++;

        Info<< "Time = " << runTime.timeName() << nl << endl;

        // --- Pressure-velocity PIMPLE corrector loop
        /*while (pimple.loop())
        {

        }*/

            #include "CO2.H"
            #include "post.H"
```

A.2. Creating Variables:

Variables like diffusivity, concentration and Henry's constant are required to create the reactive mass transfer equation. The variables are created by adding the following code at the end of createFields.H header file in the same folder:

```
////////////////////////////////////////////////////////////////////////////////////////
//read and store individual diffusivities of each phase

//DTL diffusivity of CO2 in liquid
dimensionedScalar DTLA
(
"DTLA", dimensionSet(0, 2, -1, 0, 0, 0, 0), transportProperties.lookup("DTLA")
);

//DTG diffusivity of CO2 in gas

dimensionedScalar DTGA
(
"DTGA", dimensionSet(0, 2, -1, 0, 0, 0, 0), transportProperties.lookup("DTGA")
);

//read Henry's constant

dimensionedScalar H
(
"H", dimensionSet(0, 0, 0, 0, 0, 0, 0), transportProperties.lookup("H")
);

//read second order forward rate constant

dimensionedScalar kf
(
"kf", dimensionSet(0, 0, -1, 0, 0, 0, 0), transportProperties.lookup("kf")
);

Info<< "Reading field concentration of CO2 in liquid as A\n" << endl;
volScalarField A
(
    IOobject
    (
        "A",
        runTime.timeName(),
        mesh,
        IOobject::MUST_READ,
        IOobject::AUTO_WRITE
    ),
    mesh
);

Info<< "Reading field concentration of MEA in liquid as B\n" << endl;

volScalarField B
(
    IOobject
    (
        "B",
        runTime.timeName(),
        mesh,
        IOobject::MUST_READ,
        IOobject::AUTO_WRITE
    ),
    mesh
);
```

```
Info<< "Reading field film height\n" << endl;
volScalarField fH
(
    IOobject
    (
        "fH",
        runTime.timeName(),
        mesh,
        IOobject::MUST_READ,
        IOobject::AUTO_WRITE
    ),
    mesh
);
```

Finally the CO2.H file with specie mass transfer equation and post processing post.H files are written and placed in the interFOAM_R folder. The CO2.H code is given below:

```
{
volScalarField k("k",kf*alpha1);

volScalarField Diff ("Diff",DTLA*DTGA/((alpha1*DTGA)+((1.0-alpha1)*DTLA)));

volScalarField phiC ("phiC", Diff*(1.0-H)/(alpha1+(H*(1-alpha1))));

surfaceScalarField phiD ("phiD",(fvc::snGrad(alpha1)*mesh.magSf()));

surfaceScalarField phiCf ("phiCf",(fvc::interpolate(phiC)*phiD));

fvScalarMatrix AEqn
        (
        fvm::ddt(A)+fvm::div(phi,A)-fvm::laplacian(Diff,A)+fvm::div(phiCf,A)+(k*A*B)
        );
AEqn.solve();

fvScalarMatrix BEqn
        (
        fvm::ddt(B)+fvm::div(phi,B)+(k*A*B)
        );
BEqn.solve();

}
```

The “phiCf” term in the code represents additional flux term calculated according to Equation 3.18 and “Diff” represents the diffusivity calculated according to equation 3.19. The A, B represents the concentration of the CO_2 in gas and concentration of solvent MEA in liquid phase. The equations are discretized and solved fully implicitly.

The post.H file is as shown below:

```
{

//calculate liquid holdup

forAll(mesh.C(), cellI)
        {

        if(alpha1[cellI]>0.5)
        {total_vol+=(mesh.V()[cellI])*alpha1[cellI];}

        }
reduce(total_vol,sumOp<scalar>());

//calculate interfacial area per unit volume

volVectorField alphaGrad("alphaGrad",fvc::grad(alpha1));
volScalarField magAlphaGrad("magAlphaGrad", mag(alphaGrad));//interfacial Area per unit volume
//create interfacial Area constant
volScalarField int_A("int_A",magAlphaGrad);

scalar total_int_area =0.0;
//update area for each cell
forAll(mesh.C(), cellI)
        {

        int_A[cellI]=magAlphaGrad[cellI]*mesh.V()[cellI];
        total_int_area +=int_A[cellI];

        }
//////////////////////////////////////////////////

if(runTime.outputTime())
        {
        rho.write();
        int_A.write();
        Info<<"Total liquid volume = "<<total_vol<<endl;
        Info<<"Total interfacial area= "<<total_int_area<<endl;
        }

//////////////////////////////////////////////////

//////////film height calculation//////////////////////

label patchID=mesh.boundaryMesh().findPatchID("bottom_wall");

forAll(mesh.cells(),cellI)
        {
        scalar dist=100;

        forAll(mesh.boundaryMesh()[patchID].faceCentres(),facei)
                {
                scalar temp= mag(mesh.C()[cellI]-mesh.boundaryMesh()[patchID].faceCentres()[facei]);
                if (temp<dist){dist=temp;}

                }
        fH[cellI]=dist;

        }


}
```

The post.H file calculates the total liquid holdup in the computational domain by summing the volume of all grid cells having liquid volume fraction greater than zero. The film height is calculated as a distance from the “bottom_wall” over which the liquid is flowing. The interfacial area is calculated as a gradient of volume fraction multiplied by computational cell volume. This is one of the widely used methods for calculating interfacial area (Özkan et al. 2016; Wielage 2005). Note that the interfacial area can also be calculated as the area of iso-surface with liquid volume fraction of 0.5 in paraFoam. The file also outputs the liquid holdup and interfacial area values at every time step and can also be useful in transient analysis.